NEW INSIGHTS INTO THE MAPK FUNCTION IN MEIOTIC PROGRESSION AND THE REGULATION OF OSMOSTRESS-INDUCED APOPTOSIS IN *XENOPUS* OOCYTES

Institut de Neurociències

Unidad de Bioquímica de Medicina

New insights into the MAPK function in meiotic progression and the regulation of osmostress-induced apoptosis in *Xenopus* oocytes

Memoria de tesis doctoral presentada por Jicheng Yue para optar al grado de Doctor en Neurociencias de la Universidad Autónoma de Barcelona.

Trabajo realizado en la Unidad de Bioquímica de Medicina del Departamento de Bioquímica y Biología Molecular y el Instituto de Neurociencias de la Universidad Autónoma de Barcelona, bajo la dirección del Dr. José Manuel López Blanco.

Doctorando — Director de tesis

Jicheng Yue — Dr. José Manuel López Blanco

Barcelona, 26 de septiembre de 2014

ACKNOWLEDGEMENTS

First and foremost, my deepest gratitude is to my supervisor, Dr. José Manuel López Blanco, for improving my knowledge in the area and helping me to understand my research area better. His attentive works significantly improved my research perspectives and capabilities. I am grateful for his carefully correcting grammar and notation in my writings and for circumspectly reading and commenting on this manuscript.

I owe my special gratitude to Nabil for his elaborate technical teaching. He paid a lot of attention on explaining technical tips to me. I am also deeply grateful to Dani, he helped me a lot when I came to the laboratory.

I would like to thank Roberto Pinto, Montserrat Carrascal, and Joaquín Abian, from laboratory of proteomics at Universitat Autònoma de Barcelona for mass spectrometry analysis support. I am grateful to Dr. José Lizcano and José Bayascas for their advice and concern. I am also thankful to the secretarial staffs and members of the institute who maintained all the machines in the lab so efficiently.

Last but not least, I would like to thank my parents. Nothing could come true without their constant support and patience.

I appreciate the China Scholarship Council for the continuous financial support for my PhD study and daily life, providing me with the opportunity to complete my PhD thesis at the Universitat Autònoma de Barcelona, in Spain.

INDEX

1. SUMMARY

In the model organism Xenopus laevis, oocytes at stage VI are standing in prophase (G2/M) of meiosis I indefinitely until proper hormone stimulation. A positive regulation network around the Mos/MEK/ERK cascade ensures the rapid maturation (GVBD) of the oocytes upon stimulation with progesterone. However, for the stress associated MAPK families, JNK and p38, their involvement in meiotic resumption is not so clear. Here we analyze a protein of 42 kDa detected by pJNK antibodies (XpJNK-p42) that appears around GVBD in progesterone treated oocytes. Ectopic expression of a constitutively active MEKK1 accelerates oocyte maturation through activation of the p38 and ERK signaling pathways, but not the JNK cascade. Moreover, four dormant JNK3 transcripts are described in Xenopus oocytes and none of them are activated during progesterone-induced oocyte maturation. Protein mass spectrometry analysis indicates that XpJNK-p42 is actually phosphorylated ERK2. Intriguingly, the pJNK antibody only recognizes pERK2 in mature oocytes but not in oocytes exposed to hyperosmotic shock, suggesting that a posttranslational modification of pERK2 occurs during meiotic progression. Importantly, neither ERK2 overexpression nor JNK inhibitor SP600125 affects c-Jun phosphorylation detected in mature oocytes extracts. In conclusion, JNK proteins are not involved in Xenopus oocyte maturation, and the phosphorylation of c-Jun detected in mature oocytes is independent of JNK and ERK2.

We previously reported that hyperosmotic shock induces apoptosis in Xenopus oocytes through activation of four independent pathways: p38, JNK, calpains and Smac/DIABLO release. We also reported that activation of p38β, JNK1-1, and JNK1-2 is clearly pro-apoptotic. However, several hours after hyperosmotic shock the JNK1-2 isoform disappears, suggesting some type of degradation during cell death. In addition, our previous studies did not address the role of the Bcl-2 family members in the regulation of cytochrome c release. Here we show that Xenopus pJNK1-2 is proteolyzed at Asp385 by caspase-3, and the resulting cleaved protein accelerates cytochrome c release and caspase-3 activation, thus creating a positive feedback loop. We also show that overexpression of Bcl-xL in Xenopus oocytes protect from osmostress-induced apoptosis. In oocytes expressing Bid in combination with Bcl-xL, three different types of Bid are detected: non-ubiquitinated Bid, mono- and bi-ubiquitinated Bid. All Bid types reside both in the cytosol and the mitochondria. Hyperosmotic shock rapidly induces a slight increase of mono- and bi-ubiquitinated Bid in the mitochondria. Subsequently, Bid is cleaved at Asp52 at very low levels, probably by an

initiator caspase, generating an N-terminal fragment (nBid) and a highly pro-apoptotic C-terminal fragment (tBid). When cytochrome c is released and caspase-3 is activated a massive proteolysis of non-ubiquitinated and mono-ubiquitinated Bid occurs at Asp52, mediated by caspase-3, thus creating another positive feedback loop. Although some experiments suggest that non-ubiquitinated Bid is proteolyzed faster and is more pro-apoptotic than wild type Bid, the functional effects of Bid ubiquitination are not so clear. However, the pro-apoptotic function of Bid is markedly attenuated in mutant Bid-D52N that is not cleaved by caspases, indicating that Bid proteolysis regulates osmostress-induced apoptosis. In conclusion, caspase-3 activation induced by hyperosmotic shock engages two positive feedback loops through the cleavage of JNK1-2 and Bid, thus promoting an irreversible death of the oocytes.

2. ABBREVIATIONS

AMPK	AMP-activated protein kinase
Apaf	apoptotic protease activating factor
ASK1	apoptosis signal-regulating kinase 1
Bad	Bcl-2-associated agonist of cell death
Bak	Bcl-2 antagonist killer 1
Bax	Bcl-2-associated X protein
Bcl-2	B-cell CLL/lymphoma 2
Bcl-x_L	B-cell lymphoma-extra large
Bid	Bcl-2 interacting domain death agonist
Bim	Bcl-2-interacting mediator of cell death
CDK	cyclin-dependent kinase
CPE	cytoplasmic polyadenylation element
CPEB	CPE-binding protein
cPLA2	cytosolic phospholipase A2
ERK	extracellular signal-regulated kinase
GVBD	germinal vesicle breakdown
JIP	JNK interacting protein
JNK	c-Jun N-terminal kinase
MAPK	mitogen-activated protein kinase
MAPKK or MAP2K	MAPK kinase
MAPKKK or MAP3K	MAPK kinase kinase
MBS	modified Barth´s Saline
MEKK1	mitogen-activated protein kinase kinase kinase 1
MKK4	MAP kinase kinase 4
MKK6	MAP kinase kinase 6
MKK7	MAP kinase kinase 7
MKP	MAPK phosphatase
MLK	mixed-lineage protein kinase
MOMP	mitochondrial outer membrane permeabilization

Abbreviations

OMM	outer mitochondrial membrane
PKA	cAMP-dependent protein kinase
PLK	polo-like kinase
PP2A	protein phosphatase 2A
RSK	ribosome S6 kinase
SAPK	stress-activated MAP kinase
Smac/DIABLO	second mitochondria-derived activator of caspases/ direct IAP binding protein with low pI

3. INTRODUCTION

3.1 Mitogen activated protein kinase signaling pathway

Mitogen-activated protein kinases (MAPKs), also known as MAP kinases, are serine/threonine/tyrosine specific protein kinases belonging to the CMGC (CDK/MAPK/GSK3/CLK) kinase superfamily. Its closest relative kinase family, the cyclin-dependent kinases (CDKs), is another well studied kinase group so far (Manning et al. 2002). The first MAPK discovered and characterized in mammals was ERK1 (MAPK3). Since ERK1 and ERK2 (MAPK1) are both involved in growth factor signaling, the family was termed "mitogen-activated" (Boulton et al. 1991). For quite a long time, plenty of reports about MAPK referred to ERK proteins.

As an ancient and conserved protein family, five MAPK proteins were characterized in the budding yeast *Saccharomyces cerevisiae* (Schaeffer and Weber 1999). These kinases share related structures and biochemical properties, especially, these MAPKs are activated by dual phosphorylation on a tripeptide motif (Thr-X-Tyr) located in the kinase activation loop (T-loop) (Davis R. J. 2000a).

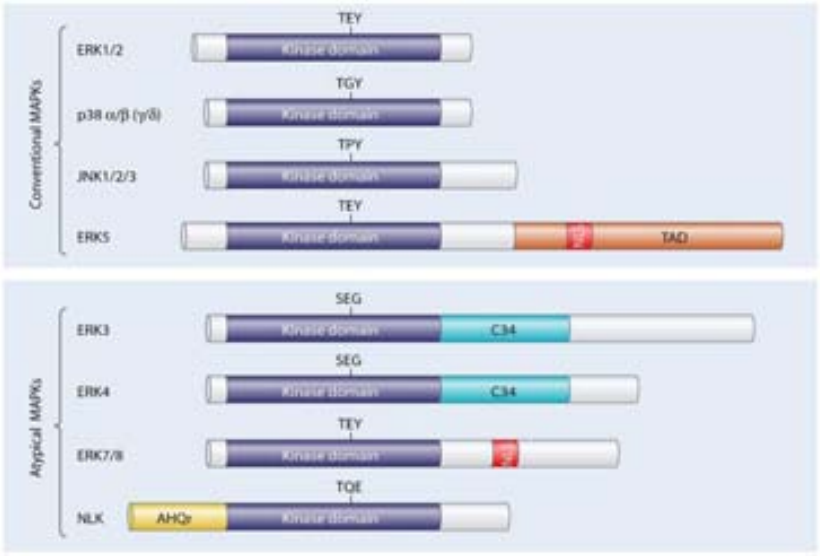

Figure 1 . **Schematic representation of the overall structures of conventional and atypical MAPKs**. All MAPKs contain a Ser/Thr kinase domain flanked by N- and C-terminal regions of different lengths. Different additional domains are also present in some MAPKs, including a transactivation domain (TAD), a nuclear localization sequence (NLS), a region conserved in ERK3 and ERK4 (C34), and a domain rich in Ala, His, and Glu (AHQr) (Cargnello and

In mammalian cells, 14 MAPKs divided into 7 groups were cloned and characterized. Besides four prototypical or conventional MAPK groups, extracellular regulated kinase (ERK1/2), C-Jun N-terminal kinase (JNK), p38 MAPK and ERK5, which work in a typical three-tiered module, at least three atypical MAPK types, ERK3/4, ERK7/8, and nemo-like kinase (NLK), which do not follow the classical three-tiered, dual-phosphorylation signaling structure, have been identified (Fig. 1) (Kholodenko and Birtwistle 2009).

In the conventional MAPK families, the ERK and p38 groups are related to kinases found in the budding yeast and contain the dual phosphorylation motifs Thr-Glu-Tyr (TEY) and Thr-Gly-Tyr (TGY) respectively. The JNK group, also known as stress-activated MAP kinase (SAPK), contains the dual phosphorylation motif Thr-Pro-Tyr (TPY) and represents a third MAPK sub-family in mammals (Davis R. J. 2000a). These mitogen activated protein kinase (MAPK) cascades process a myriad of signaling pathways stimulated by cell-surface receptors in the so called three-tiered MAPK cascade, comprising a MAPK, a MAPK kinase (MAPKK or MAP2K) and a MAPK kinase kinase (MAPKKK or MAP3K) (Fig. 2) (Kholodenko and Birtwistle 2009). MAPK signaling pathways play a pivotal role in regulating various fundamental cellular processes, including cell growth, division, migration and differentiation.

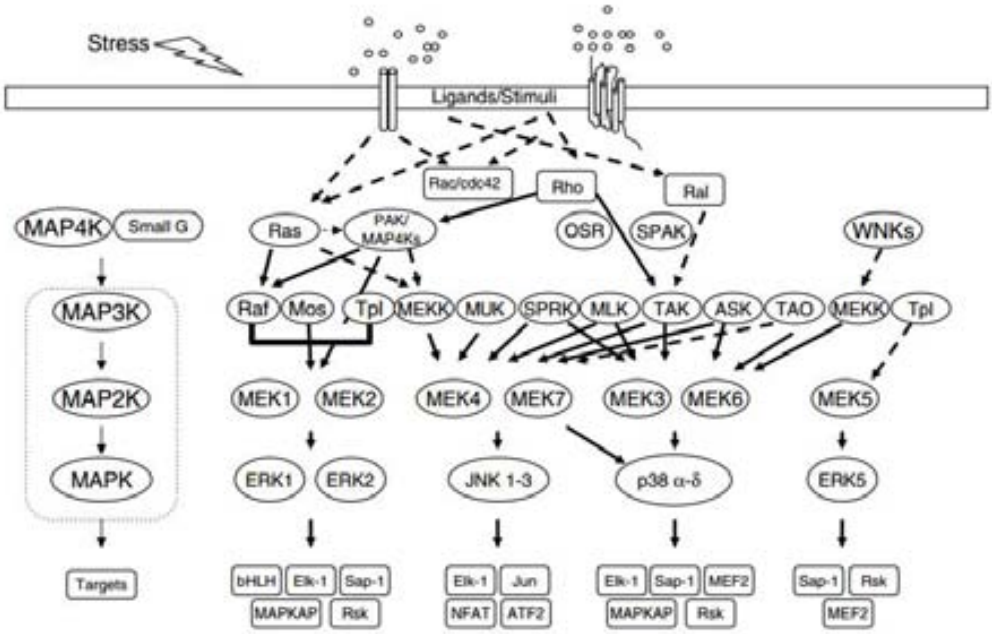

Figure 2. **MAPK cascades. Illustration of the three-tiered MAPK cascades for ERK, JNK and p38 family members** (Raman et al. 2007).

3.1.1 The ERK cascade

ERK1 which was found to be phosphorylated on residues Thr and Tyr in response to cell growth factors is the first MAPK member described in mammalians (Cooper et al. 1982, Ray and Sturgill 1988). In early 1990s, both ERK1 and ERK2 were cloned and characterized (Boulton et al. 1991). These two ERK isoforms, with molecular weight of 43 and 41 kDa and sharing 83% amino acid identity, were ubiquitously expressed in all tissues (Boulton et al. 1990). Isoforms derived from alternative splicing were described for both ERK1 (ERK1b and ERK1c) (Shaul and Seger 2006, Yung et al. 2000) and ERK2 (ERK2b) (Gonzalez et al. 1992).

MEK1/2 are the upstream kinases (MAP2K) that phosphorylate tyrosine and threonine residues in the ERK1/2 activation loop, and MAP2Ks are phosphorylated on two serine residues or a serine residue and a threonine residue in the activation loop by MAP3Ks. Raf isoforms are the best-studied MAP3Ks that regulate the ERK signaling pathways. Raf proteins are activated through binding the small G proteins of the Ras family to its N-terminus. Another well-known MAP3K is Mos. Different to Ras kinases, Mos is more restrictively selected to specific cells and stimuli, such as in Mos/MEK/ERK cascade of *Xenopus* oocytes, Mos is activated by progesterone (Raman et al. 2007, Rapp et al. 2006).

In ERK cascade proteins, the docking motif (D motif) is one crucial motif for its interaction with ERK binding proteins, including its regulators and substrates. Frequently, motifs in substrates preferred by ERK reside in the N-terminal and are characterized by a cluster of positively charged residues with two or more nearby hydrophobic residues. D motifs bind to a conserved C-terminal common docking (CD) sites identified in ERK1/2 and other MAPKs. A variety of motifs implicated in MAPK interaction were detailed described (Raman et al. 2007, Sharrocks et al. 2000, Tanoue et al. 2000).

3.1.2 The JNK cascade

C-Jun N-terminal kinase (JNK) was firstly identified as a p45 microtubule associated protein kinase in cycloheximide injected rat (Kyriakis and Avruch 1990). Later, it was notice that c-jun, a component of the AP-1 transcription factor, is regulated by MAPK via phosphorylating on two serine residues in the N-terminal in response to a variety of mitogens, and, these MAPKs include pp45 and pp42/44 kinases (Pulverer et al. 1991). The directly binding and phosphorylation was confirmed in a c-jun binding assay using extracts from UV-irradiated cells, the kinases were then named JNKs (Hibi et al. 1993).

Three distinct JNK genes have been isolated in mammalians (Dhanasekaran N and Reddy 1998). The *jnk1* and *jnk2* are ubiquitously expressed. In contrast, the *jnk3* expression pattern is relatively restricted to brain, heart, and testis. The three *jnk* genes express at least ten JNK isoforms by distinct modification in selective transcription and alternative splicing. Transcripts derived from JNK genes have two distinct 3´extension, and more transcripts are generated through alternative splicing from these original transcripts. It is clear that the alternative splicing influences the substrate specificity of the JNK isoforms by altering the binding motif of JNK to docking sites in other proteins (Gupta et al. 1996, Kallunki et al. 1994, Sluss et al. 1994).

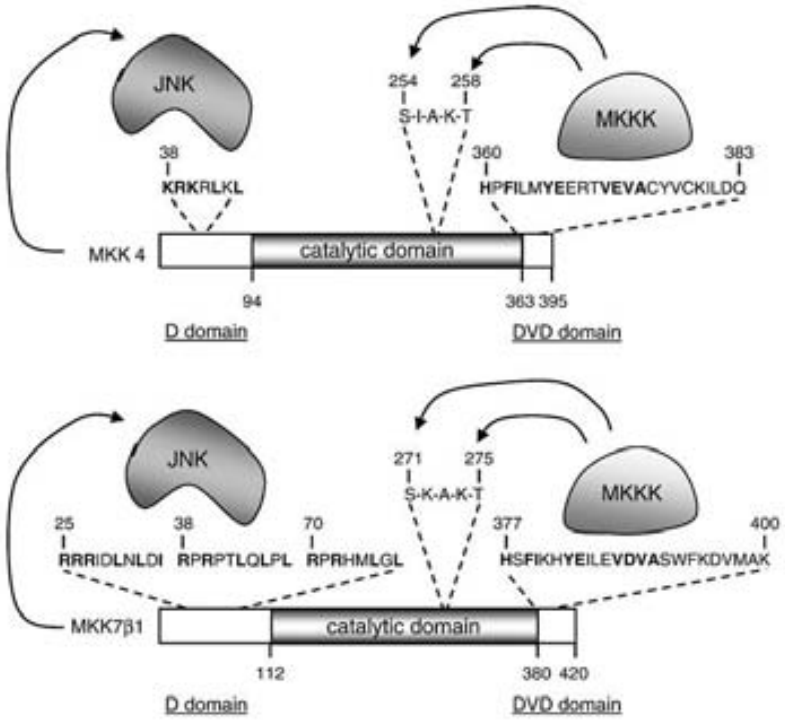

Figure 3. **Schematic illustration of functional domains identified in MKK4 and MKK7.** MAPK and MAPKKK docking domains referred as D and DVD sites in MKKs permit the formation of stable complexes between the components of the MAPK signaling pathway. These interactions contribute to accurate and efficient enzyme-substrate recognition and are essential for the specific transmission of signals from upstream kinases to the MAPKs. The D sites in MKK4 and MKK7 consist of a cluster of two to three basic residues, followed by a short spacer of 1–2 residues, and a hydrophobic-X-hydrophobic sub-motif. Unlike MKK4, MKK7 contains three weak D-sites that interact in a partially additive, partially synergistic manner to create high affinity JNK-docking platform. The specific MAPKKK MKKs interaction via the DVD site facilitates the phosphorylation of MKK4 and MKK7 at Ser and Thr residues within the S–X–A–K–T motif, by increasing the local concentration of the activating MAPKKK and altering the structure of the MKKs. Consensus-matching residues in the putative D and DVD sites of MKK4 and MKK7 are in boldface (Wang Xin et al. 2007d).

JNK proteins are activated by concomitant phosphorylation on Thr and Tyr in the TPY motif in the activation loop by MKK7 and MKK4 (SEK1). Like JNK isoforms, alternative splicing modification generates six MKK7 isoforms with different N-terminal and C-terminal and three MKK4 isoforms with distinct N-terminal. These different isoforms of MKK7 and MKK4 are biochemically different and activated by distinct MAPKKKs through different docking motif preference (Fig. 3) (Tournier et al. 1999, Wang Xin et al. 2007d). Both MKK7 and MKK4 can activate JNK, and MKK4 can also activate p38 (Fig. 2). It seems that MKK4 preferentially phosphorylates JNK on Tyr and MM7 preferentially phosphorylates JNK on Thr, indicating that MKK7 and MKK4 are not functionally exclusive and they may function cooperatively under particular circumstances (Lawler et al. 1998, Raman et al. 2007).

The MKK7 and MKK4 are also activated by dual phosphorylation on two residues in the activation loop by up tier kinase. Several MAP3Ks that phosphorylate and activate MKK4 and/or MKK7 have been isolated. Fourteen out of twenty identified MAP3Ks are proved to activate JNK via phosphorylating MKK4 or MKK7. Generally, the MAP3K is identified by transfection assay or *in vitro* protein kinase assays. It is unclear whether these MAP3Ks are physiological regulators of the JNK signaling pathway and which stimulus correspondingly activates these specific kinases (Davis R. J. 2000a). Significant progression has been made toward understanding the function of the MEKK group through targeted gene disruption techniques in mice. MEKK1 deficient mice have no gross morphological disabilities except for an eyelid closure defect (Yujiri et al. 2000) while defect of MEKK3 is lethal for mice (Yang Annie et al. 2000). Studies have demonstrated that MEKK1functions as a component of the JNK cascade. The functional consequences of MEKK1disruption in ES cells includes defects in cell migration and increase apoptosis in response to microtubule destabilizing drugs (Davis Roger J 2000b).

3.1.3 The p38 cascade

The archetypical p38 member, p38α was identified in 1994. It has a significant homology with the budding yeast Hog1, and shares 50% identity with ERK2. p38 is the second identified MAPK module in response to stress stimuli (Han J et al. 1994, Rouse et al. 1994). After the isolation of p38α, another three p38 isoforms, p38β, p38γ and p38δ, were isolated and characterized. While p38α and p38β are ubiquitously expressed in cell lines and tissues, the expression pattern of p38γ and p38δ is restricted (Cuadrado and Nebreda 2010, Jiang Yong et al. 1996, Jiang Yong et al. 1997). Even MKK4 has been shown to activate p38, MKK3 and MKK6 are supposed to be the major kinases responsible for p38 activation (Derijard et al. 1995, Han Jiahuai et al. 1996, Meier et al.

1996). MKK3/MKK6 activate(s) p38 by dual phosphorylation on Thr and Tyr in the conserved TGY motif in their activation loop. MKK6 can activate all p38 isoforms, whereas MKK3 preferentially phosphorylates the p38α, p38γ, and p38δ.

MKK3/MKK6 are activated by a great quantity of MAP3Ks, including MEKK1 to -3, MLK2/3 and ASK1 (Cuadrado and Nebreda 2010). In most contexts, MAP3Ks involved in p38 module are shared by the JNK module. In the process of investigating the role of p38 module, to eliminate the intervention between different MAPK modules, many p38 inhibitors were exploited in thousands of studies. The anti-inflammatory drug SB203580 and its close relative SB202190 specifically target and inhibit the p38α and p38β as competitive inhibitors of ATP binding (Lee et al. 2000). A novel inhibitor, BIRB0796, inhibits all p38 isoforms by blocking an allosteric binding site as well as establishing binding interactions in the ATP pocket (Pargellis et al. 2002, Regan et al. 2002).

3.1.4 Molecular scaffold proteins assemble MAPK signaling components

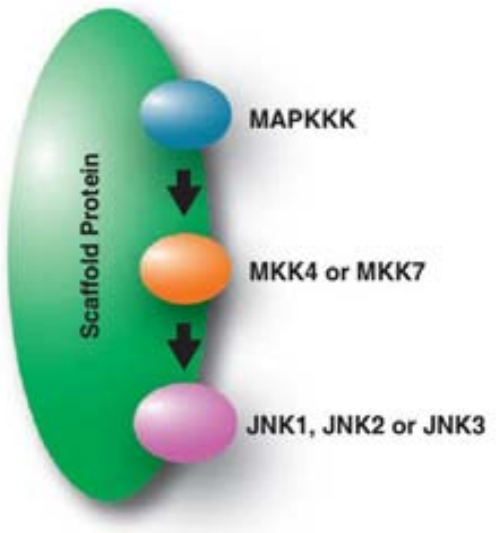

Figure 4. **Scaffold proteins mediating the structural and functional organization of the three-tier JNK signaling module.** Model of how a typical scaffold protein supports the assembly of a three-tier JNK signaling module consisting of a MAPKKK, a MAPKK (MKK4 or MKK7) and a JNK. Such scaffold proteins may play a catalytic role as well as an anchoring role depending on the nature of the scaffold protein and the cellular context (Asaoka and Nishina 2010).

Precise signaling transduction is guaranteed by proper protein-protein interactions via forming protein complexes. Generally, the interacting proteins are recruited and assembled by a third protein group, one significant protein group involved in the complex-assembly is the scaffold protein. The scaffold protein is described as protein whose main function is to bring other proteins together. Generally, these proteins have various protein docking motifs. Scaffold protein tethers signaling components together and localizes these proteins to proper areas of the cell, regulates signaling transduction precisely and insulates correct signaling proteins from competing proteins simultaneously (Shaw and Filbert 2009, Whitmarsh and

Davis 1998). Scaffold proteins are ubiquitous in MAPK cascades. For accurate signaling transmission, scaffolds have an optimal concentration, depending on the concentration of MAPK components and their affinities for the scaffold (Kholodenko and Birtwistle 2009).

A number of proteins that serve as scaffold for ERK cascade have been identified. In ERK module, upon Ras activation, scaffold protein KSR is translocated to the plasma membrane with MEK1/2 proteins, and recruits Raf-1 and ERK1/2 together to form the Raf/MEK/ERK complex, therefore facilitating the ERK activation (Morrison and Davis 2003).

For JNK cascade assembly in murine embryonic fibroblast cells, JNK is preferentially activated by MKK7 depending mainly on scaffold Axin, in contrast, MKK4 activates JNK primarily relying on scaffold LMP-1 (Zou et al. 2007). Ones intensively studied scaffold proteins in JNK module are JNK interacting protein (JIP) proteins. The JIP1 and JIP2 closely interact with JNK and MKK7 or mixed-lineage protein kinases leading to JNK activation (Meyer et al. 1999). The MLKs are a family of serine/threonine protein kinases that function in control of specific MAPK3. All the known MLKs identified by transfection in mammalian cell lines act as MAP3Ks to activate JNK and p38 pathways (Gallo and Johnson 2002).

3.1.5 Phosphatases are MAPK activity regulators

Components of MAPK cascade are all activated by phosphorylation, and protein phosphatases are supposed to be crucial regulators for MAPK activities. The dephosphorylation can impact signaling transmission both positively and negatively.

Protein phosphatase 2A (PP2A) is an important regulator in the ERK cascade. In the ERK activation event, dephosphorylation of both KSR and Raf1 on their inhibitory sites is a prerequisite for ERK complex assembly (Dougherty et al. 2005). The role of phosphatases in JNK signaling pathway regulation is poorly understood. In MAPK phosphatase (MKP)-knockout mice, it was implied that the MKPs are negative regulators of JNK signaling. Physiological inhibition of MKP can prolong JNK activation. In some circumstances, MKP inhibition was enough for JNK activation (Jeong et al. 2006). MKP family proteins may be targeted directly to JNK via mediation of scaffold proteins (Weston and Davis 2002).

3.2 *Xenopus* oocyte is an excellent system for ootidogenesis and apoptosis

Since the original studies started by John Gurdon and colleagues, oocytes from the South African clawed frog have been established as an excellent functional expression system. When injected with messenger RNA, the oocytes were able to translate the mRNA into relative proteins after a period of incubation (Gurdon et al. 1974). The large size of the oocyte (Fig. 5) facilitates the microinjection of mRNAs to express proteins in enough quantities for proper biochemical studies. Most of the mechanisms that regulate oogenesis and maturation have been discovered using *Xenopus* oocytes as a cell model.

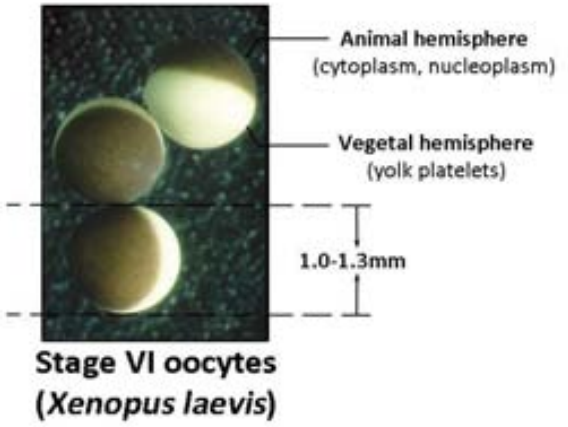

Figure 5. **Stage VI oocytes from *Xenopus laevis*.** The stage VI oocyte is tremendously large with a volume of 1 µl containing about 25µg proteins. About half of the oocyte´s volume consists of some yolk platelets which are concentrated in the lightly pigmented vegetal hemisphere, the yolk will ultimately makes its way into the gut of the tadpole and serve as energy resource. The pigmented dark brown animal hemisphere mainly contains the cytoplasm and nucleoplasm (modified from *Xenopus express*).

The *Xenopus laevis* oocyte begins as a cell slightly bigger than a typical somatic cell. At the beginning of meiotic cycle, the oocyte undergoes a round of DNA replication and then enters the prophase of meiosis I, during this stage the chromatin condenses into chromosome, then homologs pair and recombination occurs. In the following several months, the oocyte remains in a G2-like growth stage with a intact nuclear envelope (germinal vesicle envelope), and the volume of oocyte grows bigger and bigger. Once the oocyte is fully grown, it enters into the so called Dumont Stage VI, a G2 arrested state (Fig. 6). This arrest retains indefinitely in a stable environment (18ºC, 12h/12h light/dark for *Xenopus laevis*) before progesterone induction. The volume of oocyte and its ability to synthesize protein on demand make the oocyte an almost ideal single-cell experimental system (Ferrell 1999).

The process of stage VI oocyte developing into fertilizable egg is termed oocyte maturation. The maturing oocyte undergoes germinal vesicle breakdown (GVBD), followed by chromatin condensation and microtubule reorganization and formation of the metaphase spindle and

subsequent completion of the first meiosis I by emitting the first polar body. Then the oocyte enters meiosis II without the intervening interphase and is arrested in metaphase again. The maturing process completes (Fig. 6). In the maturing process, GVBD is easy to score because of a white spot appearing at the animal pole, a result of rearrangement of cortical pigment granules (Ferrell 1999). Importantly, in vitro incubation of isolated *Xenopus* oocytes at stage VI with progesterone resume the maturation process until meiosis II, facilitating the study of this biological process.

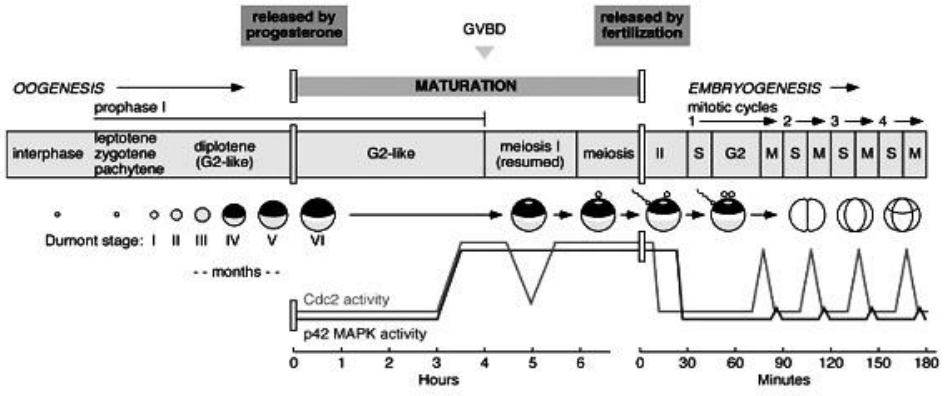

Figure 6. **Schematic view of *Xenopus* oogenesis, maturation, and early embryogenesis** (Ferrell 1999).

Besides studies of meiotic progression, *Xenopus* oocytes have also been used for research in apoptosis. A cell-free system based on *Xenopus* egg extracts was used for the seminal works describing the role of cytochrome c release from the mitochondria in the engagement of apoptosis (Newmeyer et al. 1994, Kluck et al 1997). Moreover, the role of several members of the Bcl-2 family in regulating cytochrome c release was discovered using this system. *Xenopus* egg extracts incubated at room temperature for several hours spontaneously recapitulate many events of apoptosis, including chromatin condensation, shrinkage, and fragmentation of the nuclei, even from nuclei added exogenously. This morphological changes required the presence of a dense organelle fraction enriched in mitochondria and could be blocked by the addition of baculovirus-expressed Bcl-2 protein (Newmeyer et al. 1994). Bcl-2 blocked apoptotic activity by preventing cytochrome c release from mitochondria and thereby blocking activation of caspase-3 like proteases (CPP32) and downstream apoptotic events (Kluck et al. 1997, Kuwana et al. 1998). More recently it has been discovered that the spontaneous death of the oocytes at room temperature is due to glucose-6-phosphate and NADPH depletion, which induces caspase-2 activation (Nutt et al. 2005). Caspase-2 is phosphorylated and inhibited by Calcium calmodulin-dependent kinase II (CaMKII) (Nutt et al. 2005), and protein phosphatase 1 activation by nutrient depletion would induce apoptosis through dephosphorylation and activation of caspase-2 (McCoy et al. 2013). Besides these studies with *Xenopus* egg extracts, the oocytes have been used as an easily manipulable *in vivo* system to study apoptosis induced by different stimuli. For instance, cytochrome c release was detected in isolated

intact oocytes 48h later after initiating meiotic maturation by progesterone. It seems that the default fate of unfertilized oocyte is to die through a mitochondria dependent apoptosis pathway after meiotic maturation, and it has been described that this apoptosis is regulated by JNK and Cdc2 activation (Du Pasquier et al. 2011). It has also been reported that incubation of *Xenopus* oocytes with bacterial neutral sphingomyelinase (bSMase) causes GVBD, whereas microinjection of bSMase results in apoptosis, indicating that an increase of ceramide production induced by bSMase can induce meiosis or apoptosis, depending on the location of ceramide (Coll et al. 2007, Strum et al. 1995). Although in mammalian cells it has been reported that ceramide can initiate apoptosis through a Rac1-regulated activation of the JNK/p38 cascade or ASK1-regulated p38 and JNK activation, as well as activation of the endoplasmic reticulum (ER) stress cascade (Brenner et al. 1997, Chen Chia-Ling et al. 2008, Verheij et al. 1996) in *Xenopus* oocytes it was not determined the signaling pathway responsible for ceramide-induced apoptosis. Hyperosmotic shock also induces cytochrome c release and caspase-3 activation in *Xenopus* oocytes (Bagowski et al. 2002, Martiañez et al. 2009), and several mechanisms that regulate osmostress-induced apoptosis have been discovered by our group (see introduction, section 4). Finally, *Xenopus* oocytes allow greater manipulation as a system to study the analog or digital responses in single cells for particular external stimulation or microinjected proteins (Bagowski and Ferrell Jr 2001, Martiáñez et al. 2009).

3.3 *Xenopus* oocyte maturation involves complicate regulations

Generally, progesterone is considered the hormone inducing oocyte maturation *in vivo* in *Xenopus laevis*, which is synthesized and released by follicular cells surrounding the oocyte. However, androgen, rather than progesterone, has been proposed to be the primary hormone produced in *Xenopus* ovaries (Lutz et al. 2001). Maturation can also be induced *in vitro* by insulin and insulin-like growth factor-1 via an IGF-1 receptor. However, it is unclear whether these hormones have a role in *in vivo* maturation (Ferrell 1999, Schmitt and Nebreda 2002). As we will see in this section, progesterone induces several signaling pathways in *Xenopus* oocytes, and the translational and posttranslational control of several genes is of great relevance in the maturation of the oocytes.

3.3.1 Potential progesterone receptor

In *Xenopus* oocytes, progesterone can be recognized by a plasma membrane receptor as a ligand. The receptor of progesterone does not reside in cytoplasm or nucleus, because oocytes mature only when progesterone is applied outside of the oocytes instead of microinjected into the cytoplasm or nucleoplasm (Smith and Ecker 1971). Furthermore, oocytes can also mature when incubated with steroids immobilized on agarose beads or linked to a synthetic polymer. These issues indicate that the receptor of progesterone resides on the plasma membrane and faces out (Godeau et al. 1978, Ishikawa et al. 1977). Early responses of oocytes to progesterone involve a modest inhibition of adenylate cyclase and subsequent modest decrease in cyclic AMP concentration in the oocytes, without significant alteration of cAMP phosphodiesterase activity. These responses suggest that the progesterone receptor might be a transmembrane protein coupled to heterotrimeric G proteins which inhibit adenylate cyclase. However, the functions of the G proteins are not completely understood (Ferrell 1999, Schmitt and Nebreda 2002).

An intracellular *Xenopus* progesterone receptor (XPR-1) has been implicated in meiotic maturation (Bayaa et al. 2000, Tian et al. 2000). Subsequently it was reported to be localized at the oocyte membrane (Bagowski et al. 2001b), possibly through interaction of its proline-rich motif with the SH3 domain of the c-Src protooncogene (Boonyaratanakornkit et al. 2001). Addition of a myristoilation and palmytoilation signal at the amino terminus of XPR-1 increased the amount of receptor associated to the oocyte plasma membrane and accelerated progesterone-induced oocyte maturation (Martinez et al. 2006).

A membrane-associated progesterone-binding protein from porcine liver was also purified by Nehling and his colleagues and its corresponding cDNA was cloned too (Falkenstein et al. 1996). Sequence analysis revealed that homologous cDNAs are present in human, mice, rat, and yeast (Ferrell 1999). This membrane progesterone receptor (mPR) is not termed progesterone membrane receptor component 1 (PGMRC1) and was proved located in membrane with many other progesterone binding proteins (Lösel Ralf et al. 2004). Even though PGMRC1 was originally described as steroid binding protein, current evidences support the perception that it may be involved in steroid metabolism or homeostasis and survival (Lösel Ralf M et al. 2008). Intriguingly, it is shown to be mediator of progesterone´s antiapoptotic action (Peluso et al. 2008, Peluso et al. 2006). Another distinct family of membrane progestin receptors (mPRs) has been cloned in fish and many other vertebrate species (Zhu et al. 2003). In *Xenopus laevis*, a transcript (*Xenopus* mPR, XmPR) of the mPR_{β} ortholog was cloned by RT-PCR. This protein is present on the oocyte plasma membrane, and microinjection of mRNA encoding XmPR resulted in acceleration of progesterone-

induced oocyte maturation. Binding studies in mammalian cells expressing XmPR protein confirmed specific binding of progesterone. These results suggest that XmPR might be a physiological progesterone receptor involved in meiotic resumption of *Xenopus* oocytes (Josefsberg Ben-Yehoshua et al. 2007). In *Rana pipiens* oocytes it has been reported that progesterone binds to the ouabain binding site on the N-terminal region of the alpha-subunit of Na/K-ATPase triggering a cascade of lipid second messengers and meiotic progression (Morrill et al. 2005). The authors propose that helix-helix interactions between the alpha-subunit of Na/K-ATPase and phosphatidylethanolamine-N-methyltransferase (PE-NMT) occur in the plasma membrane inducing the activation of PE-NMT and sphingomyelin synthase within seconds. (Morrill et al. 2010, Morrill et al. 2005). There are no reports about the binding of progesterone to *Xenopus* alpha-subunit of Na/K-ATPase and its role in meiotic progression.

3.3.2 Early-stage response to progesterone

Xenopus oocytes go through many changes including the metabolism of nutrient stockpile, which may supply energy for the viability and survival of the oocyte. Proteome analysis of maturing oocytes indicate that the glycolytic metabolites may be critical modulators of oocyte maturation (Berger and Wilde 2013, Nutt 2012).

One of the key earliest biochemical changes observed in maturing oocytes, as described before, is the decrease of cAMP concentration after progesterone incubation. The decrease of cAMP occurs within minutes after progesterone incubation; it lasts a few hours, and is accompanied by inhibition of the cAMP-dependent protein kinase (PKA), which has been found to be a potent inhibitor of oocyte maturation. Correspondingly, inhibition of PKA alone is enough to induce meiotic maturation in *Xenopus* oocytes (Schmitt and Nebreda 2002).

3.3.3 Polyadenylation-dependent protein synthesis is required in meiotic resumption

In *Xenopus*, oocyte maturation is independent of transcription, but it is regulated at the level of translation and post-translational modifications of proteins. Nearly two decades ago, it was found that there is a maternal stockpile of mRNAs harboring a cytoplasmic polyadenylation element (CPE) in the 3´untranslated regions (3´UTR) that may control cytoplasmic polyadenylation and translational activation. CPE is the binding platform for CPE-binding proteins (CPEB). The binding

of CPEB to the 3´UTR recruits the cleavage and polyadenylation specificity factor (CPSF) to the polyadenylation hexanucleotide (Hex, AAUAAA). Subsequently, the complex recruits the cytoplasmic poly (A) polymerase GLD2 and many other factors including eIF4 translation factors, which are required to recruit the 40S ribosomal subunit to the 5´end of the mRNA after the CPEB activation (Fig. 7) (Mendez and Richter 2001, Radford et al. 2008, Richter 2007).

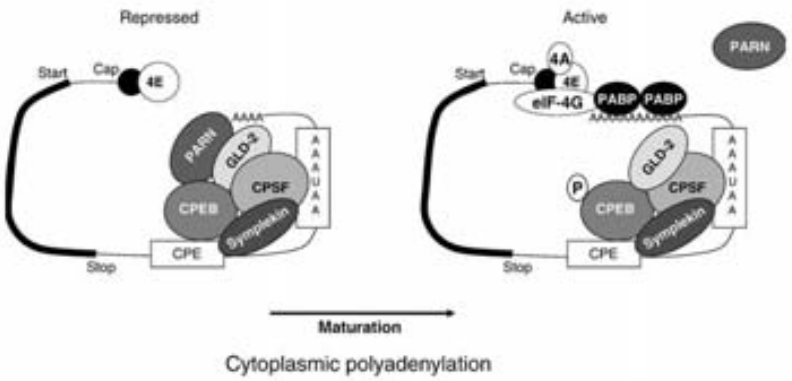

Figure 7. **The activation of CPE-mediated cytoplasmic polyadenylation.** In immature oocytes, CPE containing mRNAs already contain all the proteins necessary for polyadenylation as well as the deadenylase PARN. During oocyte maturation, phosphorylation of CPEB causes a rearrangement of the complex that leads to the ejection of PARN and the activation of the poly(A) polymerase Gld-2. 4E: eIF4E, 4A: eIF4A. For further description of this process, see the review of Radford et al. 2008 (Radford et al. 2008).

Three waves of polyadenylation were observed in meiotic progression, which were controlled by sequential activation of CPEB1 and CPEB4. For early protein synthesis during meiotic resumption or oocyte maturation, an early site-specific phosphorylation of CPEB1 (Ser174 in *Xenopus*) is essential for the polyadenylation of target mRNAs. It was reported that protein Eg2, a member of the Aurora family, is responsible for this phosphorylation(Mendez et al. 2000). Overexpression of Eg2 can accelerate progesterone induced oocyte maturation. On the contrary, the phosphatase PP1 removes this phosphate and thus inhibitis polyadenylation and translation (Radford et al. 2008, Setoyama et al. 2007, Tay et al. 2003). It was also observed that a transient activation of ERK, independent of Mos, can phosphorylate directly CPEB on four residues (T22, T164, S184, S248), but not the crucial residue Ser174. However, it has been suggested the phosphorylation mediated by ERK may prime CPEB for phosphorylation on Ser174 (Keady et al. 2007). At metaphase I, the CPEB1 phosphorylation by Cdc2 and Plx1 will result in CPEB1 degradation, and the first wave of polyadenylation ends. During this period, CPEB4 is encoded by maternal mRNA under the control of CPEB1, which will be in charge of the late or late-late wave of polyadenylation during the MI-MII progression (Fig. 8) (Igea and Méndez 2010).

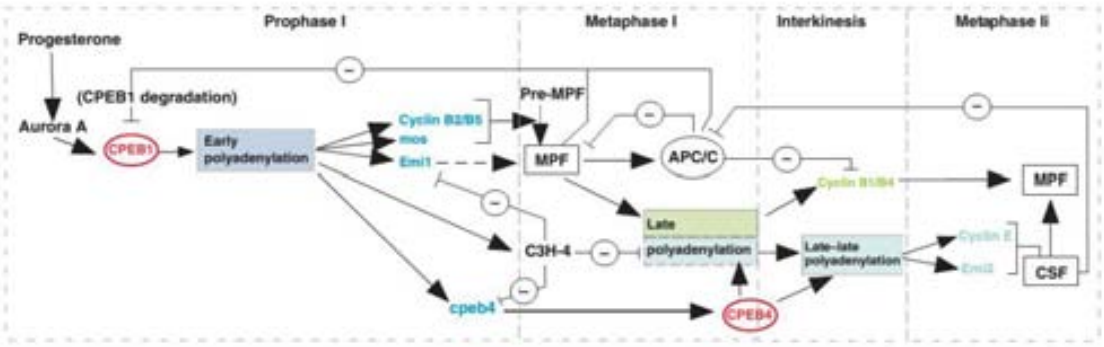

Figure 8. **Schematic diagram showing the sequential activities of CPEB1 and CPEB4 mediating the three waves of polyadenylation driving meiotic progression** (Igea and Méndez 2010).

3.3.4 MPF is one crucial factor for meiotic initiation

About 30 -60 min before GVBD, there is a significant increase of protein kinase activity and phosphorylated proteins in the oocytes. These proteins can be classified into two groups: 1) the cell cycle regulators, such as Cdc2, Cdc25, Plx1, and xPlkk1; and 2) the MAPK proteins including Mos, MEK1, ERK2, Rsk1/2 and so on (Ferrell 1999).

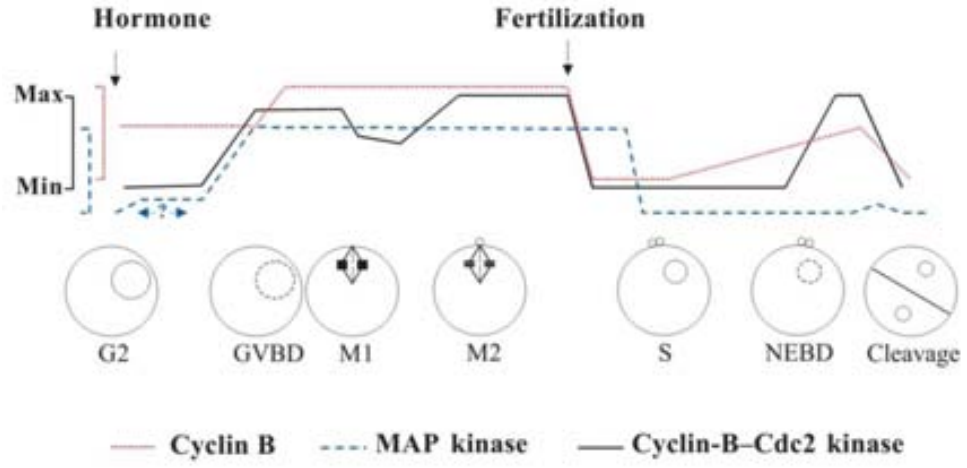

Figure 9. **Changes in *Xenopus* oocytes in the levels of cyclin B protein, and the cyclinB-Cdc2 kinase and MAP kinase activities throughout the course of meiotic maturation.** For species-specific variations, see the main text. The question mark indicates that early phosphorylation of MAP kinase has been seen, but whether or not this represents active MAP kinase is unknown. GVBD, germinal vesicle breakdown; M1, meiosis I; M2, meiosis II; NEBD, nuclear envelope breakdown (Abrieu et al. 2001).

In oocyte maturation various signals finally converge to activate MPF, which is a key complex formed of a catalytic subunit (Cdc2/Cdk1) and a regulatory subunit (Cyclin B). Once activated, MPF promotes the entry into M-phase of the first meiotic division. MPF activity falls during

anaphase I, due to partial degradation (Dupré et al. 2010). Intensive studies revealed that the function of MPF in promoting oocyte maturation is universal but the MPF activation mechanism is sort of species-dependent (Fig. 9) (Abrieu et al. 2001, Schmitt and Nebreda 2002). In *Xenopus* oocytes, there is a small stock of inactive dimer complexes named pre-MPF, which can be activated by dephosphorylation of Cdc2 on Tyr15 and Thr14 (Frank-Vaillant et al. 1999). The phosphatase responsible for this dephosphorylation is most probably Cdc25, which can be regulated by both phosphorylation and subcellular localization. Plx1 is a potential activator of Cdc25 (Qian et al. 2001), but is not clear how it is regulated during meiotic progression. The MAPK cascade is another key regulator of MPF. It has been confirmed that Mos is involved not only in the ERK cascade, but also in a mechanism that directly activates MPF and improves the stability of cyclin B which is supposed to be necessary for MPF activation (Dupré et al. 2010, Fan Heng-Yu and Sun 2004). It has also been demonstrated that ERK2 interacts with hypophosphorylated Cdc25 before meiotic induction and phosphorylates Cdc25 at T48, T138, and S205, thereby increasing Cdc25 phosphatase activity during meiotic induction (Wang Ruoning et al. 2007b). Furthermore, ERK leads to the activation of the kinase p90Rsk that in turn phosphorylates and inhibits the Cdc2 inhibitory kinase Myt1 (Ferrell 1999, Schmitt and Nebreda 2002).

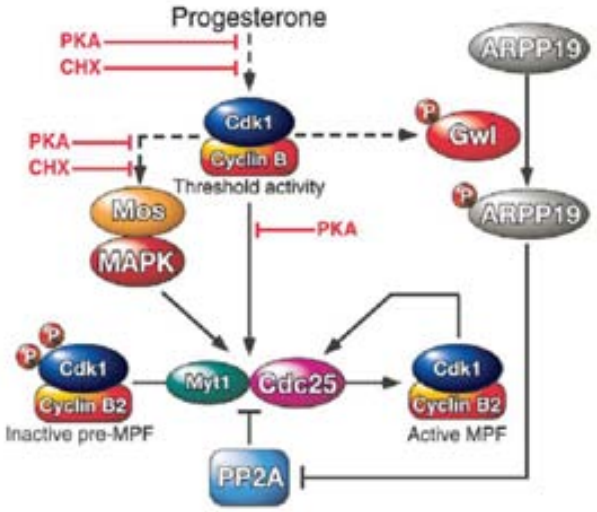

Figure 10. **Revisiting MPF activation.** MPF activation is initiated by the generation of a threshold level of active Cdk1 in response to progesterone. This step depends on the synthesis of Cyclin B and is negatively regulated by PKA. This starter amount of active Cdk1 phosphorylates its own regulatory enzymes, Cdc25 and Myt1, and induces the accumulation of Mos leading to the activation of the Mos/MAPK pathway. These reactions are under the control of PKA and are counteracted by PP2A. Therefore, the conversion of inactive pre-MPF into MPF cannot take place unless PP2A is inhibited. Gwl is activated by the threshold amount of Cdk1 activity. It phosphorylates ARPP19 at S67, leading to PP2A inhibition independently of PKA. The MPF auto-amplification loop then becomes independent of PKA activity and protein synthesis, irreversibly driving the cell into M-phase (Dupré et al. 2013).

Besides of regulation from other proteins, a MPF auto-amplification loop is also detected in *Xenopus* oocytes (Fig. 10). In this positive loop, a threshold level of cdc2 activity brings about Cdc25 activation and Myt1 inactivation, hence establishing a positive feedback loop. This positive feedback regulation is rendered via removing the inhibitory effect of PP2A by phosphorylated ARPP19 (Dupré et al. 2013) (Fig. 10). Cdc2 also phosphorylates the regulatory domain in the N-terminal of Cdc25 at a specific S/T-P motif, therefore increasing the phosphatase activity of Cdc25 (Izumi and Maller 1993, 1995). In addition, a polo-like kinase (PLK), located downstream of Cdc2, can also activate Cdc25 by phosphorylating the S/T-P motif. Therefore, PLK seems to be also involved in this positive feedback loop (Barr et al. 2004, Nakajima and Masukata 2002, Toyoshima-Morimoto et al. 2002).

3.3.5 ERK signaling pathway is one classic mediator in oocyte maturation

In the early 1980s, Mos was first identified in cells transformed by Moloney murine leukemia virus (v-mos) (Papkoff et al. 1982). Then its cellular homologue (c-mos) was isolated as a proto-oncogene. Mos is a Ser/Thr kinase and its expression is restricted to germ cells. In *Xenopus* oocytes, it accumulates during the meiotic divisions and undergoes selective proteolysis upon fertilization (Watanabe et al. 1989). There is an abundance of maternal stockpiled *mos* transcripts in arrested *Xenopus* stage VI oocytes. Mos protein appears 2 to 3 h after progesterone stimulation, before MPF activation (Sagata et al. 1989). The early translation of Mos is not sufficient to its accumulation because the ubiquitination at Lys34 induces its proteolysis. In *Xenopus* oocytes, MPF ensures Mos stability via phosphorylating the residue Ser3 in the N-terminal of Mos (Freeman et al. 1992). In 1993, it was discovered that Mos can activate ERK2 by directly phosphorylating and activating MEK1. The two amino acids phosphorylated by Mos in MEK are identical to those phosphorylated by Raf-1 (Pham et al. 1995, Posada et al. 1993). Inside the Mos/MEK/ERK cascade, the ERK2 can activate Mos in a positive feedback loop. Microinjection of activated MEK2 or ERK is sufficient to stimulate Mos accumulation implying that ERK2 could contribute to CPEB phosphorylation and activation (Gotoh et al. 1995, Howard et al. 1999, Keady et al. 2007). More recently it has been reported that ERK2 phosphorylates Cdc25 at T48, T138, and S205, thereby increasing Cdc25 phosphatase activity during meiotic induction (Wang et al. 2007).

The first found and best known physiological substrate of ERK in the oocyte is a 90-kDa protein kinase p90RSK (ribosome S6 kinase) (Jones et al. 1988). p90RSK seems to play important role in

meiotic maturation probably via inhibition of Myt1 (Palmer et al. 1998, Schmitt and Nebreda 2002). However, the Mos/MEK/ERK/p90RSK signaling pathway is dispensable for the regulation of microtubule assemble and spindle organization and even the activation of histone H3 kinase during oocyte maturation (Schmitt et al. 2002, Yu et al. 2007).

3.3.6 Involvement of JNK and p38 MAPK in meiotic resumption is not clear

Among the three MAPK families, ERK family proteins are mainly activated by mitogens and serum stimulation while the p38 and JNK families are mainly involved in response to environmental and genotoxic stresses (Ambrosino and Nebreda 2001). The role of ERK in meiotic initiation has been documented in detail, however, little is known about the function of p38 and JNK in oocyte maturation.

In fission yeast, when *spc1*, a homologue of p38 MAPK, was mutated, a G2 delay was observed, and then it was confirmed that spc1 is required for mitosis entry in fission yeast (Shieh et al. 1998, Shiozaki and Russell 1995). The function of p38 activation during G1/S transition seems to depend on the experimental systems. In *Xenopus* cell-free extracts, activated p38 induces arrest of M-phase (Takenaka et al. 1998). It has been proposed that the activation of p38γ isoform in mitosis can indirectly regulate the activity of the Chk2 kinase, which in turn phosphorylates Cdc25C (Wang Xiaofei et al. 2000).

In pig oocytes, p38 becomes active around the GVBD and maintains active until metaphase II. A specific p38 inhibitor SB203580 inhibits phosphorylation of p38 and block FSH induced pig meiotic resumption (Yamashita et al. 2009). In *Xenopus* oocyte, it has been reported that overexpression of a constitutively active MKK6, an upstream kinase of p38 proteins, accelerates progesterone-induced maturation. Furthermore, co-expression of active MKK6 with Xp38γ induces oocyte maturation in the absence of progesterone. The same authors also reported that expression of MKK6 and Xp38γ inactive mutants inhibit progesterone induced maturation (Perdiguero et al. 2003). However, it is not clear whether progesterone can activate MKK6. Moreover, co-expression of active MKK6 with Xp38γ induced the appearance of a white spot morphologycally different to the one obtained after progesterone treatment, and 50% of the mature oocytes presented abnormalities in location of the spindles (Perdiguero et al. 2003).

For JNK cascades, the meiotic regulation function seems more equivocal and less convincing evidences appear. An increase in JNK activity, measured as GST-Jun phosphorylation, has been

reported just prior to germinal vesicle breakdown (GVBD) (Bagowski et al. 2001a, Bagowski et al. 2001b). This JNK activity increased by activated Mos or MEK1 proteins (Bagowski et al. 2001b), but the JNK isoform/s responsible was/were not identified. In addition, a JNK isoform has been detected by phospho-JNK antibodies at GVBD during *Xenopus* oocyte maturation and remains phosphorylated throughout meiosis I and II (Adler et al. 2005, Du Pasquier et al. 2011, Mood et al. 2004). However, this JNK isoform has not been characterized in detail, as well as its role in meiotic maturation.

3.4 Osmotic shock stimulates *Xenopus* oocyte apoptosis

We have reported that hyperosmotic stress induces cytochrome c release and caspase-3 activation in *Xenopus laevis* oocytes (Martiáñez et al. 2009). In recent works, we observed at the very beginning of osmotic shock induced oocyte apoptosis a rapid Smac/DIABLO releases, calpain activation, and that stress associated MAPK proteins (JNK/p38) were phosphorylated around 15 min later in 300 mM sorbitol treatment. It was proved that all of these early events played some role in promoting cytochrome c and caspase-3 activation. Interestingly, caspase-3 activation in turn enhanced these events and thus positively regulated the apoptotic progression. We will review here the basic mechanisms that regulate cytochrome c release and caspase-3 activation through the Bcl-2 family members and the JNK signaling pathway.

3.4.1 Apoptosis, caspases, the extrinsic and the intrinsic apoptotic pathways

Multicellular organisms have evolved a self-demise mechanism to remove infected, damaged and unwanted cells which was referred as apoptosis (Kerr et al. 1972). Apoptotic signaling pathways have been widely studied and explosively progressed. The critical event in apoptosis is the activation of caspases, a group of cysteine protease that are the executioners of apoptosis, can cleave many cellular contents (Salvesen and Dixit 1997). Caspases comprise two distinct classes, the initiators (caspase-2, -8, -9 and -10) and the effectors (caspases-3,-6 and -7). Although general structural features are shared between the initiator and the effector caspases, their activation, inhibition and release of inhibition are differentially regulated (Riedl and Shi 2004).

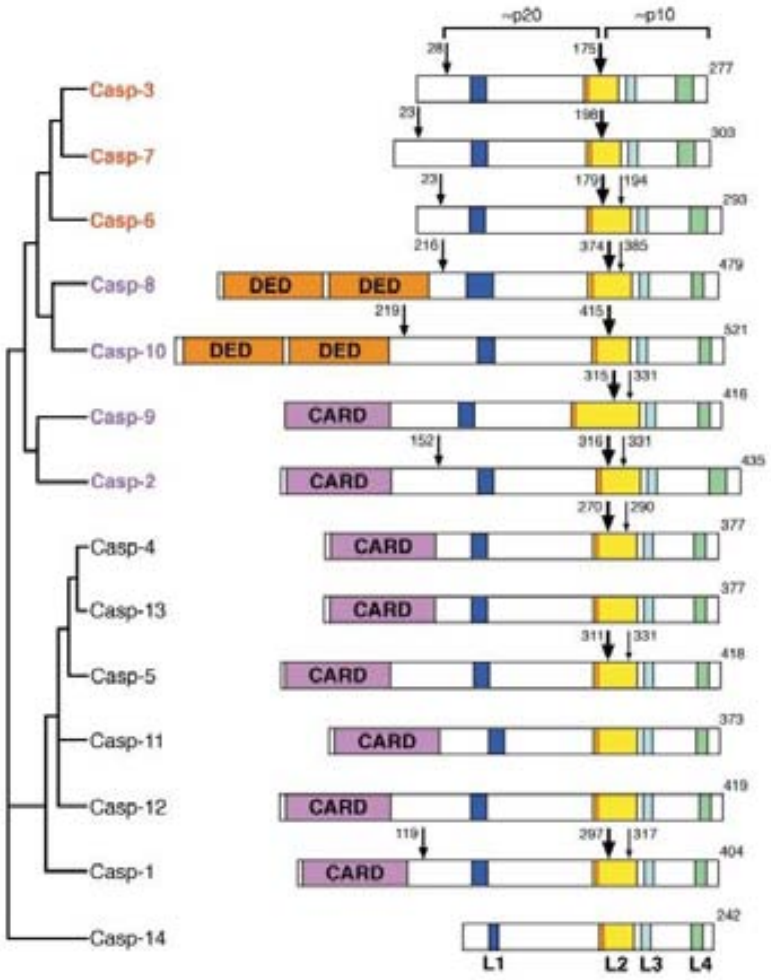

Figure 11. **Schematic diagram of the mammalian caspases.** Except caspase-11 (mouse), -12 (mouse), and -13 (bovine), all listed caspases are of human origin. Their phylogenetic relationship (left) appears to correlate with their function in apoptosis or inflammation. The initiator and effector caspases are labeled in purple and red, respectively. The position of the first activation cleavage (between the large and small subunits) is highlighted with a large arrow while additional sites of cleavage are represented by medium and small arrows. In contrast to other protease zymogens, removal of the prodomain of a caspase is unnecessary for its catalytic activity. The four surface loops (L1-L4) that shape the catalytic groove are indicated. The catalytic residue Cys is shown as a red line at the beginning of loop L2. This diagram is scaled according to the lengths of caspases and the location of functional segments (Shi 2002).

In mammalian cells, the apoptotic response is mediated through either the intrinsic pathway or the extrinsic pathway (Elmore 2007). The extrinsic pathway (caspase-8 and -10) that is responsible for elimination of unwanted cells is initiated by the binding of an extracellular death ligand to its cellular surface death receptor (such as FasL binding to Fas). The ligand-receptor complex would recruits further cytosolic factors, such as FADD and caspase-8, forming an oligomeric death-

inducing signaling complex (DISC) (Peter and Krammer 2003), thus leads to activation of the caspase-8 which leaves and activates caspase-3. The intrinsic pathway (caspases-9 and -2) that is used to eliminate cells in response to apoptotic stimuli is mediated by mitochondria. Several proteins are released from the intermembrane space of mitochondria into the cytoplasm (Wang Xiaodong 2001). Some of the well-studied proteins include cytochrome c and Smac/DIABLO and AIF. The most intriguing one of these proteins is cytochrome c. The mechanisms how cytochrome c activates caspase-9 and caspase-3 would be described in detail in next section.

These two apoptotic signaling pathways, which would finally converge on the activation of the effector caspase-3, are differentially utilized by specific apoptotic stimuli. Although these two pathways are distinct, signaling interactions between the two pathways have been detected. In certain cell types, the extrinsic pathway, initiated by cell surface receptors, such as Fas, can cross talk with the intrinsic pathway through caspase-8 mediated cleavage of Bid, truncated tBid will translocate to mitochondria and trigger Cyt C release (Li Honglin et al. 1998, Luo et al. 1998)

3.4.2 Mitochondria and mitochondrial proteins release

Mitochondria are essential organelles because they are not only the energy center in supplying ATP but also master control room in processing the cellular death program of apoptosis. In the so-called intrinsic pathway of apoptosis, signals activated by stressor receptors finally converge on regulating mitochondrial outer membrane permeabilization (MOMP), enabling protein release from the mitochondrial inter-membrane space. The release of soluble proteins is a key event in initiating caspase activation in the cytosol (Kroemer et al. 2007, Vaux 2011). One key protein released from mitochondria is cytochrome c (Cyt c). Cyt c was first identified as an essential component of the mitochondrial electron transport chain. It was then identified as one of three apoptotic protease activating factors (Apafs) for caspase activation (Jiang Xuejun and Wang 2000). The role of Cyt c in apoptosis was systematically established both biochemically and genetically. First, purified Cyt c can trigger caspase activation in a cell free system using extracts from healthy cells (Liu et al. 1996). Second, apoptosome activity can be obtained in vitro by reconstituting Cyt c, Apaf-1, and caspase-9 in the presence of ATP/dATP (Li Peng et al. 1997). Apaf-1 is another indispensable component of the apoptosome besides Cyt c. Crystal structure analysis shows that the inactive Apaf-1 protein may exist in a compact close form, probably through intramolecular interaction between the N-terminal CARD domain and the C-terminal WD40 repeats. The compact Apaf-1 is not accessible to procaspase-9. Deletion of the WD40 repeats results in Apaf-1 constitutively binding and activating caspase-9, indicating that the inactive Apaf-1 is in an auto-inhibited state (Bao et al. 2005, Hu et al.

1998). Upon Cyt c binding to the WD40 region, Apaf-1 interaction is loosened. Then, ATP/dATP bound to the nucleotide-binding domain induces Apaf-1 conformational change (Kim Hyun-Eui et al. 2005). The Apaf-1 at this state can co-assemble with six other subunits to form a symmetric wheel-shaped structure, a platform ready to recruit procaspase-9 to form the active apoptosome (Shi 2008).

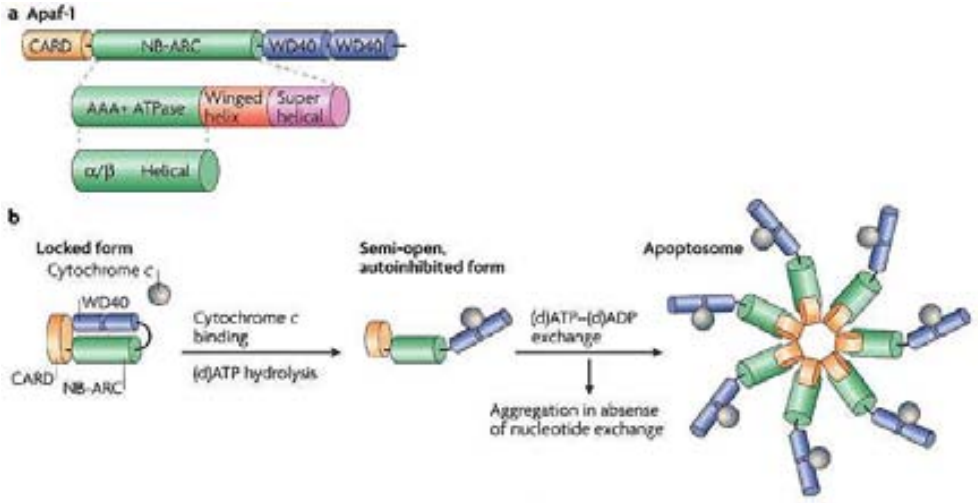

Figure 12. **Apaf-1 and cytochrome c induced caspase-3 activation.** a. Apaf-1 can be divided into three functional units: the N-terminal caspase-recruitment domain (CARD), which is responsible for recruiting caspase-9; a nucleotide-binding and oligomerization domain (NB-ARC), which is responsible for (d)ATP-dependent oligomerization, and the WD40 region, which is responsible for binding of cytochrome c. The NB-ARC consists of an ATPase region. This region is followed by a winged-helix and a superhelical domain. b. Apoptosome formation. In the absence of an apoptotic signal, Apaf-1 exists in a locked autoinhibited form. Following an apoptotic signal, the binding of cytochrome c to the WD40 region of Apaf-1 releases the lock leading to a semi-open, still autoinhibited, form of Apaf-1. This rearrangement is concurrent with the hydrolysis of the bound nucleotide to (d)ADP (Riedl and Salvesen 2007).

Smac is another important protein released from mitochondria in apoptosis. Smac was identified by its ability to enhance Cyt C mediated caspase-3 activation (Du et al. 2000). Vaux´s lab isolated the same protein with the name DIABLO via Co-IP with XIAP (X-linked inhibitor of apoptosis protein) (Verhagen et al. 2000). Smac/DIABLO facilitates caspase activation by neutralizing caspase protein inhibitors (IAPs), such as XIAP (Srinivasula et al. 2000). Smac/DIABLO competes with mature capase-9 and caspase-3 for interaction with XIAP thereby enhancing the release of mature caspase-9 and -3 from the inhibitor (Srinivasula et al. 2001). In addition, released Smac/DIABLO can disrupt the TRAF2-cIAP1 complex to trigger Cyt c independent cell death (Wang Chunxin and Youle 2009). XIAP can polyubiquitinate both mature caspase-9 and Smac/DIABLO besides of its block binding to Smac/DIABLO (Morizane et al. 2005).

Smac/DIABLO and Cyt C reside in the same narrow space in the mitochondria. However, some stimuli seems to induce a differential release of both proteins. It has been reported that TNFα-induced apoptosis generates jBid, a cleaved Bid induced by JNK activation, which translocates to mitochondria to trigger Smac/DIABLO but not Cyt c release (Deng Yibin et al. 2003). Consistently, overexpression of Bidᐃ25, a mimic of jBid, only induces Smac/DIABLO release. Cephalostatin, a bis-steroidal marine natural product, induces selective release of Smac/DIABLO and subsequent apoptosis (Dirsch et al. 2003). It has also been reported that inhibition of mitochondrial fission in apoptosis prevents Cyt c release more than Smac/DIABLO release (Parone et al. 2006). The mechanism involved in this differential release is not clear, but a pool of cytochrome c is thighly bound to (Cortese et al. 1998) and oxidative modification of cardiolipin, as a consequence of ROS production, might be important for mobilization of cytochrome c (Ott et al. 2002).

3.4.3 Bcl-2 family members are key components in regulating mitochondrial out membrane permeability

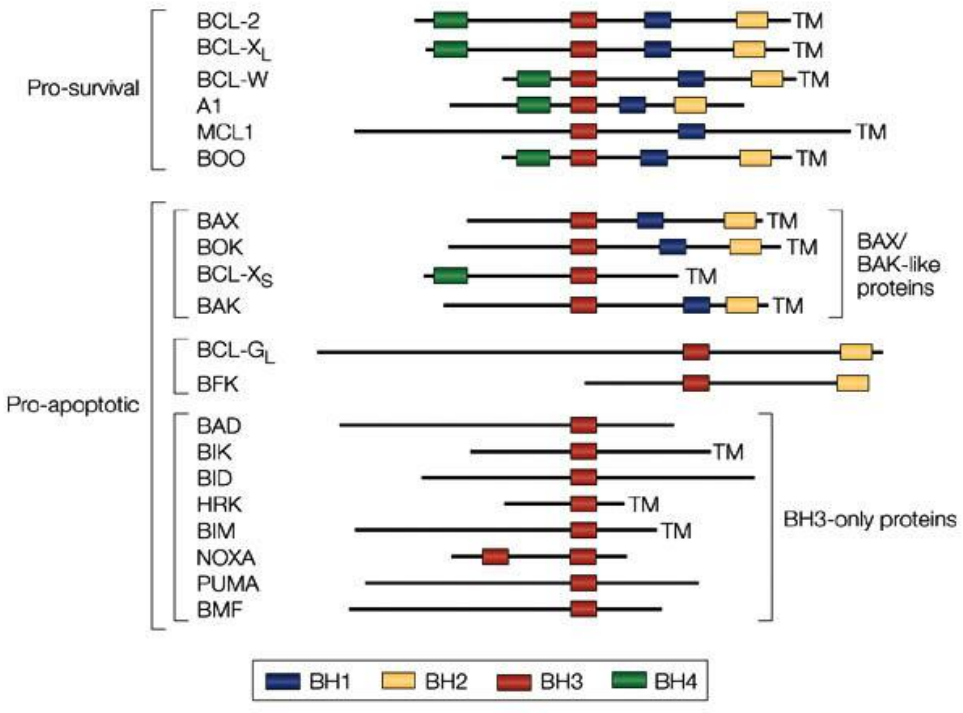

Figure 13. **Diagrammatic representation of the mammalian B-cell lymphoma 2 (BCL-2) family** (Strasser 2005).

Original information about Bcl-2 family proteins came from *C. elegans*, in which four genes Egl-1, Ced-3, Ced-4 and Ced-9 involved in phenotype change were classified (Muzio et al. 1996). Shortly

after, 13 Ced-9 homologues (known as multi-region Bcl-2 proteins) and a number of highly divergent proteins analogous to Egl-1 (known as BH3-only proteins) were identified in mammalian cells. The common feature of Bcl-2 members is that they contain one or more Bcl-2 homology (BH) domain. Within the Bcl-2 family, the evolutionary relationship between multi-region Bcl-2 family members and BH3-only proteins (other than Bid) is distant. Phylogenetic analysis indicates that the multi-region proteins Bcl-2, Bcl-xl, Bax and Bid share a common origin, and other BH3-only proteins evolved later (Billen et al. 2008). Generally, Bcl-2 family proteins are subdivided into three groups based on their pro- or anti- apoptotic action and the Bcl-2 homology (BH) domains they possess (Fig. 13). The interactions between the three groups determine MOMP and apoptosis (Chipuk et al. 2010).

Anti-apoptotic Bcl-2-like proteins (e.g., Bcl-2, Bcl-x_L, Bcl-w, and Mcl-1) and proapoptotic Bax-like proteins (e.g., Bax, Bak, and Bok) consist of four BH domains (Kvansakul et al. 2008). On the other hand, the proapoptotic BH3-only proteins (e.g., Bid, Bim, Bad, Bmf, Bik, Blk, Noxa, Puma) possess only a short motif called the BH3 domain. The anti-apoptotic Bcl-2 proteins are generally located in OMM, but may also be in the cytosol or ER membrane. The Bcl-2-like proteins possess various membrane insertion domains and have been reported to interact with different lipids when targeted to membranes (Petros et al. 2004). The proapoptotic Bcl-2 members consist of the BH3-only proteins and a number of multi-BH3 domain proteins (effectors). BH3-only proteins that only bind to the anti-apoptotic repertoire are referred to as ‘‘sensitizer’’ or ‘‘derepressor’’, whereas the ones interacting with both the anti-apoptotic proteins and the effectors are classified as activators, such as Bid (Bcl-2-interacting domain death agonist), Bim (Bcl-2-interacting mediator of cell death), Bad (Bc-2 antagonist of cell death) and Noxa (Martinou and Youle 2011). Bid and Bim can interac with the anti-apoptotic repertoire, as well as with the effectors directly inducing Bak and Bax oligomerization and MOMP. Therefore, they are referred as ‘‘direct activators’’ (Giam et al. 2008, Shamas-Din et al. 2011).

Bid, first cloned in 1996 as a novel death agonist that heterodimerises with either BAX or Bcl-2, is a member of the BH3-only proteins that plays a crucial role in regulating the permeability of the OMM. Bid contains eight α-helices, the BH3 region located in helix 3 comprises a region of sequence homology to other Bcl-2 proteins which is required for interaction with both pro-apoptotic Bax and anti-apoptotic protein Bcl-x_L (Wang Kun et al. 1996) (Fig. 14a). Bid also contains a large unstructured loop (amino acids 42–79) that separates helices 2 and 3. This loop contains a variety of sites that are subjected to post-translation modifications, regulating Bid localization and apoptotic function (Kvansakul et al. 2008) (Fig. 14a). In 1998, Bid was identified as a caspase-8 substrate. The resulted tBid translocates to mitochondria and initiates mitochondrial protein release. The

cleavage site of caspase-8 in human Bid is Asp60 (Li Honglin et al. 1998) and in *X. laevis* is Asp52 (Saitoh et al. 2009). Removal of the N-terminal fragment has been suggested to increase the number of exposed hydrophobic residues thereby facilitating its binding to membranes (McDonnell et al. 1999). It was shown that cardiolipin, a negatively charged lipid specific to mitochondria, mediates the specific targeting of tBid to MOM (Lutter et al. 2000) and that the membrane protein MTCH2/MIMP was also a major facilitator of tBid insertion into the MOM (Zaltsman et al. 2010). MTCH2/MIMP may enhance tBid function by facilitating interactions with cardiolipin rich regions (Shamas-Din et al. 2011). In addition, caspase-3 can also cleave human Bid at Asp60 (Slee et al. 2000). Similar cleavage sites for non-caspase proteases were also detected in human Bid, such as Gly70 for calpain, Arg71 for cathepsins and Asp75 for granzyme B. Studies shown that granzyme B treatment of cells resulted in cleavage of Bid, accumulation of tBid at mitochondria and release of cytochrome c that was not inhibited by caspase inhibitors, similar effects were observed for protease calpain. Tissue extracts from normal mice treated with lysosomal extracts released cytochrome c, however similar treatment in tissue extracts from Bid-/- mice failed to release cytochrome c, indicating that Bid may also be cleaved by cathepsins (Cirman et al. 2004, Reiners Jr et al. 2002, Sutton et al. 2003, Sutton et al. 2000). Finally, human Bid cleavage at Leu25 by an unknown protease is described in a JNK dependent manner to generate a large C-terminal fragment (jBid) that could accumulate at mitochondria like tBid (Deng Hongbin et al. 2008).

In summary, when Bid was cleaved by proteases, the C-terminal product accumulates at mitochondria. This implicates the N-terminus of Bid as a negative regulatory sequence that prevents the mitochondrial localization of Bid, thereby preventing apoptosis. After cleavage by caspase-8, the N-terminus of Bid (nBid) remains attached to tBid, possibly masking the BH3 domain. However, it was shown that only tBid inserts while nBid remains in solution (Lovell et al. 2008).The inhibitory role of the N-terminal fragment was elegantly demonstrated by Tan and colleagues. They concluded that the N-terminal fragment negatively regulates the exposure of the BH3-domain and thereby its binding to the OMM (Mandic et al. 2002).

Bid cleavage mediated by caspase-8 can be attenuated when residues in the vicinity of the cleavage site are phosphorylated. In human Bid phosphorylation of Thr59 (Bid is cleaved after Asp60) severely inhibited Bid cleavage by caspase-8 (Degli Esposti et al. 2003). Similarly, phosphorylation of murine Bid (at Ser61 and Ser64) also attenuated its cleavage by caspase-8 (Desagher et al. 2001). *Xenopus* Bid is mono- and bi- ubiquitinated in egg extracts, and not degraded by the proteasome (Saithoh et al. 2009). There are at least three sites important for ubiquitination (K18, K21, K37), located close to the cleavage site Asp52. However, it is not clear the role of mono- and bi-uiquitinated Bid in apoptosis (Saitoh et al. 2009).

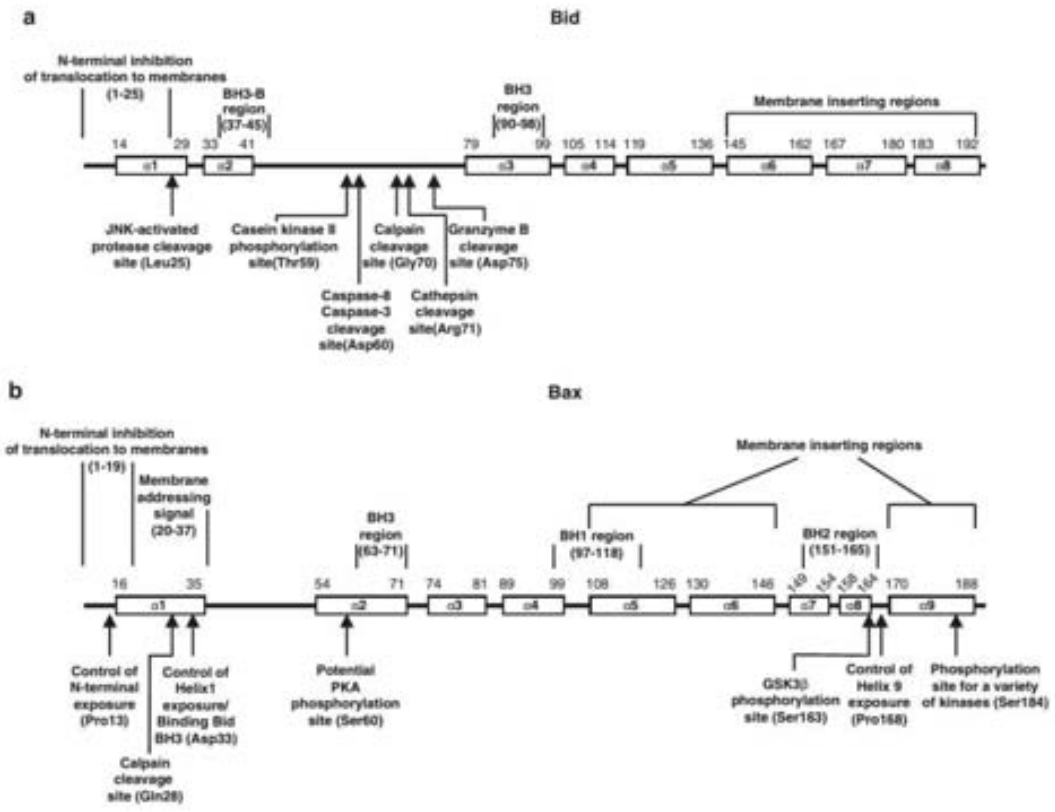

Figure 14. **Regions and residues of Bid and Bax that regulate binding to membranes and apoptotic function.** The human Bid protein (a) and the human Bax protein (b) are depicted. Bid contains 195 amino acids and 8α-helices whereas Bax contains 192 amino acids and 9α-helices. The numbers above each α-helix indicate the starting and ending amino acids for that helix. The regions of Bid and Bax that control recruitment of the proteins to membranes and function, including the BH regions and domains believed to insert into membranes, are indicated above the proteins. Where appropriate, parentheses indicate the amino acids that correspond to a particular region. Individual amino acids that regulate binding to membranes or are subjected to posttranslational modifications that regulate binding to membranes are indicated below the proteins, with parentheses indicating the identity and number of each amino acid (Billen et al. 2008).

The effector proteins, Bcl-2 antagonist killer 1 (Bak) and Bcl-2-associated x protein (Bax) were originally described to contain only BH1-3 motifs; however, structure-based alignment of global Bcl-2 family proteins revealed a conserved BH4 motif (Kvansakul et al. 2008). Upon activation, Bak and Bax homo-oligomerize into proteolipid pores within the OMM to promote MOMP. It was reported that the Bak/Bax complex seems to be indispensable in regulating MOMP. The proapoptotic function of Bax/Bak was proved by the extreme resistance of *bax−/− bak−/−* DKO cells to a variety of apoptotic stimuli, and Cyt C release from the mitochondria was not detected (Wei et al. 2001).

Bak is constitutively inserted in the outer mitochondiral membrane (OMM) by a C-terminal transmembrane domain. In contrast, Bax is mainly cytosolic with a minor fraction loosely attached to mitochondria. It has been observed that Bax constantly travels back and forth from the cytoplasm to mitochondria (Edlich et al. 2011). Several reports suggested that the mitochondrial sub-population of Bax could be treated as a measure of the stress experienced by the cells. Once attached to mitochondria, Bax can be retrotranslocated to the cytosol by Bcl-x_L or other prosurvival Bcl-2 proteins which would ensure that Bax does not chronically accumulate at the OMM to reach a critical level that could promote Cyt c release (Martinou and Youle 2011). Unlike Bid, Bax does not require a cleavage-activation to enable its pro-apoptotic function. However, the binding of Bax to mitochondria-bound tBid can drive the translocation of Bax from cytoplasm to the mitochondrial outer membrane. Early tudies suggested that the recruitment of Bax might be regulated by a proposed C-terminal TM region, TM sequence release not only potentiates its insert into membranes, but also opens the hydrophobic binding pocket where it resides. Then studies indicate that N-terminal conformational changes in Bax is required for its insert into the mitochondria membrane, the N-terminus of Bax contains regions that both positively and negatively regulate the targeting of Bax to membranes. The conformational changes at both the N- and C- terminal of Bas may due to phosphorylation occurring in these regions (Billen et al. 2008).

BH3-only proteins and antiapoptotic Bcl-2 proteins are positive and negative regulators of Bax/Bak complex respectively. The protein tBid has been originally described as a direct activator of Bax, inducing a conformational change of the Bax N-terminus, to modulate Bax insertion and oligomerization in the OMM (Eskes et al. 2000). Many groups have confirmed the contribution of other BH3-only proteins, Bim and Puma, to this process. However, the mechanism how BH3 only proteins induce apoptosis is not clear (Lovell et al. 2008). Three different models have been proposed to explain the regulation of apoptosis by Bcl2 family members (Fig. 15).

In a “membrane-embedded together” model proposed by Andrews and colleagues, it was described that tBid first inserts in the membrane, then recruits Bax and other antiapoptotic proteins, including Bcl-xl and Bcl-w. It seems both anti- and pro- apoptotic proteins are activated by recruiting sensitizer BH3-only proteins (Shamas-Din et al. 2011). This conferred an ambiguous role on the BH3-only proteins. The tBid, is capable of inducing MOMP in cells. Similar evidence exists for Bim-meidated Bak/Bax activation, and for PUMA promoting Bak/Bax activation. Bid and Bim BH3 peptides induce Bak and Bax oligomerization and pore-forming activity with isolated mitochondria or large unilamellar vesicles (Chipuk and Green 2008, Kuwana et al. 2005, Letai et al. 2002)

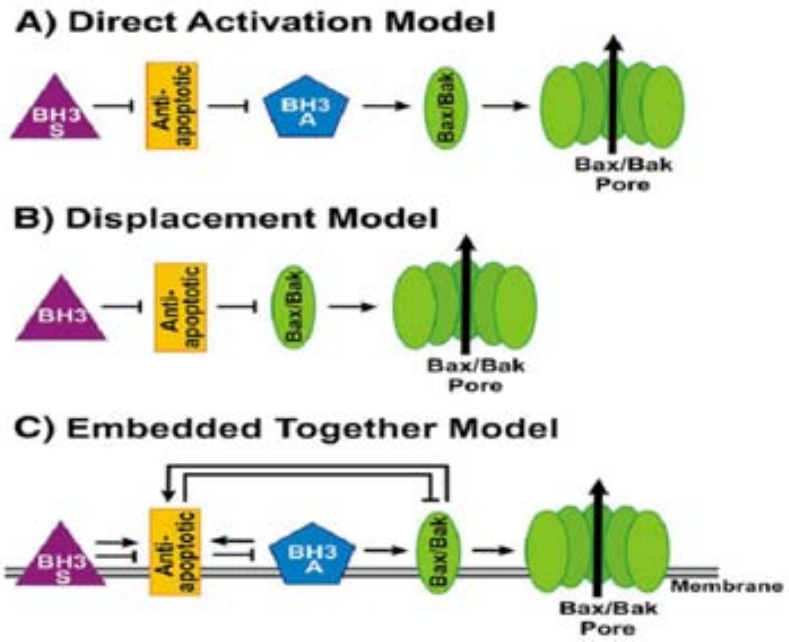

Figure 15. **Overview of the three models of regulation of apoptosis by Bcl-2 family proteins.** BH3-S and BH3-A represent sensitizer and activator BH3-only proteins, respectively. A) The Direct activation model proposes that activator BH3-only proteins are required for activating Bax and Bak. Anti-apoptotic proteins inhibit the activator BH3-only proteins but not Bax and Bak to suppress apoptosis. Sensitizer BH3-only proteins displace the activator BH3-only proteins from the anti-apoptotic proteins to promote apoptosis. B) The Displacement model postulates that Bax and Bak are constitutively active in cells and must be sequestered by anti-apoptotic proteins for cell survival. BH3-only proteins only play the sensitizer role and inhibit their respective anti-apoptotic proteins to promote apoptosis. Both the direct activation and the displacement model do not define a role for the membrane. C) Embedded together model highlights the active role of the membrane where Bcl-2 family proteins insert into and change their conformations that dictate their functions. Cytoplasmic anti-apoptotic proteins are recruited to membranes and are activated by both sensitizer and activator BH3-only proteins as well as Bax/Bak. At the membrane, anti-apoptotic proteins inhibit the activator BH3-only proteins and Bax/Bak to prevent MOMP. Sensitizer BH3-only proteins displace the activator BH3-only proteins and Bax/Bak from the anti-apoptotic proteins to promote apoptosis. Activator BH3-only proteins recruit Bax to the membrane to induce MOMP and apoptosis. These interactions are reversible and are governed by equilibrium constants that are altered by the concentrations and interactions of the proteins with each other and with membranes (Shamas-Din et al. 2011).

3.4.4 JNK activation are implicated in both intrinsic and extrinsic apoptotic signaling pathways

.It has been reported that JNK1 is involved in ultraviolet C and γ-radiation-induced apoptosis (Chen Yi-Rong et al. 1996). In 2000, evidence came up from the studies of embryonic fibroblasts derived from *JNK1-/- & JNK2-/-* mice. These MEF cells displayed remarkable resistance to UV induced

apoptosis (Tournier et al. 2000). The function of JNK3 in apoptosis was also explored through *JNK3-/-* mice, in the mutant mice the phosphorylation of c-Jun and the transcriptional activity of the AP-1 transcription factor complex were markedly reduced, and the reduction in seizure activity and hippocampal neuron apoptosis was prevented. (Yang Derek D et al. 1997). Furthermore, it has been reported that activated JNK is involved in both transcription-dependent and transcription-independent apoptotic mechanisms, which could cooperate through activation of specific transcription factors and directly modifying apoptosis associated proteins (Davis R. J. 2000a, Dhanasekaran Danny N and Reddy 2008) (Fig. 16).

Phosphorylated c-Jun by JNK translocates to nucleus and regulates a vast of transcription factors which result in regulation of a wide range of proteins including increased expression of pro-apoptotic proteins and decreased expression of anti-apoptotic proteins (Dhanasekaran Danny N and Reddy 2008, Raman et al. 2007). In addition, JNKs play an essential role in regulating the pro- and/or anti- apoptotic proteins residing in the mitochondria (Schroeter et al. 2003). It has been shown that the activation of JNK is indispensable for cytochrome C release, because *JNK1-/- & JNK2-/-* MEFs fail to show cytochrome C release in front of various apoptotic stimuli (Tournier et al. 2000). Similarly, redistribution and conformational changes of Bax/Bak cannot be observed in JNK-deficient cells (Lei et al. 2002). Some researches show that Bid cleavage induced by JNK activation may play an essential role in this process (Madesh et al. 2002). For instance, in TNF-α induced apoptosis of Hela cells, JNK activation has been proven to induce caspase-8 independent cleavage of Bid to get a 21kDa fragment (jBid) which translocates to mitochondria and selectively promotes Smac/DABLO release (Deng Yibin et al. 2003). It has been reported that other pro-apoptotic BH3-only family proteins were also modulated by JNK signaling, such as Bim and Bmf (Lei and Davis 2003). During UV-induced apoptosis of HEK293K cells, Bim and Bmf are released from their sequestering proteins because of their phosphorylation by JNK. The released Bim and Bmf subsequently activate Bax and/or Bak (Lei et al. 2002, Makani et al. 2002, Putcha et al. 2003). In another way, phosphorylated Bim can neutralize the activity of anti-apoptotic proteins, such as Bcl2 and Bcl-x_L, thereby releasing Bcl-x_L and/or Bak from inhibition (Puthalakath and Strasser 2002). Another BH3-only pro-apoptotic member regulated by JNK is Bad. Generally, the pro-survival kinases, such as Akt-1, PAK-1 and PKA, inhibit the activity of Bad by phosphorylation at Ser136 or/and Ser112, and phosphorylated Bad is sequestered by 14-3-3 family proteins (Gross et al. 1999). In contrast, JNK specifically phosphorylates Bad at Ser128 thereby sequestering its interaction with 14-3-3 family proteins (Wang Xiao-Tian et al. 2007c). Furthermore, JNK seems to release sequestered Bad from 14-3-3 protein by phosphorylating 14-3-3 protein at Ser184 (Sunayama et al. 2005, Tsuruta et al. 2004).

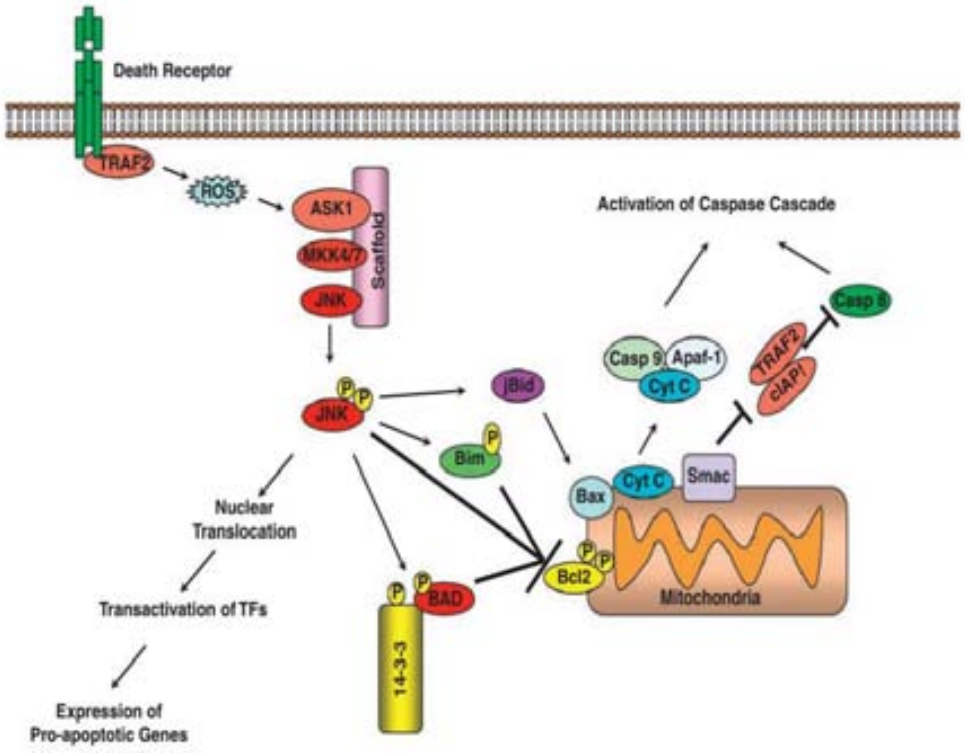

Figure 16. **Nucleus- and mitochondria- targeted signaling by JNK.** JNK can promote apoptosis by two distinct mechanisms. In the first mechanism targeted at the nuclear events, activated JNK translocates to the nucleus and transactivates c-Jun and other target transcription factors (TF). JNK can promote apoptosis by increasing the expression of pro-apoptotic genes through the transactivation of c-Jun/AP1-dependent or p53/73 protein-dependent mechanisms. In pathways directed at mitochondrial apoptotic proteins, activated JNK translocates to mitochondria. There, JNK can phosphorylate the BH3-only family of Bcl-2 proteins to antagonize the anti-apoptotic activity of Bcl-2 or Bcl-X_L. In addition, JNK can stimulate the release of cytochrome c (Cyt C) from the mitochondrial inner membrane through a Bid-Bax-dependent mechanism, promoting the formation of apoptosomes consisting of cytochrome c, caspase-9 (Casp 9) and Apaf-1. This complex initiates the activation of caspase-9-dependent caspase cascade. In another mechanism, JNK can promote the release of Smac/DIABLO (Smac) that can inhibit the TRAF2/IAP1 inhibitory complex, thereby relieving the inhibition on caspase-8 to initiate caspase activation. In addition, by phosphorylating Bad and its sequestering partner 14-3-3, JNK can promote Bad-mediated neutralization of the Bcl-2 family of anti-apoptotic proteins. Finally, JNK can phosphorylate Bcl2 for suppressing its anti-apoptotic activity. These nuclear and mitochondrial events regulated by JNK need not be mutually exclusive (Dhanasekaran Danny N and Reddy 2008).

It has been reported that Bax is also a JNK substrate. The JNK-mediated Bax phosphorylation may cause Bax activation (Kim Bong-Jo et al. 2006), and Bax has also been reported to be sequestered by 14-3-3 proteins, like Bad, via interaction with the C-terminal region of 14-3-3 protein (Weston and Davis 2007). Additionally, JNK may regulate the anti-apoptotic Bcl-2 family members. It has been shown that JNK can phosphorylates Bcl-2, Bcl-x_L and Mcl-1 thereby suppressing their anti-apoptotic functions (Dhanasekaran Danny N and Reddy 2008, Srivastava et al. 1999, Yamamoto et

al. 1999). Interestingly, besides the MOMP regulation function via modifying Bcl-2 family members, another anti-apoptotic function has been reported for JNK1-1 that JNK interacts with Apaf1 and cytochrome c to inhibit the apoptosome complex (Tran et al. 2007).

4. OBJECTIVES

The general objectives of this project are to investigate the role of MAPK proteins in meiotic maturation and the role of JNK1-2 proteolysis and Bcl-2 family members in the regulation of osmostress-induced apoptosis in *Xenopus* oocytes. The specific aims of the research project are:

- To address whether JNK proteins are key factors for oocyte maturation.
- To identify which protein/JNK isoform is phosphorylated and detected by the pJNK antibody in mature oocytes and the upstream kinase responsible for its phosphorylation.
- To identify the cleavage site and the protease responsible for JNK1-2 proteolysis induced by osmostress and to understand the biological role of JNK1-2 proteolysis during osmostress-induced apoptosis.
- To investigate the function of Bcl-2 family members on hyperosmotic shock-induced apoptosis.
- To analyze the posttranslational modifications of Bid induced by hyperosmotic shock and their effect to Bid function.

5. MATERIALS AND METHODS

5.1 Plasmid constructs and *in vitro* transcription

5.1.1 RT-PCR

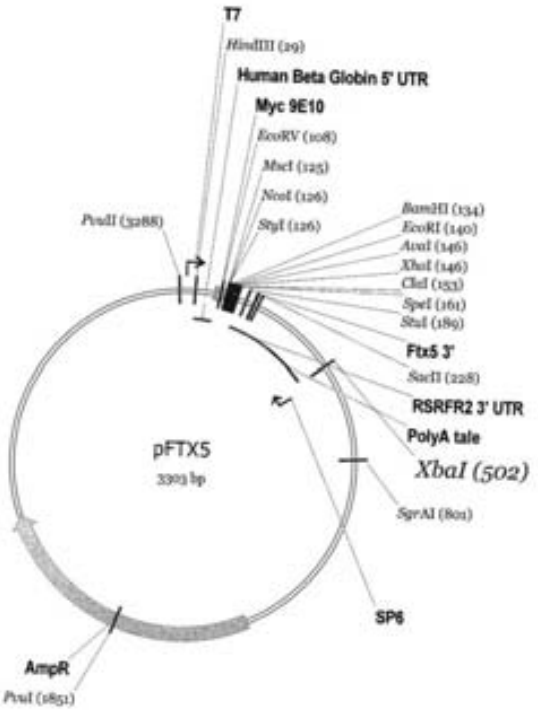

Figure 17. **Map of the cloning and expression vector pFTX5.** pFTX4 is same to pFTX5, except for not including Myc sequence.

Total RNA was isolated from stage VI oocytes with the method described by McGrew (McGrew et al. 1989), and kept at -70ºC. First-strand cDNA was synthesized with reverse transcriptase (Fermentas) in a 20 µL reaction using 250 ng of total RNA and poly (dT) primer. Reaction mixture was incubated for 1 h at 42ºC and subsequently for 10 min at 70 ºC to terminate the reaction, chilled on ice and stored at -20ºC.

In order to clone complete coding sequences of selected genes, 2 µL of RT reaction mixture was used in a 50 µL PCR reaction with specific primers which were synthesized in Sigma-Aldrich Corporation with specific restriction enzyme sites inserted before the start codon or after the stop codon, corresponding to the multiple cloning sites of FTX5 (with a Myc tag sequence in the 5´end) or/and FTX4 (without Myc tag), the plasmids used for cloning (Fig. 17). The PCR reaction pools were assembled as follow:

- 5 µl Pwo Super Yield PCR Buffer with Mg2+
- 2 µl RT product
- 1 µl dNTPs Mix (10 mM)

- 1.25 µl sense primer (20 µM) *
- 1.25 µl antisense primer (20 µM) *
- 39 µl H_2O
- 0.5 µl Pwo Super Yield DNA polymerase (5U/µl)

* For specific primers, see Table 1.

PCR reaction was performed as follow:

- 95ºC, 5 min
- 95ºC, 45 sec
- 60ºC, 45 sec
- 72ºC, 3 min

} 30x

- 72ºC, 10 min
- 4ºC, hold.

Table 1. Primers for RT-PCR and site-directed mutagenesis

OBJECTIVE	ORIENTATION	SEQUENCE (5´-3´)	RESTRICTION ENZYME
H. sapiens JNK2-1	S	GCCCCATGGCAGACAGTAAATGACAGT	Nco I
	AS	GCCCTCGAGTTACTGCTGCATCTGTGCTGAAGG	Xho I
X. laevis JNK1-1	S	GCCCCGGCACGAAGCAAGCGTGACAGC	Nco I
	AS	GCCCTCGAGTTACTGCTGCACCTGTGCTAAAGG	Xho I
X. laevis JNK1-2	S	GCCCCATGGCAAGAAGCAAGCGTGACAACAATTTT	Nco I
	AS	GCCCTCGAGTCATCATCGACAGCAACCCAG	Xho I
X. laevis JNK1-2Δ412	S	GCCCCATGGCAAGAAGCAAGCGTGACAACAATTTT	Nco I
	AS	GCCCTCGAGTTAGTCTGTGTCTGAG	Xho I
X. laevis JNK1-2 (D412A)	S	TGCCCTCAGACACAGCCAGCAGCCTTGAAAC	
	AS	GTTTCAAGGCTGCTGGCTGTGTCTGAGGGCA	
X. laevis JNK1-2Δ385	S	GCCCCATGGCAAGAAGCAAGCGTGACAACAATTTT	Nco I
	AS	GCCCTCGAGTTAATCAGTTACTGCTGCAC	Xho I
X. laevis JNK1-2 (D385A)	S	GTGCAGCAGTAACTGCTGGTTCCCAGGCTCA	
	AS	TGAGCCTGGGAACCAGCAGTTACTGCTGCAC	
JNK3 sequencing	S	GTGAATTGTTGCAGTGCAGGC	
	AS	GGGTTTCGCAGGCAGGCGGC	
X. laevis JNK3-1	S	GCCCCATGGCCCGTCATTTCTTGTATAACTGCAG	Nco I
	AS	GCCCTCGAGTCACTGCTGCACCTGTG	Xho I
X. laevis JNK3-2	S	GCCCCATGGCCCGTCATTTCTTGTATAACTGCAG	Nco I
	AS	GCCCTCGAGTCACCTGCAACAACCGA	Xho I
X. laevis	S	GCCCCATGGCCAAAAGCAAAGTTGACAACCAG	Nco I

JNK3-3	AS	GCCCTCGAGTCACCTGCAACAACCGA	Xho I
X. laevis JNK3-4	S	GCCCCATGGCCAAAAGCAAAGTTGACAACCAG	Nco I
	AS	GCCCTCGAGTCACTGCTGCACCTGTG	Xho I
X. laevis MKK7	S	GCCCCATGGCGGCGTCCTCCCTGGAGCAGAAACTCT	Nco I
	AS	GCCCTCGAGCTACCTGCCGAAAAATGGCAGGTTTTG	Xho I
X. laevis MKK7-DED	S	GGGCGCCTTGTGGACGACAAGGCAAAGGAGAGGGATGCAG GCTGTGCTGC	
	AS	GCAGCACAGCCTGCATCCCTCTCCTTTGCCTTGTCGTCCACA AGGCGCCC	
X. laevis MKK7 (K146M)	S	GGACACGTCATCGCAGTTATGCAAATGCGTCG	
	AS	CGACGCATTTGCATAACTGCGATGACGTGTCC	
X. laevis MKK7-3A	S	GGCGCCTTGTGGACGCCAAGGCAAAGGCGATTTCTGCAGGC TGTGCTGC	
	AS	GCAGCACAGCCTGCAGCCCTCGCCTTTGCCTTGGCGTCCACA AGGCGCC	
X. laevis caspase-10	S	GCCCCATGGATTTCAATTCCATGCTTCTCCGT	Nco I
	AS	GCCCTCGAGTTATGGACTGTTTTCTTGACAAG	Xho I
X. laevis caspase-10 (C385S)	S	GTTTTTTATACAAGCGAGCCAAGGGAGATATACAC	
	AS	GTGTATATCTCCCTTGGCTCGCTTGTATAAAAAAC	
X. laevis ERK2a	S	GCCGGATCCATGGCAGCGGCAGGAGCTG	Bam HI
	AS	GCCCTCGAGTCAGTACCCTGGCTGGAATCGAGC	Xho I
X. laevis ERK2b	S	GCCGGATCCATGGCAGCGGCAGCGGCCT	Bam HI
	AS	GCCCTCGAGTCAGTACCCTGGCTGGAATCGAGC	Xho I
X. laevis ERK2b (T184S)	S	CAGACCATGATCACTCTGGCTTTCTCACAG	
	AS	CTGTGAGAAAGCCAGAGTGATCATGGTCTG	
X. laevis ERK2b (T193S)	S	CACAGAATATGTAGCCTCTCGCTGGTACAGAGC	
	AS	GCTCTGTACCAGCGAGAGGCTACATATTCTGTG	
X. laevis Bcl-xl	S	GCCCCATGGAGGGCAGCAGTAGAGATCTGGTGG	Nco I
	AS	GCCCTCGAGCTATCGGCGCCTCATGTAGCAGAC	Xho I
X. laevis Bak	S	GCCCCATGGTCTCTTCCGCATGTGAAGTAGAGTT	Nco I
	AS	GCCCTCGAGTCAGGTCAATCGTTGAAGCAGAAAC	Xho I
X. laevis Bax	S	GCCGGATCCCATGGAGCCGGTGGGGATTGT	Bam HI
	AS	GCCCTCGAGTTAGGACATCTTCCAGATGGCAAGA	Xho I
X. laevis Bid	S	GCCCCATGGGTCTGAATGTGAAGACGATTCTCG	Nco I
	AS	GCCCTCGAGTCACCTCTGTCTAGCGAGACGCTC	Xho I
X. laevis nBid	S	GCCCCATGGGTCTGAATGTGAAGACGATTCTCG	Nco I
	AS	GCCCTCGAGTCAATCAGTTTCCAGATCCCCATC	Xho I
X. laevis tBid	S	GCCCCATGGGAAACGTCCAATTCAGATCTACAG	Nco I
	AS	GCCCTCGAGTCACCTCTGTCTAGCGAGACGCTC	Xho I
X. laevis Bid (D52N)	S	GGGGATCTGGAAACTAATGGAAACGTCCAATTC	
	AS	GAATTGGACGTTTCCATTAGTTTCCAGATCCCC	
X. laevis Bid (K18/21R)	S	TGGAGATCGACATAAGGAATCACAGAGATGAATTCTGGGA	
	AS	TCCCAGAATTCATCTCTGTGATTCCTTATGTCGATCTCCA	
X. laevis Bid (K37R)	S	GCGAGGGAAGAGGGGAGGTTAGTGGCACAGATG	
	AS	CATCTGTGCCACTAACCTCCCCTCTTCCCTCGC	

5.1.2 DNA purification

PCR products were purified by agarose gel electrophoresis. To prepare 1% agarose gel, 1 g agarose was dissolved in 100 ml 1X TAE (40mM Tris, 20mM acetic acid, and 1mM EDTA, pH 8.0). ´´SYBR Safe DNA gel stain´´ (Invitrogen) at a dilution of 1:10.000 was added to the gel to visualize the DNA band under UV irradiation.

The proper band was cut and recovered through the kit ´´Illustra GFX PCR DNA and Gel Band Purification Kit´´ of GE Healthcare, and quantified by agarose gel electrophoresis. To indicate the molecular weight and quantify the DNA, lambda DNA EcoRI/HindIII Marker was used in the electrophoresis.

5.1.3 DNA digestion

DNA digestion was performed with the corresponding restriction enzymes and buffers (Fermentas) following the recipe below:

- 10x buffer 10µl
- DNA/FTX vector 5µg
- restriction enzyme 2µl
- nuclease-free water to 100µl

The mixture was gently mixed by pipetting up and down and spined down briefly to collect all samples at the bottom of the tubes. Samples were incubated at appropriate temperature (usually 37°C) for 2 h following the manufacturer's instructions. Finally, DNA products were purified with ¨Illustra GFX PCR DNA and Gel Band Purification Kit¨.

5.1.4 DNA ligation and transformation

PCR products were ligated to FTX5/FTX4 vectors (Figure 1). Accurate ligation clones were selected after transformation of *E. coli* DH5α ultracompetent cells (Inoue et al. 1990).

DNA ligation reaction was assembled in a microcentrifuge tube on ice using a molar ratio of 1:3 (vector to insert for the indicated DNA sizes). The components for a 20 µl reaction follow the recipe below:

- 10X T4 DNA Ligase Buffer 2 µl

- Vector DNA (FTX4/5) 50 ng
- Insert DNA 50 ng (depending of DNA size)
- Nuclease-free water to 19 µl
- T4 DNA Ligase (Fermentas) 1 µl

The reaction was gently mixed by pipetting up and down and spined down briefly. Then the mixture was incubated at 16°C overnight or at room temperature for 10 minutes.
For transformation, 50 µl of competent cells were incubated with 10 µl of DNA ligation mix on ice for 30 min. Transformed cells were selected on LB plate with Ampicillin (50 µg/ml).

5.1.5 Plasmid extraction

Single colonies from the LB plate were selected and added to 5 ml LB medium containing 50 µg/ml Ampicillin, and then incubated at 37°C with 200 rpm shaking overnight. Bacterial cells were harvested by centrifugation at the maximum speed for 1 min. Plasmids were prepared using ¨GenElute™ Plasmid Miniprep Kit¨ according to the instruction manual. Finally, the plasmids were eluted with 50µl nuclease-free water. Generally, the plasmids were sequenced as described below.

5.1.6 Site-directed mutagenesis and DNA sequencing

For construction of interested mutants used in different experiments, PCR-based mutagenesis was employed to mutate specific amino acids in the coding sequences. Wild-type cDNA cloned in the FTX5/4 vector was used as template and oligonucleotides for site-directed mutagenesis were designed based on the QuikChange® Primer Design Program (Agilent Technologies) (Table 1). The mutagenesis processes were performed according to QuikChange® Site-Directed Mutagenesis Kit instruction manual. Briefly, we used high fidelity Pfu Turbo DNA polymerase (Stratagene, Ref. 600250) for the PCR reaction, and the following mix reaction was prepared:

- 5 µl 10x Cloned Pfu reaction buffer
- 1 µl DNA template (10 ng/µl)
- 1 µl dNTPs (10 mM)
- 0.7 µl sense primer (20 µM)*
- 0.7 µl antisense primer (20 µM)*
- 40.6 µl H2O

- 1 µl Pfu Turbo DNA polymerase (2.5 U/µl)

* For specific primers, see Table 1.

The PCR conditions were:

- 95ºC 30 s
- 95ºC 30 s
- 55ºC 1 min } 16 cycles
- 68ºC 5 min
- 4ºC hold

After PCR reaction, the parental DNA was eliminated by adding 1 µl of the restriction enzyme Dpn I (10 U/µl) directly into the tube and incubating the mix for 2.5 h at 37ºC (without the restriction enzyme buffer). The PCR product obtained was transformed into E. coli DH5α ultracompetent cells and individual colonies were selected in agar plates by their resistance to ampiciline. Minipreps were obtained from single colonies and plasmids were purified using GenElute™ Plasmid Miniprep Kit and sequenced as described below.

5.1.7 DNA sequencing

All cloned genes and mutations generated were confirmed by DNA sequencing using the "BigDye® Terminator v3.1 Cycle Sequencing Kit" purchased from Applied Biosystems with the following reaction set:

- 1.5 µl 5x Big Dye buffer
- 1 µl DNA template (400 ng/µl)
- 1 µl sequencing primer (5µM) (Table 2)
- 1 µl Big Dye
- 5.5 µl H20

Table 2. Primers for DNA sequencing

NAME	SEQUENCE (5´-3´)	Tm(ºC)	ORIENTATION
T7	TAATACGACTCACTATAGGG	50.8	Sense
SP6	ATTTAGGTGACACTATAG	42.6	Antisense
FTX5 reverse	CCAGGGTGGATTGAGTCCAG	66.9	Antisense

Parameters for sequencing were seted as follow:

- 96ºC, 6 sec
- 96ºC, 30 sec
- 50ºC, 15 sec } 24 cycles
- 60ºC, 4 min
- 4ºC, hold

To precipitate the sequencing product, the 10 µl reaction pool was mix thoroughly with 40 µl ethanol/sodium acetate precipitation buffer (650 µl ethanol 100%, 30 µl sodium acetate 3M pH 5.2, 130 µl water) and left on desk for 15 min at room temperature. Then the mix was centrifuged at 14.000 rpm for 15 min at 4ºC to get sequencing product pellet. The pellet was washed one time with 70% ethanol and centrifuged at 14.000 rpm for 5 min at 4ºC. Then the pellet was dried at room temperature for 10 min before sent to Servei de Genòmica i Bioinformàtica of Universidad Autónoma de Barcelona.

5.1.8 *In vitro* transcription

In vitro transcriptions of capped RNAs (cRNAs) were performed using mMESSAGE mMACHINE® T7 Transcription Kit (Ambion®). DNA templates used for transcription were linearized at the Xba I or Sgr AI site, then about 1 µg linearized DNA was used in a 20 µL reaction assembly as described in its instruction manual. After incubated at 37ºC for two hours, extra DNA was removed by incubating with 1 µL TURBO DNase at 37ºC for 15 min and terminated by adding 115 µL H_2O and 15 µL Ammonium Acetate stop solution. The RNA was extracted with phenol/chloroform and precipitated with 1 volume of isopropanol, the resulting mRNA was resuspended in water to a final concentration of 1 mg/ml, as compared to RNA standards in denaturing gel electrophoresis as described below.

Table 3. cRNAs prepared for oocyte microinjection

cRNAs	Source	Vector	Mutation	Notes
MEKK1Δ	*Mus musculus*	FTX5	Deletion of aminoacids from 1 to 351 from wild type MEKK1	Constitutively active
MEKK1-KM	*Mus musculus*	FTX5	Mutation of aminoacid Lys-432 to Met of MEKK1Δ	Catalytically inactive
MKK7-DED	*Xenopus laevis*	FTX4	Mutation of aminoacids Ser-268, Thr-272, and Ser-274 to Asp, Glu and Asp	Constitutively active

			of wild type MKK7	
MKK7-3A	*Xenopus laevis*	FTX5	Mutation of aminoacids Ser-268, Thr-272, and Ser-274 to Ala of wild type MKK7	Catalytically inactive
MKK7-KM	*Xenopus laevis*	FTX5	Mutation of aminoacid Lys-146 to Met of wild type MKK7	Catalytically inactive
JNK1wt	*Homo sapiens*	FTX5	Wild type human JNK1	
JNK-AF	*Homo sapiens*	FTX5	Mutation of aminoacid Thr-183 and Tyr-185 to Ala and Phe respectively of human wild type JNK1	Cannot be phosphorylated and constitutively active
JNK-KR	*Homo sapiens*	FTX5	Mutation of aminoacid Lys-56 to Arg of human wild type JNK1	Catalytically inactive
JNK1-1	*Xenopus laevis*	FTX5	Wild type JNK1	
JNK1-2	*Xenopus laevis*	FTX5	Wild type JNK1	
JNK1-2 (D385A)	*Xenopus laevis*	FTX5	Mutation of aminoacid Asp-385 to Ala of wild type JNK1-2	A potential caspase-3 recognizing site in JNK1-2 was mutated.
JNK1-2 Δ385	*Xenopus laevis*	FTX5	Deletion of aminoacids 386 to 426 from wild type JNK1-2	
JNK1-2 (D412A)	*Xenopus laevis*	FTX5	Mutation of aminoacid Asp-412 to Ala of wild type JNK1-2	A reported caspase-3 recognizing site in JNK1 and JNK2 was mutated (Enomoto et al. 2003).
JNK1-2 Δ412	*Xenopus laevis*	FTX5	Deletion of aminoacids 412 to 426 from wild type JNK1-2	
JNK2-1	*Homo sapiens*	FTX5	Wild type	
JNK3-1	*Xenopus laevis*	FTX5	Wild type	
JNK3-2	*Xenopus laevis*	FTX5	Wild type	
JNK3-3	*Xenopus laevis*	FTX5	Wild type	
JNK3-4	*Xenopus laevis*	FTX5	Wild type	
ERK2a	*Xenopus laevis*	FTX5	Wild type	
ERK2b	*Xenopus laevis*	FTX5	Wild type	
ERK2 b(T184S)	*Xenopus laevis*	FTX5	Mutation of aminoacid Thr-184 to Ser of wild type ERK2b	An autophosphorylation site previously found in human ERK2 (Thr188) (Lorenz et al. 2008).
ERK2 b(T193S)	*Xenopus laevis*	FTX5	Mutation of aminoacid Thr-193 to Ser of wild type ERK2b	
MKK6-DD	*Homo sapiens*	FTX5	Mutation of aminoacids Ser-207 and Thr-211 to Asp of wild type MKK6	Constitutively active
p38α	*Xenopus laevis*	FTX5	Wild type	

p38α-KR	*Xenopus laevis*	FTX5	Mutation of aminoacid Lys-54 to Arg of wild type p38α	Catalytically inactive
p38α-AF	*Xenopus laevis*	FTX5	Mutation of aminoacids Thr-181 and Tyr-183 to Ala and Phe respectively of wild type p38α	Cannot be phosphorylated and constitutively active
p38β	*Xenopus laevis*	FTX5	Wild type	
p38β-KR	*Xenopus laevis*	FTX5	Mutation of aminoacid Lys-52 to Arg of wild type p38β	Catalytically inactive
p38β-AF	*Xenopus laevis*	FTX5	Mutation of aminoacids Thr-179, Tyr-181 to Ala, Phe of wild type p38β	Cannot be phosphorylated and constitutively active
p38γ	*Xenopus laevis*	FTX5	Wild type	
p38γ-DA	*Homo sapiens*	FTX5	Mutation of aminoacid Asp-179 to Ala of wild type p38γ	Dominant negative and catalytically inactive
p38δ	*Xenopus tropicalis*	FTX5	Wild type	
p38δ-KR	*Xenopus tropicalis*	FTX5	Mutation of aminoacid Lys-54 to Arg of wild type p38δ	Catalytically inactive
p38δ-AF	*Xenopus tropicalis*	FTX5	Mutation of aminoacids Thr-180, Tyr-182 to Ala, Phe of wild type p38δ	Cannot be phosphorylated and constitutively active
caspase-10	*Xenopus laevis*	FTX5	Wild type	
caspase-10 (C384S)	*Xenopus laevis*	FTX5	Mutation of aminoacid Cys-384 to Ser of wild type caspase-10	Catalytically inactive
Bcl-xl	*Xenopus laevis*	FTX5/ FTX4	Wild type	
Bak	*Xenopus laevis*	FTX5/ FTX4	Wild type	
Bax	*Xenopus laevis*	FTX5/ FTX4	Wild type	
Bid	*Xenopus laevis*	FTX5	Wild type	
Bid (D52N)	*Xenopus laevis*	FTX5	Mutation of aminoacid Asp-52 to Asn of wild type Bid	A reported Caspase-8 recognizing site in Bid was mutated (Kominami et al. 2006).
Bid (Ub)	*Xenopus laevis*	FTX5	Mutation of aminoacids Lys-18, Lys-21, and Lys-37 to Args of wild type Bid	Three reported ubiquitin -ation sites are mutated (Saitoh et al. 2009).
tBid	*Xenopus laevis*	FTX5	Fragment of aminoacids from 53 to 184 of wild type Bid	
nBid	*Xenopus laevis*	FTX4	Fragment of aminoacids from 1 to 52 of wild type Bid	

5.1.9 RNA quantification

The cRNAs obtained by *in vitro* transcription were quantified in denaturing 1% agarose gel electrophoresis. To prepare the gel, 0.5 g agarose was dissolved in 36 ml water by heating and then when it was cooled down to about 60ºC, 5 ml 10X MOPS running buffer (0.1 M Sodium Acetate, 0.01 M EDTA, 0.4 M MOPS, pH 7.0) and 9 ml 37% formaldehyde (12.3 M) were added. After polymerization the gel was assembled in the tank and covered with 1X MOPS running buffer.
0.5 µl RNA sample was diluted with 14.5µl nuclease-free water and then 5 µl denaturing buffer (65 µl 10X MOPS Buffer, 113 µl Formaldehyde, 323 µl Formamide, 0.5 µl Ethidium Bromide Stock (10mg/ml)) was added. The samples were heated at 85ºC for 10 min and then chilled on ice for 10 min. 10 µl sample with 2 µl loading buffer (50% glycerol, 10 mM EDTA pH 8.0, 0.6% orange G) were analyzed in the electrophoresis.

5.2 Oocyte manipulation and sample collection

5.2.1 Oocyte isolation

Oocytes were obtained from sexually mature *Xenopus laevis* females (purchased from Centre d'Elevage de Xenopes, Montpellier, or from Xenopus Express, Vernassal, France) via a minimally invasive surgery. *Xenopus* was anesthetized in 0.02% benzocaine. Then, portions of ovary were removed through a small incision on the abdomen. The incision was sutured and the animal was kept in a separate tank until it had fully recovered from the anesthesia. Frog was then returned to a large tank in which all the frogs were kept to recover at least 4 weeks until the next surgery. The tissue was dissected into small pieces if the ovaries were healthy enough to use. Oocytes were defolliculated for 3h at 18ºC with collagenase/dispase (0.8 mg/ml (Sigma), 0.48 mg/ml (Roche)) in MBS (5 mM HEPES, 88 mM NaCl, 1 mM KCl, 1 mM $MgSO_4 \cdot 7H_2O$, 2.5 mM $NaHCO_3$, 0.7 mM $CaCl_2$, pH 7.8) with gentle agitation. The defolliculated oocytes were then washed thoroughly with MBS and transferred to a petri dish. Stage VI oocytes in good state were sorted manually and incubated overnight in MBS at 18ºC. The next day, healthy survivors were selected and transferred to another petri dish containing fresh MBS. Pools of oocytes were treated with drugs at concentrations and times indicated or injected with cRNAs and treated as described below.

5.2.2 Oocyte injection

Stage VI *Xenopus* oocytes were microinjected near their equator with 50 nL (5 ng) of the corresponding cRNAs using a Nanoject II™ Automatic Nanoliter Injector (Drummond Scientific Company). Injected oocytes were incubated 18 h at 18ºC and poor oocytes were eliminated the next day before proper manipulation. Pools of 20 oocytes were collected at the indicated times before or after treatment. In some experiments, oocytes were injected with cytochrome c from horse heart (c-7752, Sigma).

5.2.3 Progesterone stimulation and GVBD percentage calculation

For stimulating *Xenopus* oocyte maturation, 3 µg/mL progesterone (from 1000x stock solution dissolved in ethanol) at final concentration was used in MBS. Mature oocytes were identified by the white spot at the animal pole. The number of GVBD oocytes was counted and samples were collected every hour as described. The percentage of mature oocyte was quantified by the number of mature oocytes/number of total oocytes.

5.2.4 Hyperosmotic treatment

To investigate oocyte response to hyperosmotic shock, oocytes were treated with 300 mM sorbitol in MBS. Samples were collected at indicated times and samples were prepared as described below.

5.2.5 Inhibitor usage

In order to inhibit specific protein activities, oocytes were either pre-incubated for 1 h or injected with proper inhibitors before designed manipulation as described below. When oocytes were preincubated and then treated with progesterone or 300 mM sorbitol, the final concentration of inhibitor was maintained in the medium. We used a higher concentration of inhibitors compared to mammalian cells due to specific properties of *Xenopus* oocytes (presence of vitelline membrane and the yolk) that reduce the actual concentration of drugs at the cell membrane. In general, IC50 values are approximately 10 to 20-fold higher when the drugs are applied to the extracellular surface of *Xenopus* oocytes (Thomas et al. 2001, Thomas et al. 2004).

Table 4. Inhibitors used in oocyte manipulation

Inhibitor	Target	Final concentration	Supplier
SP600125	JNK MAPK	25 µM (b), 50 or 100 µM (a)	Calbiochem
BIRB796	p38 MAPK	50 or 100 µM (a)	Axon Medchem
MDL28170	Calpains	50 µM (a)	Sigma
U0126	MEK1	50 µM (a)	Calbiochem
FR 180204	ERK MAPK	50 µM (a)	Calbiochem
Z-VAD-fmk	caspases	50 µM (a)	Bachem
Z-DEVD-fmk	caspase-3	50 µM (a)	Calbiochem
TI-JIP153-163	JNK MAPK	5 or 10 µM (b)	Calbiochem

a. pre-incubation with indicated final concentration in MBS or 300mM sorbitol;

b. injected with indicated final concentration.

5.3 Sample preparation and analysis

5.3.1 Oocyte lysis and mitochondrial/ cytosolic fraction preparation

Fresh oocytes were lysed by pipetting up and down in 200 µl (pools of 20 oocytes) of ice-cold lysis buffer (0.25 M sucrose, 0.1 M NaCl, 2.5 mM $MgCl_2$, 20 mM HEPES, 1 mM EDTA, 1 mM EGTA, pH 7.2) containing protease inhibitors (10 µg/ml leupeptin, 1 mM PMSF, 10 µg/ml aprotinin) and phosphatase inhibitors (50 mM β-glycerolphosphate, 50 mM sodium fluoride, 1 mM sodium orthovanadate, 5 mM sodium pyrophosphate). Samples were clarified by centrifugation at 14.500 rpm for 5 min and supernatants were collected and processed for western blotting or activity assay as described below.

For subcellular fractionation, 30 oocytes were lysed in the lysis buffer and the extract obtained was centrifuged at 1.000 g for 5 min at 4ºC to remove lipids and the yolk. The supernatant was isolated and centrifuged at 16.000 g for 15 min at 4ºC. The supernatant obtained (cytosolic fraction) was stored at -20ºC, and the pellet (mitochondrial fraction) was resuspended in 50 ul of lysis buffer and stored at -20ºC too (Brun et al., 1981).

5.3.2 Immunoprecipitation

For denaturing IP, 10 oocytes were lysed in 50 µl lysis buffer. Then the 50 µl protein extract was denatured with 10µl 6x denaturing buffer (375 mM Tris-HCl pH 6.8, 600 mM dithiothreitol, 9% SDS) at 95ºC for 10 min and then purified through chloroform-methanol precipitation method (Wessel and Flügge 1984). The pellets were then resuspended in 50 µl of resuspension buffer (100 mM Tris, pH 11.3% SDS, 3 mM DTT) by heating to 65ºC for 5 min and 95ºC for 10 min. 450 µl of IP cell lysis buffer (20 mM Tris (pH 7.5), 150 mM NaCl, 1 mM EDTA, 1 mM EGTA, 1% Triton X-100, 2.5 mM Sodium pyrophosphate, 1 mM β-glycerophosphate, 1 mM Na_3VO_4, 1 µg/ml Leupeptin) was then added to the protein suspension (Campbell and Hardwick 2003). 0.5 µl of the pJNK antibody was added to 100 µl cell lysate, and the mixture was incubated overnight at 4ºC with gentle rocking. 10 µl G agarose beeds slurry (washed two times with IP buffer) were added to the lysate and incubated with gentle rocking for 2 h 4ºC. A 30 s centrifugation was then performed at max speed at 4ºC. The pellet was washed 3 times with 500 µl of IP cell lysis buffer. The sample was kept on ice during washes. For immunoblotting analysis, the pellet was resuspended with 6 µl 5× Laemmli sample buffer (50 mM Tris HCl, pH 6.8, SDS 2%, 100 mM dithiothreitol, 10% glycerol), vortex and centrifuged for 30 s. The sample was incubated at 100ºC for 5 min and centrifuged for 30 s before was loaded to SDS-PAGE gels for analysis.

In order to get high quality immunoprecipitation product for mass spectrometry analysis, a Pierce® Crosslink Immunoprecipitation Kit (Thermo Scientific) was applied. 10 µl pJNK antibodies were incubated with 20 µl protein A/G plus agarose for 1 h in 1X coupling buffer to bind the antibody to the agarose. The crosslink reaction was performed via incubating antibody-bound agarose with 450 µM DSS in 1X coupling buffer for 1 h. In the IP reaction, 20 µl antibody-crosslinked agarose were incubated with 200 µl denatured lysate and washed as described above with kit supplied columns. Finally, samples were eluted with 0.2% TFA elution buffer and concentrated before mass spectrometry. The antibody-crosslinked agarose can be regenerated and reused in the next Immunoprecipitation reactions.

5.3.3 Mass spectrometry identification

The pool of several immunoprecipitations (samples eluted in 0.2% TFA) was concentrated and sent to Laboratori de Proteomica CSIC/UAB, Facultat de Medicina, Universitat Autònoma de Barcelona, for mass spectrometry analysis. Briefly, the sample was separated on SDS-PAGE electrophoresis and visualized with a compatible mass spectrometric silver staining (acetic acid was used as a fixer

instead of glutaraldehyde). The gel band obtained with the target protein was cut and the protein in the gel slice digested in situ with trypsin. The tryptic extracts were analyzed by LC-MS/MS in data-dependent mode. The MS system used was an LTQ XL Orbitrap (ThermoFisher) equipped with a nanoESI ion source. LC-MS/MS spectra were searched using SEQUEST (Proteome Discoverer v1.4, ThermoFisher). The database used for searching was obtained from Uniprot (organism: Xenopus). Peptide identifications were filtered at 1% FDR and only proteins identified with two or more peptides and peptide rank 1 were considered.

5.3.4 Western Blot

Samples collected were denatured in Laemmli sample buffer at 100ºC and subject to 10% or 14% SDS/PAGE. Generally polyacrylamide gels for electrophoresis were prepared from commercial 40% acrylamide (37.5 :1 acrylamide:bis, Bio-Rad, Cat. No. 161-0148), except for special gels for detecting protein shift induced by phosphorylation which were prepared from 30% polyacrylamide (100 :1 acrylamide:bis, Sigma).

Table 5. Gel preparation buffer for SDS-PAGE

For 100 ml Lower Gel Buffer (4x)	For 100 ml Upper Gel Buffer (4x)
18.17 g Tris base	6.06 g Tris base
2 ml 20% SDS	2 ml 20% SDS
Adjust pH to 8.8 with HCl.	Adjust pH to 6.8 with HCl.

Polyacrylamide gels were prepared as described in table 6 depending on the final acrylamide concentration in the separating gel.

Table 6. Polyacrylamide gel recipes (2 gels)

	Lower Gel			Upper Gel
	8%	10%	14%	3%
4x buffer (ml)	4	4	4	2
40% acrylamide (ml)	3.2	4	5.6	0.6
H_2O (ml)	8.8	8	6.4	5.4
PSA (µl)	60	60	60	32
TEMED (µl)	20	20	20	8

To get a proper separation resolution, electrophoresis was performed in Laemmli Runing Buffer 1X (Table 7) at 150V for 1 h and, subsequently, proteins were transferred to Immobilon-P membranes (Millipore) in Transfer Buffer with 10% methanol (Table 7) at 400mA for 2 h.

Table 7. Electrophoresis buffer for SDS-PAGE

For 1L Laemmli Running Buffer (10x)	For 1L Transfer Buffer (10x)
30.3 g Tris Base	144 g glycine
144.1 g Glycine	30.2 g Tris base
50ml 20% SDS	

To make 1X Transfer Buffer with 10% methanol: Mix 100 ml of 10 x Transfer Buffer, 100 ml of methanol and 800 ml of dH2O per liter.

Uniformity of samples loading was verified by Ponceau (Sigma) staining of the blots. Membranes were blocked for 1 h with 5% dried skimmed milk in TBST (50 mM Tris, 150 mM NaCl, 100 mM KCl, pH 7.4, and 0.1% Tween20), washed several times with TBST, and then incubated overnight with the specific primary antibody (see Table 8) diluted 1:1000 in TBST containing 5% bovine serum albumin (BSA).

Table 8. Antibodies used in identification of *Xenopus* oocyte proteins

Antibody	Product Number	Supplier
AMPKα	#2532	Cell Signaling Technology
Phospho - AMPKα (Thr172)	#2531	Cell Signaling Technology
SAPK/JNK	#9252	Cell Signaling Technology
Phospho - SAPK/JNK (Thr183/Tyr185)	#9251	Cell Signaling Technology
JNK(FL)	SC-571	Santa Cruz Biotechnology
MAPK10 (N-term)	AP14264a	ABGENGT
p44/42 MAPK (Erk1/2) (137F5) Rabbit mAb	#4695	Cell Signaling Technology
Phospho-p44/42 MAPK (Erk1/2) (Thr202/Tyr204) (D13.14.4E) XP™ Rabbit mAb	#4370	Cell Signaling Technology
cleaved caspase-3 (Asp175)	#9661	Cell Signaling Technology
Cytochrome C	556433	BD Pharmingen
Phospho-cPLA2 (Ser505) Antibody	#2831	Cell Signaling Technology
p38 α/ß (H-147)	sc-7149	Santa Cruz Biotechnology

Phospho-p38 MAP Kinase (Thr180/Tyr182) antibody	#9211	Cell Signaling Technology
Smac Antibody	#2409	ProSci Inc
monoclonal anti-β-actin	A19789	Sigma-Aldrich
monoclonal anti-Myc	M4439	Sigma-Aldrich
monoclonal anti-ATP-synthase α	A21350	Invitrogen

Antibody binding was detected next morning by washing the membranes with TBST several times and incubating for 1 h at room temperature with horseradish peroxidase–coupled secondary antibody (anti-Rabbit from Cultek, Ref 31460; or anti-Mouse from Bio-Rad, Ref. P0260) diluted 1:3000 with TBST containing 5% dried skimmed milk. Membranes were washed several times with TBST and signals were detected using Fuji films and enhanced chemiluminescence (ECL) reagents.

Table 9. ECL solutions

Solution A	Solution B
5 ml 1 M Tris pH 8.5	5 ml 1 M Tris pH 8.5
250 µl 0.5 M p-Coumaric acid	32 µl 30% H_2O_2
250 µl 250 mM Luminol	Make up to 50 ml with H_2O
Make up to 50 ml with H_2O	

5.3.5 Stripping of PVDF membranes

In order to remove primary and secondary antibodies of first western blot and reuse the PVDF membranes in a second analysis, membranes were incubated in ´´Stripping buffer´´ (100 mM 2-mercaptoetanol, 2% SDS, 62.5 mM Tris-HCl pH 6.7) at 50°C for 30 min with gentle agitation. Then, the membranes were washed with TBS-T three times and incubated with 5% non-fat milk for 1 h. Subsequently, western blot was performed as described above.

5.4 Activity assays

5.4.1 Caspase-3 Activity Assay

Caspase-3 activity was measured in terms of DEVDase activity assay in 96 cells opaque plates. 25 µl cytosolic fraction (corresponding to 2.5 oocytes) were assayed with 50 µl 2× Reaction Buffer (20% Glycerol, 40mM Hepes, 4mM DTT, pH 7.5) and 25 µl lysis buffer. Before the reaction assembly, 20 µl 10 mM synthetic peptide Z-DEVD-AMC (Peptide Institute, Inc.) was added to 980µl 2x Reaction Buffer. Generally, 2 reactions were performed for each sample. Fluorescence at 360 nm for excitation and at 460 nm for emission was measured after incubation of the samples for 60 min at 37ºC.

Caspase-3 activity was determined as the concentration of fluorescent AMC formation from Z-DEVD-AMC substrate, and represented as arbitrary units (AU) of caspase-3 activity, giving value 1 to non-treated oocytes or oocytes injected with H_2O.

5.4.2 JNK and ERK kinase assays

Fresh oocytes were lysed by pipetting up and down in 200 µl (pools of 20 oocytes) of ice-cold kinase buffer (20 mM Hepes pH 7.6, 20 mM MgCl2, 10 mM β-glycerophosphate, 0.5 mM sodium orthovanadate, 2 mM dithiothreitol) containing protease inhibitors (10 µg/ml leupeptin, 1 mM PMSF, 10 µg/ml aprotinin). Samples were clarified by centrifugation at 14.500 rpm for 5 min and supernatants were collected for activity assay (performed the same day that the lysis). JNK activity was measured using GST-cJun (1-79) (Sigma, C3233) as a substrate, and ERK activity using myelin basic protein (MBP) (Sigma, M1891). Briefly, 5 µl of oocytes extract (equivalent to 10 µg of protein) were incubated with 3 µg of substrate (GST-cJun or MBP) in kinase buffer with protease inhibitors (total volume of reaction 20 µl) containing 50 µM ATP and 2 µCi [γ32P] ATP at 30ºC for 30 min with moderate shaking (800 rpm). The amounts added for a reaction, based on the stocks prepared in the laboratory, were as follow:

- 5 µl oocytes extract (2 µg/µl)
- 3 µl GST-cJun or MBP (1 µg/ µl)
- 1 µl ATP (1 mM)
- 0.2 µl [γ32P] ATP (10 µCi/µl)

- 10.8 µl kinase buffer with protease inhibitors

The reaction was stopped by adding 5 µl of 5x Laemmli Buffer and heating the samples at 100ºC for 5 min. The phosphorylated proteins were resolved by SDS-PAGE (15% polyacrylamide gel for GST-cJun and 12% for MBP) at 150V for 1 h. The gel was washed briefly with Laemmli Running Buffer and signals were detected by autoradiography by exposure with Fuji films at -80ºC.

5.4.3 Statistical analysis

Most of the experiments described have been repeated at least three times. Due to the variability in the absolute values obtained using different frogs we decided to present here only a representative graph or Western blot for each experiment instead of the statistical analysis. Otherwise indicated, the independent experiments performed showed similar results, leading to the same conclusions.

6. RESULTS

A. Insights into the role of MAPK function in meiotic progression

6.1 Various kinases are activated during meiotic initiation

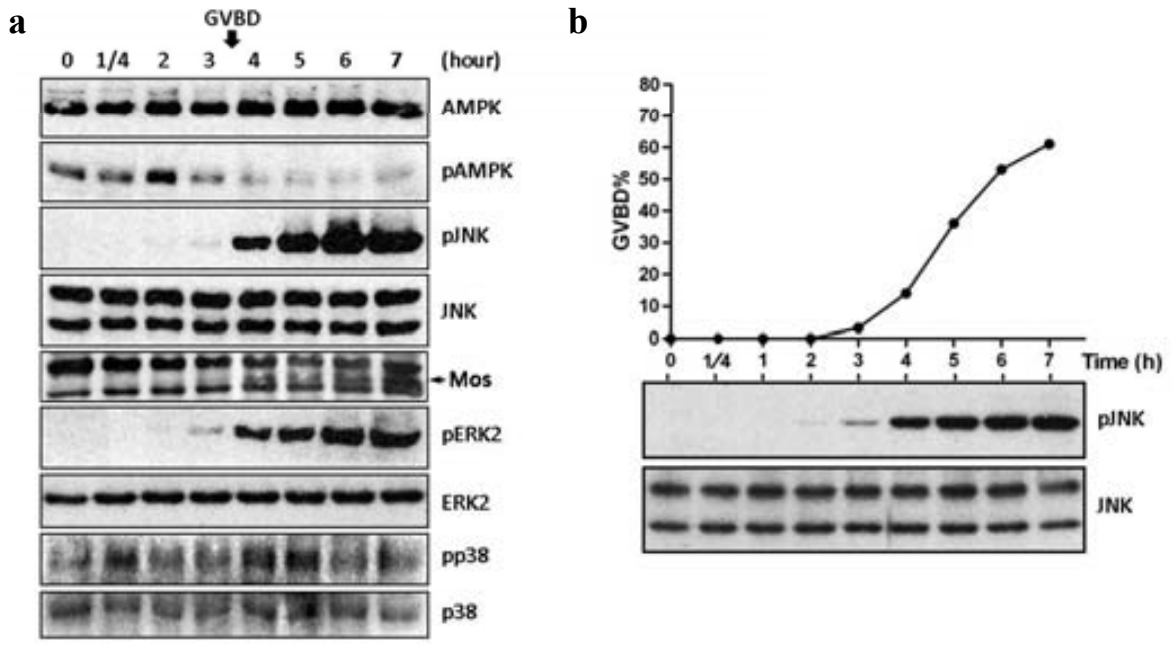

Figure 18. **Protein kinases phosphorylated during Xenopus oocyte maturation.** *Xenopus* oocytes were incubated with 3 µM progesterone in MBS and samples were collected at indicated time points and analyzed by western blot as described. (a) MAPK proteins are phosphorylated during meiotic progression. (b) The levels of pJNK detected by western blot correlates well with maturation kinetics.

Xenopus oocytes go through many changes in progesterone-induced meiotic initiation. One of the key earliest biochemical changes observed in frog oocytes after progesterone incubation is a decrease of cAMP, which has also been observed in mouse and rat. In mouse oocytes AMP-activated protein kinase (AMPK) is activated during meiotic progression and it has been suggested that the decrease of cAMP would induce AMPK activation via an unclear mechanism (Chen Jing and Downs 2008, Chen Jing et al. 2006, Downs et al. 2002). AMPK is an important regulator of cellular energy status and can be activated by an increase of AMP levels or Ca^{2+} levels (Hurley et al. 2005). As shown in Figure 18, *Xenopus* oocytes incubated with 3 µM progesterone induced

phosphorylation of AMPK at 2 h, before GVBD. The AMPK activation was a transient event, since pAMPK decreased after GVBD along with oocyte maturation. The MAP kinase cascade proteins, including Mos, MEK1, and ERK2 are crucial mediators in oocyte meiotic resumption (Ferrell 1999). In mature oocytes, ERK2 was activated rapidly around the GVBD, which occurred between 3-4 h, and remained highly active and unchanged (Fig. 18a). As a crucial upstream activator of ERK2, Mos protein levels were increased almost at the same time (Fig. 18a). Treatment of *Xenopus* oocytes with progesterone also induced phosphorylation of the stress protein kinases JNK and p38. As we can see in Figure 18b, the phosphorylation of JNK increased abruptly at 4 h, and was maintained high for the next hours corresponding to the kinetics of oocyte maturation. The phosphorylation of JNK was well correlated with pERK2 levels.

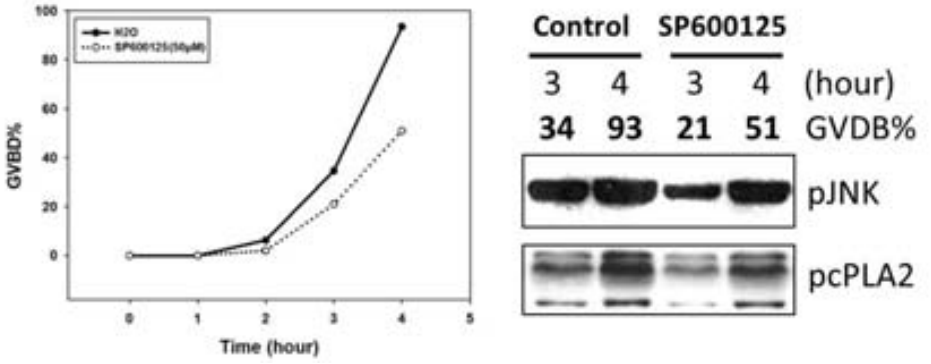

Figure 19. **The JNK inhibitor SP600125 decreases the maturation of *Xenopus* oocytes and the levels of pJNK.** *Xenopus* oocytes were incubated with progesterone in MBS with or without JNK inhibitor SP600125 (50 µM), GVBD percentage was calculated and samples were collected both at 3 h and 4 h. Samples were then analyzed by western blot. pcPLA2 levels were measured as marker of JNK activation.

Additionally, the JNK inhibitor SP600125 decreased the accumulation of pJNK and the maturation process (Fig. 19). As a control of JNK activity, we measured the phosphorylation levels of cytosolic phospholipase A2 (cPLA2), a protein previously described as substrate of JNK (Davis Roger J 1995, Gubern et al. 2009). However, the JNK inhibitor TI-JIP153-163 did not affect the maturation of *Xenopus* oocytes (data not shown). The MAPK p38 showed two peaks of phosphorylation: the first one occurred at the very beginning of progesterone treatment and was a transient event, and the second one was observed around 4 h. The levels of pp38 were low and could only be detected after a long exposure of the films. The above results indicate that the protein kinases AMPK, JNK and p38 are activated during meiosis at different times and with different strength and duration, suggesting that they might have different roles in meiotic progression.

6.2 Constitutively active MEKK1 accelerates progesterone-induced meiotic resumption

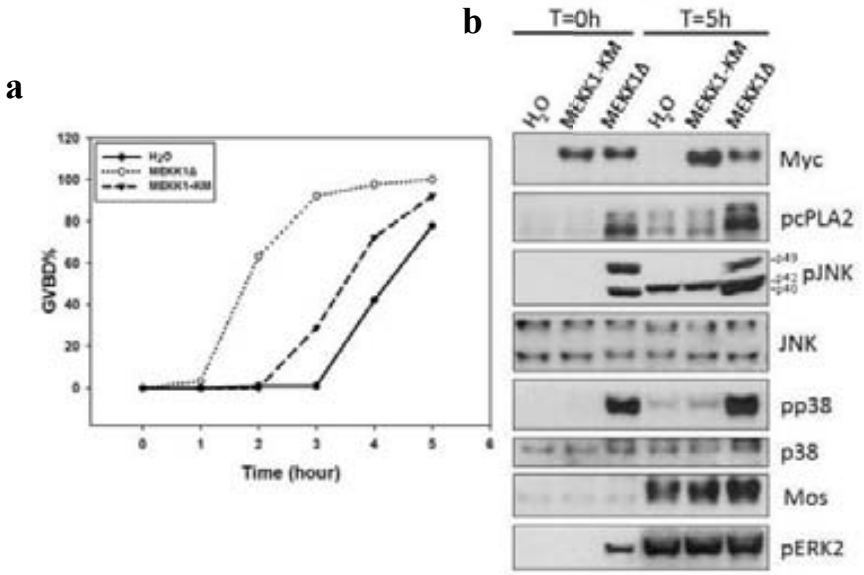

Figure 20. **Constitutively active MEKK1 (MEKK1Δ) accelerates progesterone-induced oocyte maturation.** *Xenopus* oocytes were injected with catalytically inactive MEKK1 (MEKK1-KM), constitutively active MEKK1 (MEKK1Δ) or water, and treated with progesterone 18 h later. GVBD percentage was calculated and samples were collected every hour. Samples were then analyzed by western blot. (a) MEKK1Δ speeds up meiotic progression. (b) MEKK1Δ activates MAPK family proteins without any treatment and progesterone treatment induces XpJNK-p42.

It is well known that the upstream protein kinase MEKK1 activates JNK and p38 (Davis Roger J 2000b, Wagner and Nebreda 2009). In order to investigate the role of the stress protein kinases JNK and p38 in meiotic progression, we injected a cRNA of a constitutively active mutant of MEKK1 (MEKK1Δ) into *Xenopus* oocytes to activate JNK and p38 proteins. If JNK and p38 signaling pathways play any role in meiotic progression, we should expect that ectopic expression of MEKK1Δ in *Xenopus* oocytes would modify the kinetics of maturation induced by progesterone.

As shown in figure 20a, expression of MEKK1Δ accelerated meiotic maturation compared with water-injected oocytes or with oocytes expressing a catalytically inactive mutant of MEKK1 (MEKK1-KM). Both protein kinases (MEKK1 and MEKK1-KM) were efficiently expressed in the oocytes (Fig. 20b, myc blot) and MEKK1Δ induced the phosphorylation of JNK, p38 and ERK, whereas MEKK1-KM did not activate any of these signaling pathways, as expected. Activation of JNK and p38 by MEKK1Δ was also confirmed by an increase of cPLA2 phosphorylation, which has been reported to be a substrate for both protein kinases (Davis Roger J 1995, Gubern et al. 2009,

Zarubin and Jiahuai 2005). However, ERK2 was also activated by MEKK1Δ (Fig. 20b) as some authors have reported before (Minden et al. 1994). Progesterone treatment activated the three signaling pathways, as expected (Fig. 20b, 5h). Interestingly, the expression of MEKK1Δ induced the phosphorylation of two JNK isoforms with molecular weights of 40 and 49 kDa, whereas progesterone treatment induced the phosphorylation of a protein of different molecular weight (42 kDa) (Fig. 20b, pJNK). Surprisingly, it was proved that the total JNK antibody recognized the 40 and 49 kDa proteins, but not the 42 kDa protein (Fig. 20b, JNK). To distinguish this phosphorylated protein from the 40 and 49 kDa isoforms, we named it XpJNK-p42.

6.3 Ectopic expression of human JNK1 or JNK2 isoforms do not modify progesterone-induced oocyte maturation

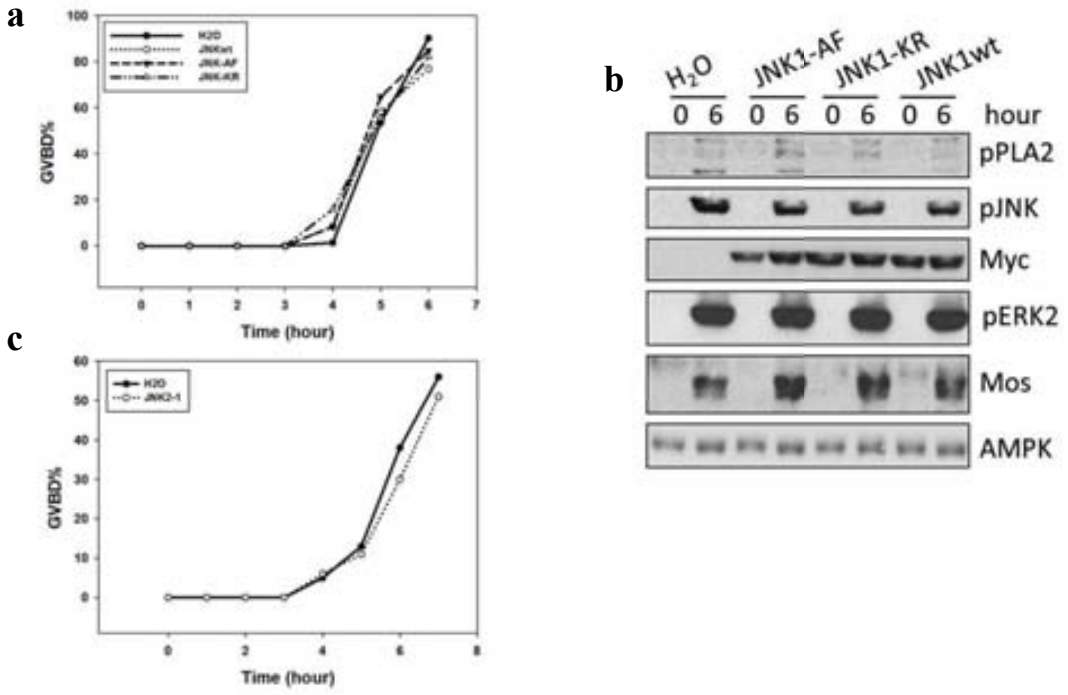

Figure 21. **Ectopic expression of human JNKs does not affect *Xenopus* oocyte maturation.** Human JNK wild type isoforms (JNK1 and JNK2-1) and catalytically inactive mutants of JNK1 (JNK-AF, JNK-KR) were overexpressed in *Xenopus* oocytes. Oocytes were then incubated with progesterone and GVBD percentage was calculated every hour. Water injected oocytes were treated as control group. Samples were collected at 0 h and 6 h and analyzed in western blot. (a) Overexpression of human JNK1 (wild type or mutants) does not impair meiotic kinetics. (b) Expression of human JNK1 wild type or catalytically inactive mutants (AF, KR) do not increase XpJNK-p42 levels. (c) Expression of human JNK2-1 isoform does not change oocyte maturation kinetics.

To address the role of different JNK isoforms in the regulation of oocyte maturation, we expressed human JNK1 wild type or catalytically inactive mutants JNK1-AF or JNK1-KR in *Xenopus* oocytes. Although these proteins were efficiently expressed (Fig. 21b, Myc blot), there were no significant differences in the percentage of mature oocytes induced by progesterone treatment (Fig. 21a). The increase of pJNK levels detected by Western blot after progesterone treatment was similar in water-injected and JNK1-injected oocytes (Fig. 21b, pJNK), indicating that human JNK1 is not phosphorylated by progesterone treatment.

Although there are no JNK2 isoforms described in *Xenopus*, we expressed human JNK2-1, which did not affect progesterone-induced maturation (Fig. 21c). Western blot showed that human JNK1 and JNK2-1 can be detected with the total JNK antibody (data not shown).

6.4 Co-expression of human JNK1 with MEKK1Δ does not modify meiotic acceleration induced by MEKK1Δ

The accelerated maturation of the oocytes induced by MEKK1Δ could be due to activation of the JNK signaling pathway, since JNK activation was observed before progesterone treatment (Fig. 22b). To address this issue, we injected the oocytes with the cRNAs of wild type human JNK1 or catalytically inactive mutants (JNK1-AF or JNK1-KR) combined with MEKK1Δ respectively and compared their kinetic of meiotic progression with MEKK1Δ or water-injected oocytes.

As shown in figure 22a, there were no significant differences in the acceleration of meiotic progression induced by MEKK1Δ or by MEKK1Δ + JNK1wt. The expression of MEKK1Δ and JNK1wt were confirmed by Western blot (Fig. 22b, myc and JNK blots) and by an increase of cPLA2 phosphorylation. MEKK1Δ induced the activation of JNK, ERK and p38 signaling pathways, as described before. Compared to XpJNK-p42, human JNK1 with a myc tag in the N-terminal has also a molecular weight of 42kDa, but it was well recognized with the total JNK antibody and was phosphorylated by MEKK1. It is clear that MEKK1Δ did not modify the levels of XpJNK-p42 induced by progesterone, but accelerated the apperance of this protein in correlation with increased Mos levels, pERK2 and the percent of mature oocytes (Fig. 22b). In accordance with the kinetics of maturation (Fig. 22a), there were no differences between MEKK1Δ and MEKK1Δ + JNK1wt in the levels of Mos, pERK2 or pp38. As a control of total protein loading we measured AMPK levels. This result, and the previous data, clearly indicates that progesterone treatment induces phosphorylation of a p42 protein recognized by the pJNK antibody (XpJNK-p42), but not by the total JNK antibody, and that ectopic expression of MEKK1Δ activates two different JNK

isoforms (p40 and p49), not activated during meiotic progression. It is also clear that overexpression of human JNK1 does not modify the acceleration of meiosis induced by MEKK1Δ.

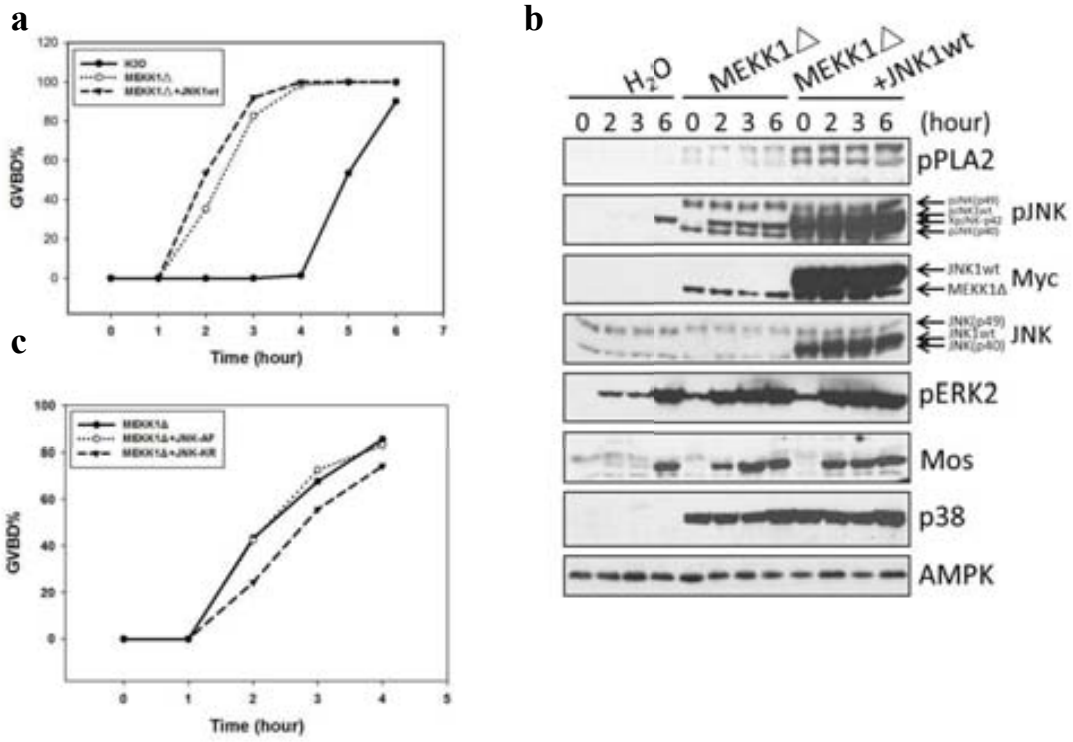

Figure 22. **Overexpression of human JNK1 does not increase MEKK1Δ-induced meiotic acceleration.** Human wild type JNK1 or its catalytically inactive mutants JNK-AF and JNK-KR were co-expressed with MEKK1Δ respectively in *Xenopus* oocytes. Oocytes were incubated with progesterone and GVBD percentage was calculated every hour comparing with water injected oocytes as a control. Samples were collected at different times and analyzed by western blot. (a) Expression of human JNK1wild type does not alter MEKK1Δ-induced meiotic acceleration. (b) Samples from (a) were collected at 2, 3 and 6 h, and analyzed by western blot. (c) Expression of human JNK-AF does not modify meiotic acceleration induced by MEKK1Δ.

Expression of MEKK1Δ with catalytically inactive mutant JNK1-AF did not modify the acceleration of meiosis, but the mutant JNK1-KR slightly reduced the percentage of mature oocytes (Fig. 22c), although this result was not consistently repeated in replicate experiments (data not shown). When oocytes expressing MEKK1Δ were incubated with SP600125, the meiotic acceleration induced by MEKK1Δ was attenuated (Fig. 23).

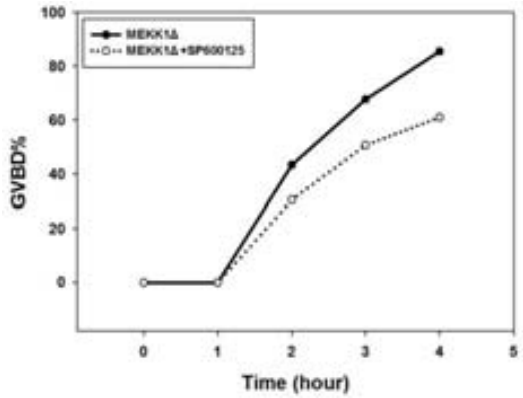

Figure 23. **The JNK inhibitor SP600125 attenuates MEKK1Δ-induced acceleration of meiosis.** *Xenopus* oocytes expressing MEKK1Δ were treated with progesterone in the presence or absence of the JNK inhibitor SP600125 (50μM). GVBD percentage was calculated every hour.

6.5 Constitutively active MKK7 does not accelerate meiotic progression

To address more specifically the role of JNK cascade in progesterone-induced meiotic progression, we microinjected a wild type MKK7, a constitutively active mutant (MKK7-DED), or two catalytically inactive mutants (MKK7-KM, MKK7-3A) and treated the oocytes with 3 μM progesterone.

As shown in Figure 24a, the oocytes injected with wild type or mutants MKK7 matured with the same kinetics that of water-injected oocytes. The constitutively active mutant MKK7-DED induced the phosphorylation of the p40 and p49 JNK isoforms, but did not activate the ERK or the p38 signaling pathways (Fig. 24b). The p40 and p49 JNK isoforms activated by MKK7 were also activated by hyperosmotic shock (Fig. 24b), as previously reported (Martiáñez et al. 2009). Recently, we have characterized these isoforms as *Xenopus* JNK1-1 and JNK1-2, which differ in the C-terminal domain obtained by differential splicing of the JNK1 gene (Messaoud NB, These Dissertation, 2014). Progesterone treatment induced the phosphorylation of XpJNK-p42, clearly different to the p40 and p49 JNK isoforms. Furthermore, co-overexpression of MKK7-DED and *Xenopus* JNK1-1 or JNK1-2 did not increase progesterone-induced oocyte maturation, but on the contrary decreased it (Fig. 24c).

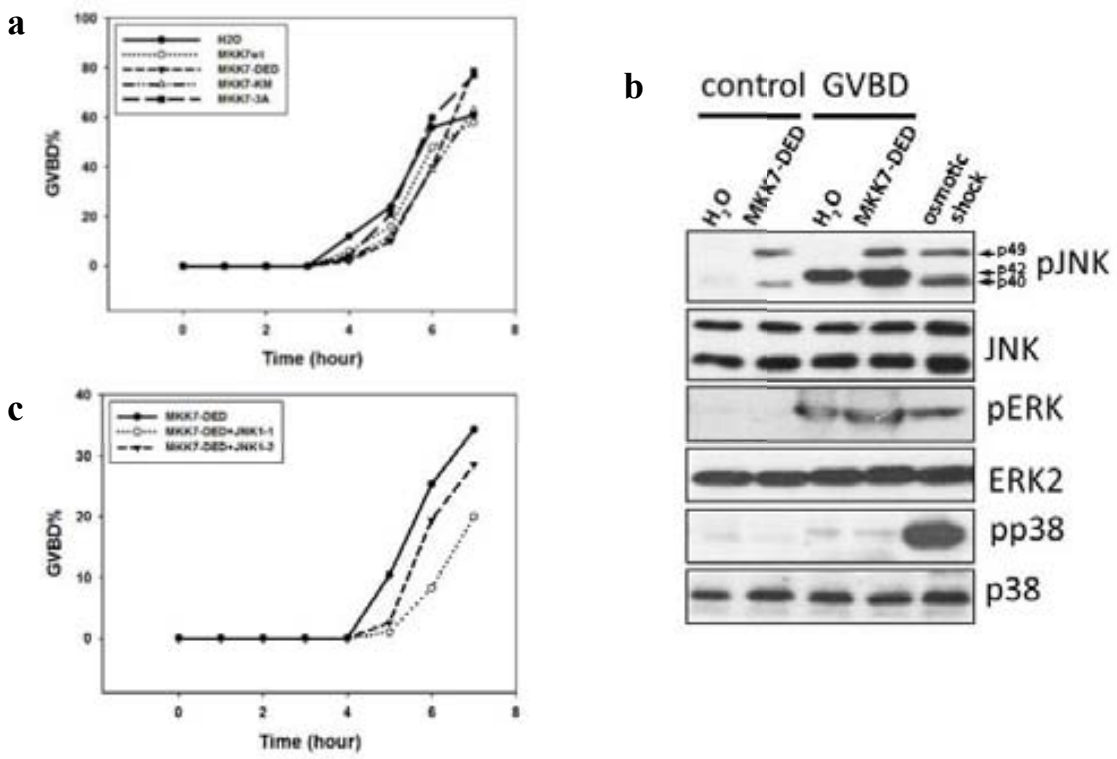

Figure 24. **MKK7 does not modify progesterone-induced maturation.** Wild type MKK7, constitutively active mutant MKK7-DED, catalytically inactive mutants MKK7-KM or MKK7-3A, or a combination of MKK7-DED with JNK1-1 or JNK1-2 respectively were overexpressed in *Xenopus* oocytes. Then oocytes were treated with progesterone and GVBD percentage was calculated every hour. Samples were analyzed by western blot at last. (a) Ectopic expression of wild type, constitutively active or catalytically inactive MKK7 mutants do not affect maturation kinetics of *Xenopus* oocytes. (b) MKK7-DED activates *Xenopus* JNK1 proteins, but not ERK, p38 or XpJNK-p42. Oocytes expressing MKK7-DED or water injected oocytes were treated with progesterone and samples were collected at GVBD and analyzed by western blot comparing with untreated oocytes. Some oocytes were treated with 300mM sorbitol (osmotic shock) for 1 h to induce activation of p40 and p49 JNK1 isoforms. (c) Overexpression of JNK1-1 or JNK1-2 combined with MKK7-DED slightly reduces progesterone-induced maturation.

6.6 Cloning of JNK3 isoforms in Xenopus laevis oocytes

Generally, unlike JNK1 and JNK2, JNK3 exhibits a restricted expression, primarily in the central nervous system (Martin et al. 1996). However, for the sake of bringing to light the XpJNK-p42, we cloned several complete coding regions from *Xenopus* stage VI oocytes by RT-PCR. PCR primers were designed based on *Xenopus tropicalis* JNK3 coding sequences, as JNK3 proteins are quite conserved in different species. In *Xenopus* JNK3 sequences, there are two potential start codons and also two stop codons. The specific sequence between the first and second start codon that was obtained via alternative splicing will determine which start codon should be chosen and an insertion

of a 5-nucleotide before the stop codon which also results from alternative splicing will determine which stop codon would be selected. In other words, exon alternative selection indicates the start and stop of the coding region, giving to different JNK3 isoforms (Fig. 25a).

a

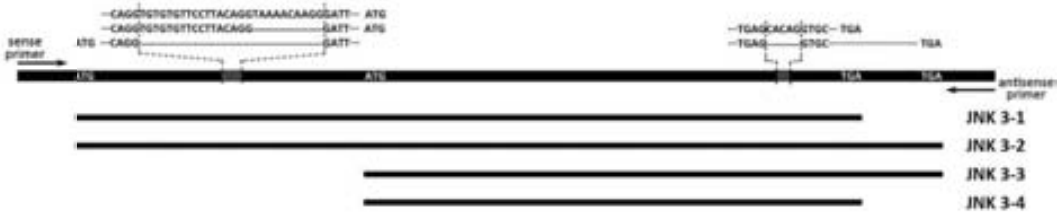

b

c

	H. sapiens	*X. laevis*
JNK3-1	**422AA**	**441AA**
JNK3-2	**464AA**	**483AA**
JNK3-3	**426AA**	**445AA**
JNK3-4	**277AA**	/
	/	**403AA**

Figure 25. **Four JNK3 isoforms were cloned from *Xenopus laevis* oocytes.** In order to clone JNK3 isoforms from *Xenopus laevis*, reverse transcription was performed using oligo (dT) as primer. PCR primers were designed based on conserved sequences in *Xenopus tropicalis* JNK3 transcripts with the sense and antisense primers residing before start codon or stop codon respectively as depicted above. Finally, 10 PCR fragments were sequenced and four different JNK3 isoforms were detected. (a) Schematic representation of *Xenopus* JNK3 isoforms. (b) JNK3-1 is quite conserved between human and *Xenopus* except for a 19aa insertion (square box) in *Xenopus* isoforms. (c) Four JNK3 isoforms are reported in humans and four were cloned in *Xenopus laevis* by RT-PCR. The table indicates the molecular weight of the predicted proteins obtained.

Sense and antisense primers were designed based on sequence before the first start codon or after the last codon of *Xenopus tropicalis* JNK3. Ten complete-coding-region clones were sequenced and four JNK3 isoforms were obtained, which demonstrates that *Xenopus laevis* stage VI oocytes contain at least four poly A JNK3 transcripts obtained by alternative splicing. Subsequently, these four JNK3 isoforms were subcloned to vector FTX5, adding a Myc tag to the N-terminal. Sequence

alignment of JNK3-1 shown that JNK3 proteins are quite conserved between human and *Xenopus laevis*, the only specificity of *Xenopus* proteins is that a distinct 19 amino acids insert was detected which leads to a higher molecular weight than human proteins (Fig.25b and c).

6.7 Ectopic expression of JNK3 isoforms does not affect meiotic progression in *Xenopus* oocytes

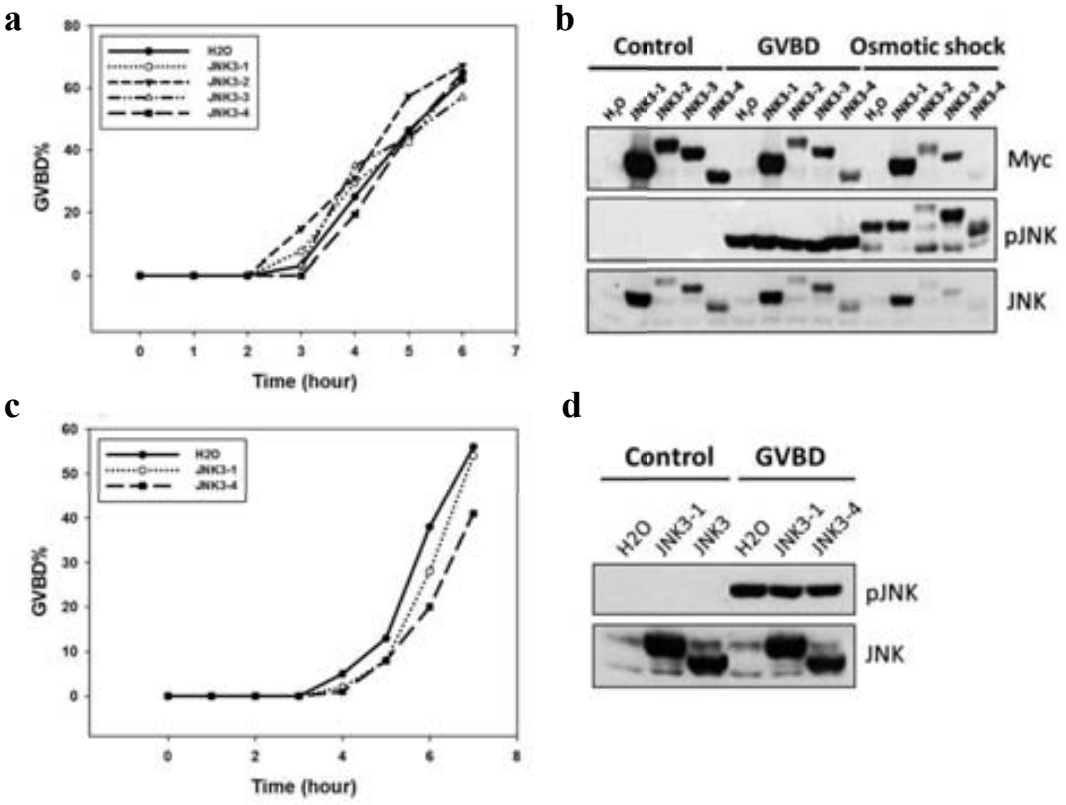

Figure 26. **JNK3 proteins are not involved in meiotic progression.** *Xenopus* JNK3-1, 3-2, 3-3, 3-4 with Myc tag or JNK3-1, 3-4 without Myc tag were overexpressed in *Xenopus* oocytes. Then oocytes were treated with progesterone or 300 mM sorbitol (osmotic shock). GVBD percentage was calculated in the oocytes treated with progesterone every hour. Samples were collected at GVBD or 1 h after osmotic shock and analyzed by western blot. (a) Overexpression of different *Xenopus* JNK3 isoforms with Myc tag in the N-terminal do not modify oocyte maturation kinetics. (b) *Xenopus* JNK3 isoforms are not phosphorylated during oocyte maturation, but are phosphorylated by hyperosmotic shock. (c) Overexpression of JNK3 isoforms 3-1 and 3-4 without Myc tag do not alter meiotic progression. (d) JNK3-1 and JNK3-4 without myc tag are detected by western blot with total JNK antibody and do not modify XpJNK-p42 levels in progesterone treated oocytes.

To confirm their characteristics and function in response to progesterone and osmotic shock, these four JNK3 isoforms with myc tag were ectopically expressed in *Xenopus* oocytes. 18 h after

microinjection of the corresponding cRNAs, the oocytes were treated either with 3 µg progesterone or 300 mM sorbitol in MBS. As shown in figure 26a, neither of these four JNK3 isoforms modified the kinetics of oocyte maturation. Western blot analysis indicated that none of the isoforms were phosphorylated at GVBD, although the proteins were well expressed (Fig. 26b). In contrast, the four JNK3 isoforms were phosphorylated in response to hyperosmotic shock, like *Xenopus* JNK1 isoforms and can be recognized by western blot with the JNK antibody (Fig. 26b).

Considering that the Myc tag may impair the molecular structure of JNK3 and that JNK3-1 and JNK3-4 have very similar molecular weights to JNK1-2 (p49) and XpJNK-p42 respectively, we cloned JNK3-1 and JNK3-4 without a Myc tag at the N-terminal. Expression of JNK3-1 or JNK3-4 without Myc tag did not affect oocyte meiotic progression (Fig. 26c). Moreover, JNK3-1 and JNK3-4 without tags did not modify the levels of expression of XpJNK-p42 induced by progesterone, although both isoforms were well detected by western blot with the total JNK antibody (Fig. 26d). Since total JNK antibody detected by western blot all the four overexpressed JNK3 isoforms, it seems that there is no expression, or tiny amounts, of endogenous JNK3 proteins in cytosolic extracts of stage VI oocytes, although the mRNAs are present.

6.8 XpJNK-p42 is a posttranslational modification of pERK2 induced by progesterone

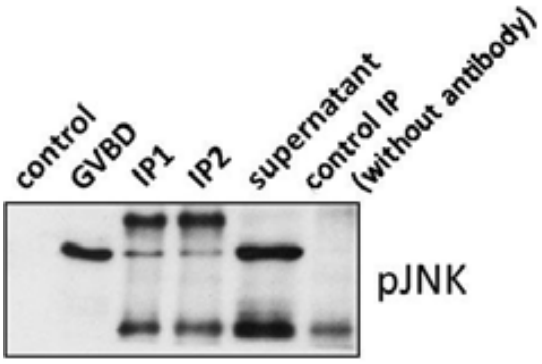

Figure 27. **The affinity of pJNK to XpJNK-p42 is weak.** In denaturing immunoprecipitation, 0.5µl pJNK antibodies were incubated with 100 µl denatured IP lysate overnight, and 20µl sepharose G proteins were added to the lysate the next day. The mixture was incubated for 2 h with gentle up-and-down shake. Two repeats were performed. For one repeat, the sepharose G proteins were then washed 3 times (IP1) and another 5 times (IP2). The sepharose G proteins were boiled in 20µl 1X Laemmli sample buffer and analyzed by western blot.

To reveal the true feature of XpJNK-p42, crosslinking immunoprecipitation and mass spectrometry analysis were performed. Denaturing protein immunoprecipitation with pJNK antibody showed that

its affinity to XpJNK-p42 was very weak (Fig. 27). To collect enough sample for mass spectrometry analysis, elution of many crosslink immunoprecipitation reactions were pooled, and concentrated by centrifugal vacuum. The final sample was run in a 10% polyacrylamide-SDS gel and stained with silver; the band corresponding to 42k Da was cut and analyzed by mass spectrometry.

Mass spectrometry analysis shown that XpJNK-p42 may be pERK2 (pMAPK1). In MS analysis report, 18 unique peptides of mitogen-activated protein kinase1 (ERK2) covering 46.81% of the whole protein were recognized (Table 10).

To prove that phosphorylated ERK2 is recognized by pJNK antibody we cloned and expressed ERK2 in *Xenopus* oocytes. Using total RNA from stage VI oocytes, we cloned by TR-PCR two different sequences corresponding to ERK2, which we named ERK2a and ERK2b that are different only in a few amino acids. These two isoforms were cloned into FTX5 plasmid and *in vitro* transcribed into cRNAs that were injected and expressed in *Xenopus* oocytes. Since the proteins expressed contain a Myc tag, they have a higher molecular weight than endogenous ERK2.

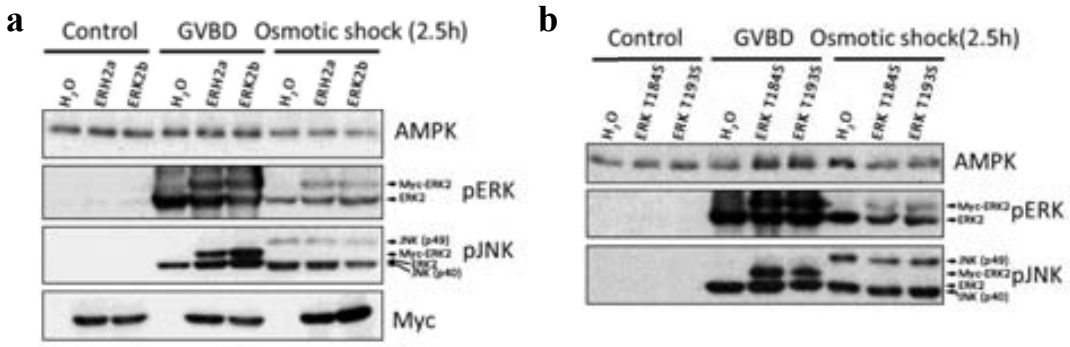

Figure 28. **The XpJNK-p42 induced by progesterone is confirmed to be pERK2.** Both wild type ERK2a and ERK2b or mutants ERK T184S and T193S of ERK2b were overexpressed in *Xenopus* oocytes. Subsequently these oocytes were treated with progesterone or 300 mM sorbitol (osmotic shock). Samples of control oocytes, mature oocytes, and 300 mM sorbitol treated oocytes (2.5 h) were collected and analyzed by western blot. (a) pERK2 induced by progesterone can be recognized by pJNK antibody but pERK2 induced by osmotic shock can not. (b) Mutations of Thr184 or Thr193 to Ser of wild type ERK2b do not affect its phosphorylation and detection by pJNK antibody.

Either progesterone treatment or osmotic shock treatment induced the phosphorylation of endogenous ERK2 and ectopically expressed ERK2a and ERK2b (Fig. 28a). Intriguingly, ERK2 phosphorylated at GVBD induced by progesterone was also recognized by pJNK antibody but not ERK2 phosphorylated by osmotic shock. Only the endogenous p49 and p40 JNK1 isoforms were detected by pJNK antibody in oocytes treated with osmotic shock (Fig. 28a). This implied that the protein recognized by pJNK antibody is pERK2 and that some posttranslational modification occurs

after progesterone treatment but not after osmotic shock treatment, which allows ERK2 to be recognized by pJNK antibody.

Potential phosphorylation sites (T184 and T193) in ERK2b around the TEY motif (170-FGLARVADPDHDH**T**(184)GFL**TEY**VA**T**(193)RWYRAPEIMLNSKGYTK -210) were mutated to Ser to scan for potential phosphorylation sites that may impair the recognition by pJNK antibody. Unfortunately, these mutations did not affect the recognition of ectopic ERK2 by pJNK antibody (Fig. 28b). Therefore, the modification induced by progesterone in ERK2 that allows recognition by pJNK antibody needs farther studies.

Table 10. Mass Spectrometry Report

Accession	Description	Score	Coverage	# Proteins	Unique Peptide	# Peptides	# PSMs	# AAs	MW [kDa]	calc. pI						
P26696	Mitogen-activated protein kinase 1 OS=Xenopu	69.08	46.81	1	16	16	21	361	41.2	6.76						
	Sequence	# PSMs	# Proteins	# Protein Groups	Protein Group Accession	Modifications	ΔCn	q-Value	PEP	XCorr	Charge	MH+ [Da]	ΔM [ppm]	RT [min]	# Missed Cleavages	
	A2	High	AIPTIEQMKDVYIVQDLMETDLYK	1	1	1	P26696		0.0000	0	8.88E-11	5.49	3	2743.36063	1.32	41.53	1	
		High	DLKPSNLLLNTTCDLK	2	1	1	P26696	C13(Carbamidomethy	0.0000	0	1.03E-11	5.41	2	1844.97832	-0.21	33.41	0	
		High	DVYIVQDLMETDLYK	1	1	1	P26696		0.0000	0	2.48E-12	5.06	2	1844.90007	0.74	41.19	0	
		High	YINLAYIGEGAYGMVCSAHDNVNK	1	1	1	P26696	C16(Carbamidomethy	0.0000	0	1.52E-10	4.31	3	2659.22916	0.43	37.88	0	
		High	TQHLSNDHICYFLYQILR	1	1	1	P26696	C10(Carbamidomethy	0.0000	0	3.61E-14	4.23	3	2321.15183	0.96	41.21	0	
		High	DVYIVQDLMETDLYK	1	1	1	P26696	M9(Oxidation)	0.0000	0	8.05E-10	4.17	2	1860.89543	0.97	36.59	0	
		High	RHENEIGINDIIR	2	1	1	P26696		0.0000	0	3.3E-08	4.05	2	1681.93718	-0.78	33.39	1	
		High	DLKPSNLLLNTTCDLKICDFGLAR	1	1	1	P26696	C13(Carbamidomethy	0.0000	0	5.46E-13	4.03	3	2777.43235	-0.08	39.17	1	
		High	ISPEHQTYQQR	2	1	1	P26696	C10(Carbamidomethy	0.0000	0	1.17E-06	3.74	2	1565.71477	-1.15	23.84	0	
		High	AIPTIEQMKDVYIVQDLMETDLYK	1	1	1	P26696	M7(Oxidation)	0.0000	0	0.000585	3.34	3	2759.35270	0.28	39.26	1	
		High	YSYGAVLVIR	1	1	1	P26696		0.0000	0	9.43E-05	2.86	4	1209.64553	-2.66	21.14	0	
		High	ALDLLDKPLTPNPVK	1	1	1	P26696		0.0000	0	0.001758	2.64	3	1755.94352	-1.98	39.12	1	
		High	GQAFDVGPR	1	1	1	P26696		0.0000	0	0.005985	2.35	2	946.47161	-2.70	23.79	0	
		High	SDPGLAR	1	1	1	P26696	C7(Carbamidomethyl)	0.0000	0	0.001036	2.17	2	951.46977	-2.04	28.21	0	
		High	ELPEETAR	1	1	1	P26696		0.0000	0	2.51E-05	2.02	2	1107.56621	-1.73	29.84	0	
		High	YINLAYIGEGAYGMVCSAHDNVNK	1	1	1	P26696	C16(Carbamidomethy	0.0000	0.002	0.03209	2.75	4	2914.39614	-6.49	37.60	1	
		High	ALDLLDK	1	1	1	P26696		0.0000	0.002	0.04711	2.26	2	787.45464	-1.78	28.54	0	
		High	NYLLSLPHK	1	1	1	P26696		0.0000	0.003	0.09383	1.53	3	1084.61249	-2.30	28.95	0	
A2RG80	Actin, cytoplasmic 2 OS=Xenopus laevis GN=ac	52.29	44.27	4	10	10	14	375	41.8	5.48						
P02350	40S ribosomal protein S3-A OS=Xenopus laevis	50.05	56.50	1	12	12	16	246	27.0	9.66						
P15308	Protein B4 OS=Xenopus laevis GN=b4 PE=1 SV	49.99	34.07	2	11	11	17	273	29.3	10.11						
Q00387	Serine protease inhibitor A6 OS=Xenopus laevis	46.97	41.97	1	10	10	12	436	49.5	8.06						
Q5U4L0	LOC100101274 protein OS=Xenopus laevis GN	45.15	37.81	1	5	8	14	320	35.3	5.25						
Q7ZY52	Glyceraldehyde-3-phosphate dehydrogenase OS	44.89	51.65	1	10	14	17	333	35.8	8.05						
Q80153	40S ribosomal protein S3a-A OS=Xenopus laevi	43.47	43.18	1	11	11	15	264	29.9	9.72						
Q6GQB2	MGC80199 protein OS=Xenopus laevis GN=gtf7	41.48	51.88	1	14	14	16	266	29.9	10.54						
P08429	60S ribosomal protein L14-A OS=Xenopus laevis	40.64	35.10	1	12	12	18	396	44.9	11.08						
Q8AY70	Glyceraldehyde-3-phosphate dehydrogenase ty	31.38	24.92	1	4	8	10	333	35.9	8.25						
Q6DJI0	40S ribosomal protein S8 OS=Xenopus laevis G	30.71	37.50	1	6	6	8	208	24.0	10.37						
Q7L2G6	Creatine kinase isozyme IV (Fragment) OS=Xen	30.55	25.76	2	7	7	9	361	40.4	6.92						
Q8AVX2	RpS6-a protein OS=Xenopus laevis GN=rps6 PE	28.63	25.34	1	6	6	8	296	34.1	9.64						
P49401	60S ribosomal protein L4 OS=Xenopus laevis G	26.41	31.56	1	9	9	10	263	29.6	10.15						
O12975	Fructose-bisphosphate aldolase OS=Xenopus la	25.48	27.20	1	6	6	8	364	39.4	8.29						
Q6DJF7	60S ribosomal protein L6 OS=Xenopus laevis G	24.59	29.84	1	6	6	10	258	29.7	10.84						
Q6P4B3	Malate dehydrogenase, cytoplasmic OS=Xenop	23.49	23.05	1	5	5	7	334	36.4	6.92						
Q3B813	MGC130910 protein OS=Xenopus laevis GN=rp	22.81	34.96	1	9	9	10	246	28.7	10.78						
Q68RQ4	RNA-binding motif protein, X chromosome OS=	22.77	17.30	1	7	7	8	370	40.3	9.98						
Q91719	Cortical granule lectin OS=Xenopus laevis GN=	21.58	23.64	1	3	6	8	313	34.3	5.67						

6.9 ¨JNK activity¨ induced by progesterone is independent of JNK and ERK2 activation

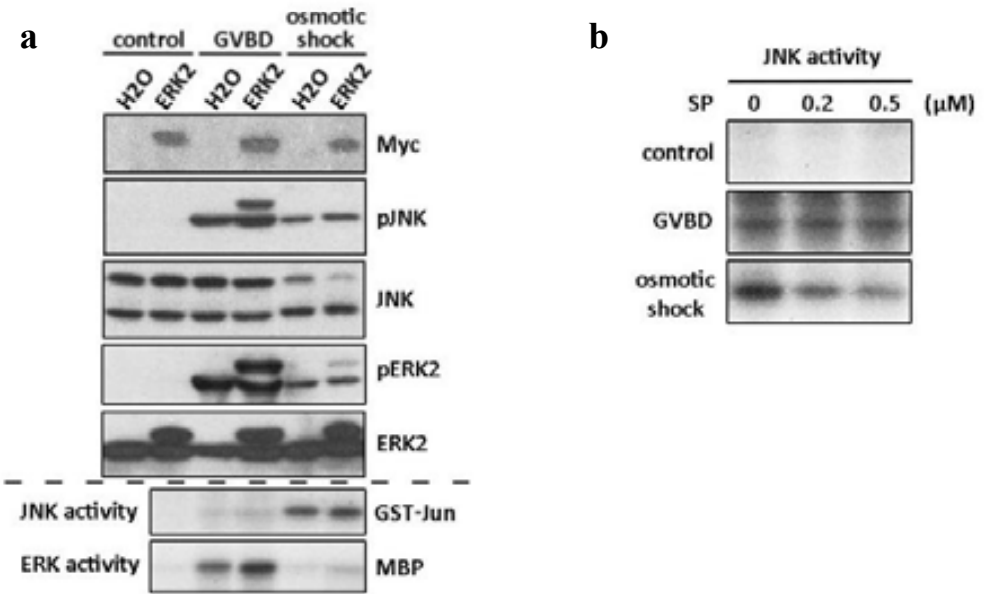

Figure 29. **JNK and ERK activities in *Xenopus* oocytes overexpressing ERK2.** Oocytes overexpressing ERK2 were treated with progesterone to induce maturation (GVBD) or with 300 mM sorbitol (osmotic shock) for 2 h. Samples of control oocytes, mature oocytes, and osmotic treated oocytes were collected and analyzed by western blot or kinase activity assay. To check the effect of JNK inhibitor on JNK activity, different concentrations (0.2 μM, 0.5 μM) of SP600125 were used. (a) Overexpression of ERK2 increases ERK activity but not JNK activity. (b) JNK inhibitor SP600125 inhibits JNK activity in osmotic shock treated oocytes but not in mature oocytes induced by progesterone (GVBD).

It has been reported that meiotic progression induced by progesterone activates JNK in *Xenopus* oocytes, measuring the activity as phosphorylation of the GST-jun substrate. (Bagowski et al. 2001a). It was also reported by the same authors that there is no significant ERK activity in oocytes subjected to hyperosmotic shock.

We analyzed the phosphorylation levels of ERK2 and JNK by western blot and measured their activity by using MBP or GST-jun as substrate, respectively, in *Xenopus* oocytes treated with progesterone to induce meiotic progression (GVBD) or in oocytes treated with osmotic shock to induce activation of the endogenous JNK1 isoforms. We compared oocytes injected with water and oocytes injected with ERK2b with a Myc tag in the N-terminal. As shown in figure 29a, expression of ERK2 did not have any significant effect on JNK or ERK phosphorylation levels in nontreated oocytes. JNK and ERK activity were also undetectable in non-treated oocytes (Fig. 29a, low panels). Progesterone treatment induced phosphorylation of ERK2, which was also detected with pJNK

antibodies, and a significant ERK activity, incremented in the oocytes expressing ectopic ERK2, but very low levels of JNK activity were observed in progesterone treated oocytes with or without expression of ectopic ERK2. On the contrary, osmotic shock induced phosphorylation of ERK2 and JNK1 and high levels of JNK activity, which was not incremented by ERK2b ectopic expression (Fig. 29a, low panel). The level of ERK2 activity induced by hyperosmotic shock was low and slightly increased by ERK2 ectopic expression. Of note, the p49 JNK1 isoform is not observed in the oocytes treated with osmotic shock, since p49 is proteolyzed when caspase-3 is activated by osmostress (see next section). In conclusion, JNK activity induced by progesterone is very low in *Xenopus* oocytes and independent of ERK2 activity.

Additionally, as shown in figure 29b, the JNK inhibitor SP600125 clearly inhibited the JNK activity induced by osmotic shock but not the JNK activity detected in mature oocytes, indicating that the GST-jun phosphorylation (JNK activity) induced by progesterone is JNK independent.

6.10 ERK signaling pathway inhibitors decrease MEKK1Δ-induced acceleration of meiosis

ERK signaling pathway is a classic cascade in regulating meiotic resumption. As described above, the protein kinase MEKK1Δ activates ERK2 without progesterone treatment. We used inhibitors of the ERK signaling pathway, U0126 or FR180204, to evaluate the contribution of ERK2 to MEKK1Δ-induced acceleration of meiosis. U0126 is a selective inhibitor of MAP kinase kinases, MEK1 and MEK2 which prevents the activation of ERK proteins (Favata et al. 1998). FR180204 is a selective and cell-permeable inhibitor of ERK proteins. The compound inhibits ERK1/2 in an ATP competitive manner and blocks their activities (Ohori et al. 2005). When oocytes were treated with the inhibitor U0126 or FR180204 18 h after microinjection of MEKK1Δ, there were no differences in maturation kinetics compared with MEKK1Δ injected oocytes without inhibitors (Fig. 30a). However, when the oocytes were pre-incubated for 1 h with the corresponding inhibitors before microinjection and also maintained in the medium after MEKK1Δ injection, there was a significant decrease in maturation in the oocytes incubated with U0126 and nearly a complete inhibition of the oocytes incubated with FR180204 (Fig. 30b).

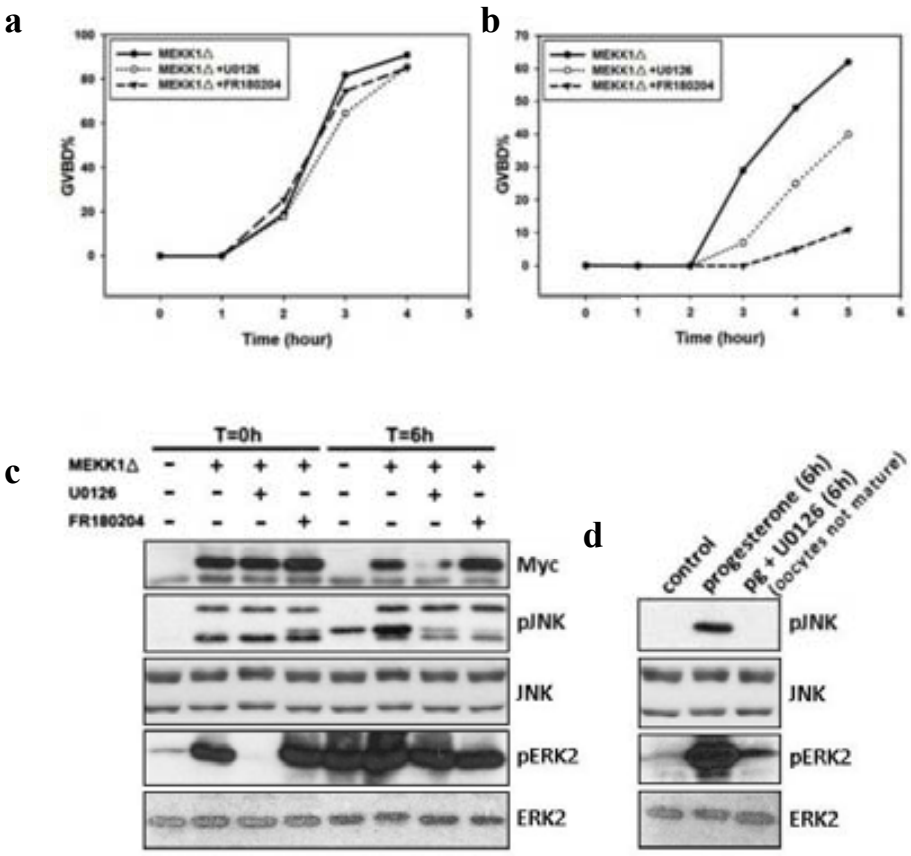

Figure 30. **Inhibitors of the ERK signaling pathway inhibitors decrease MEKK1Δ-induced acceleration of meiosis.** *Xenopus* oocytes were treated with inhibitors of the ERK signaling pathway after or before MEKK1Δ injection. These oocytes were treated with progesterone 18 h after the injection. Oocyte mature percentage was calculated every one hour and samples of control oocytes and oocytes 4 h or 5 h after progesterone treatment were collected and analyzed by western blot. (a) Oocytes incubated with inhibitors U0126 or FR180204 (50 μM) 18 h after microinjection of MEKK1Δ do not have different maturation kinetics to that of MEKK1Δ injected oocytes without inhibitors. (b) Oocytes pre-incubated for 1 h with the inhibitors U0126 or FR180204 (50 μM) and maintained in the medium after MEKK1Δ injection have reduced maturation that MEKK1Δ injected oocytes without inhibitors. (c) Western blot shown that inhibitor U0126 blocks phosphorylation of ERK2 induced by MEKK1Δ, but not induced by progesterone treatment in MEKK1Δ injected oocytes. (d) U0126 partially blocks ERK2 phosphorylation recognized by pERK antibodies and completely blocks ERK2 phosphorylation recognized by pJNK antibodies in *Xenopus* oocyte maturing process induced by progesterone.

MEKK1Δ expression induced phosphorylation of ERK2, which was completely blocked by pre-incubation with inhibitor U0126 (Fig. 30c). Not surprisingly, ERK2 was phosphorylated even in the presence of the inhibitor FR180204. These results indicate that a proper ERK function is crucial for oocyte maturation and that ERK signaling pathway activation contributes to MEKK1Δ-induced acceleration of meiosis.

Interestingly, ERK2 was phosphorylated in the presence of the inhibitor U0126 at 5 h after progesterone treatment (Fig. 30c), implying that a MEK1/2 independent signaling pathway may be responsible for ERK2 phosphorylation. In non-injected oocytes, the phosphorylation of ERK2 is markedly reduced by incubation with U0126, but not completely blocked, pointing also to a MEK1/2 independent pathway of phosphorylation (Fig. 30d). What is clear is that the levels of pERK2 (XpJNK-p42) detected with pJNK antibodies correlate quite well with the percent of mature oocytes (GVBD), whereas this is not true for pERK2 levels detected with pERK antibodies (Fig. 30c and d).

We proposed that pERK antibodies recognizes both early and late phosphorylation of ERK2, whereas pJNK antibodies recognize only late phosphorylation of ERK2, highly associated to GVBD. Of note, it is surprising that the inhibitor FR180204 increased the phosphorylation of ERK2 detected by pJNK antibodies at time 0 h (Fig. 30c). We do not have an explanation for the presence of this band in the western blot. More experiments should be performed to confirm this results and to discard that this band is not a result of JNK1-2 proteolysis, which could appear in apoptotic oocytes (see next section).

6.11 The role for p38 isoforms in regulating meiotic progression

It has been reported that ectopic expression of constitutively active MKK6-DD, an upstream kinase of p38, accelerates meiotic maturation through activation of 38γ (Perdiguero et al. 2003). Since p38 was activated by MEKK1Δ, we addressed the role of p38γ in the MEKK1Δ-induced acceleration of meiosis. As shown in figure 29a, expression of a dominant negative p38γ mutant (p38γ-DA) reduced significantly the meiotic acceleration caused by MEKK1Δ. We also addressed the role of p38 isoforms in combination with MKK6-DD, a more specific activator of the p38 signaling pathways that does not activate the JNK or ERK signaling pathways (data not shown). Co-expression of MKK6-DD with different p38 isoforms accelerated oocyte maturation to various extents depending on the combination. When p38γ and MKK6-DD were co-overexpressed in *Xenopus* oocytes, the oocytes matured spontaneously without progesterone stimulation as reported previously (Perdiguero et al. 2003). For the other p38 isoforms expressed in combination with MKK6-DD, we observed a ranking of acceleration of meiosis as follow p38δ>p38β> p38α (Fig. 31b).

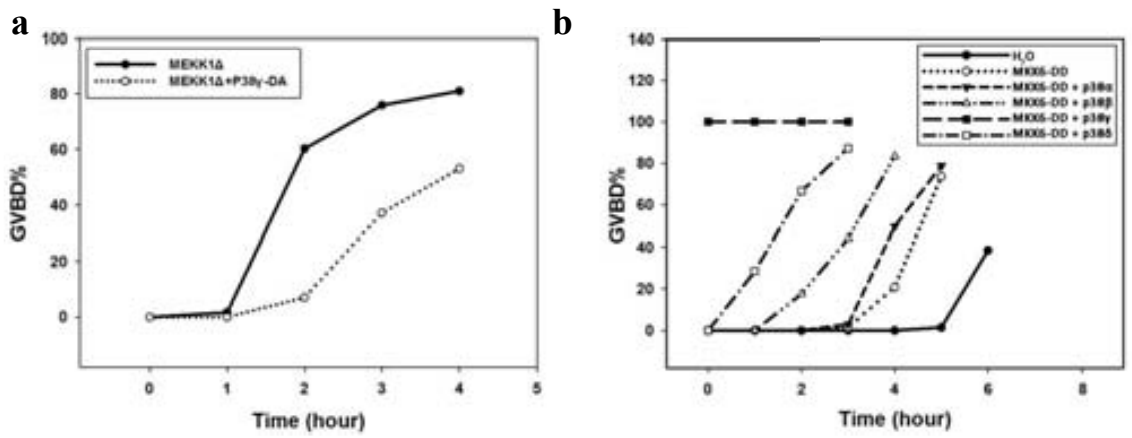

Figure 31. **p38 proteins are involved in MEKK1Δ/MKK6-DD induced meiotic acceleration.** Constitutively active MEKK1Δ or MKK6-DD were overexpressed in *Xenopus* oocytes combined with dominant negative p38γ mutant (p38γ-DA) or with different p38 wild type isoforms (p38α, β, δ, γ). Then the oocytes were treated with progesterone and GVBD percentage was calculated every one hour. (a) Catalytically inactive mutant p38γ-DA decreases MEKK1Δ-induced meiotic acceleration. (b) Constitutively active MKK6-DD combined with p38 isoforms accelerates meiotic progression.

However, when the wild type p38 isoforms or their mutants, were overexpressed, the maturation of the oocytes induced by progesterone was not affected (Fig. 32a and 32b). Western Blot indicated that all proteins were well expressed (Fig. 32c, Myc blot). The p38 total antibodies could only recognize p38α and p38γ isoforms (Fig. 32c), but all pp38 isoform can be recognized by pp38 antibodies as described before in our laboratory (Messaoud NB, Thesis Dissertation, 2014). As shown in figure 32c, overexpression of p38α and p38β slightly increased the basal phosphorylation state at time 0 h. However, progesterone treatment for 8 h did not induce any phosphorylation of the p38 isoforms (Fig. 32c). These results pose some doubts about the relevance of p38 isoforms in the regulation of meiotic progression (see discussion).

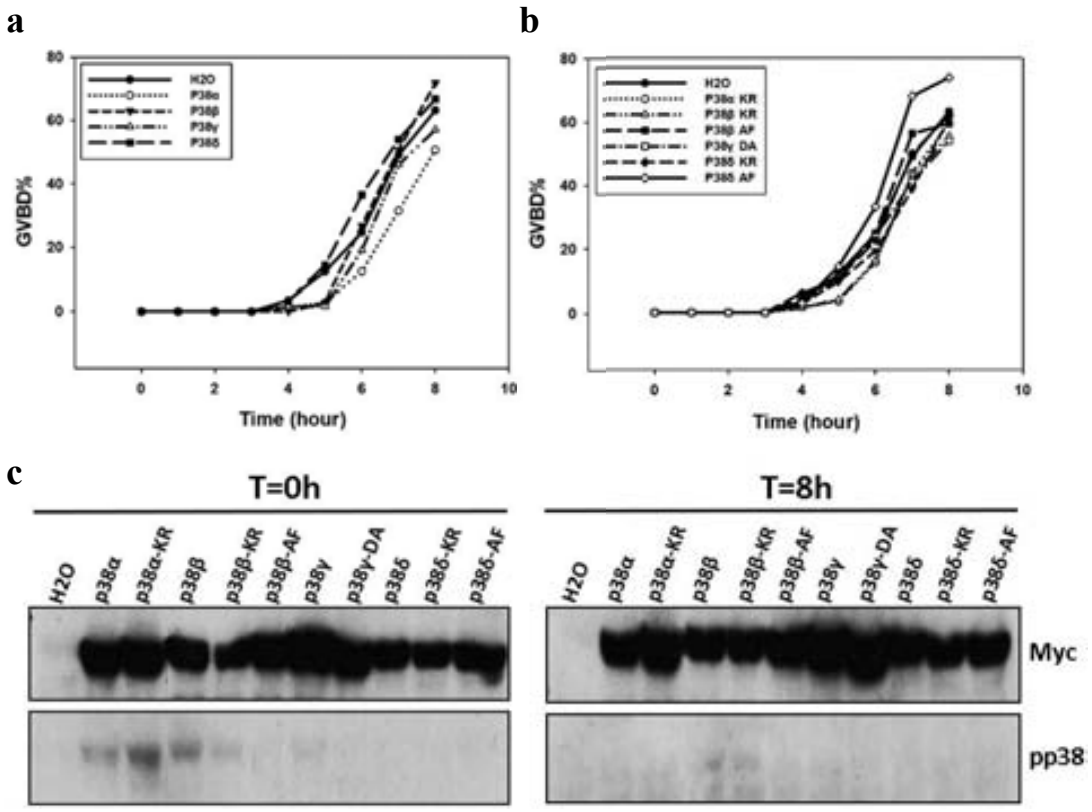

Figure 32. **p38 MAPKs might not be implicated in meiotic progression.** cRNAs of wild type p38 isoforms or their catalytically inactive mutants were injected into *Xenopus* oocytes and 18 h later these oocytes were treated with progesterone, GVBD percentage was calculated every hour and samples of oocytes at 0h and 8h were collected and analyzed by western blot. (a) Expression of wild type p38 isoforms or (b) their catalytically inactive mutants do not affect progesterone induced oocyte maturation. (c) No phosphorylated p38 proteins are detected after progesterone treatment even though these proteins are efficiently expressed. The total p38 antibody recognizes only p38α and p38γ isoforms.

B. Insights into the function of JNK1-2 and Bcl-2 family members in the regulation of osmostress-induced apoptosis.

Previous work in our laboratory has characterized in detail the time-course events during osmostress-induced apoptosis of *Xenopus* oocytes and the role of stress protein kinases, calpains, caspases, Smac/DIABLO and cytochrome c in the cell death program (Messaoud NB, Thesis Dissertation, 2014). Four independent pathways early activated by hyperosmotic shock regulate late cytochrome c release and caspase-3 activation: p38, JNK, calpains and Smac/DIABLO release. We have proposed that osmostress-induced apoptosis is basically a program of three acts: 1) rapid release of Smac/DIABLO and calpain activation, with progressive JNK/p38 phosphorylation followed by, 2) maximum and sustained JNK/p38 activity in cooperation with calpains and

Smac/DIABLO to induce the release of cytochrome c and caspase-3 activation and finally, 3) multiple feedback loops engaged by caspase-3 activation, including calpain activation and p38 phosphorylation, that would determine an irreversible death (Messaoud NB, Thesis Dissertation, 2014). We have also characterized the p38 and JNK isoforms activated by hyperosmotic shock: p38α, p38β, p38γ, JNK1-1, and JNK1-2, and we have demonstrated a clear pro-apoptotic effect in three isoforms: p38β , JNK1-1 and JNK1-2 (Messaoud NB, Thesis Dissertation, 2014). However, we did not address the role of the Bcl-2 family members in the regulation of cytochrome c release. Moreover, we realized that several hours after hyperosmotic shock the JNK1-2 isoform disappeared, suggesting some kinds of proteolysis. Here, we characterized the mechanism of JNK1-2 proteolysis induced by osmostress and its role in apoptosis. In addition, we studied the role of Bcl-2 family members, especially Bid, in the regulation of osmostress-induced apoptosis.

6.12 Osmostress induces the proteolysis of JNK1-2 by caspase-3 at Asp385 and engages a positive feedback loop increasing the release of cytochrome c and caspase-3 activation

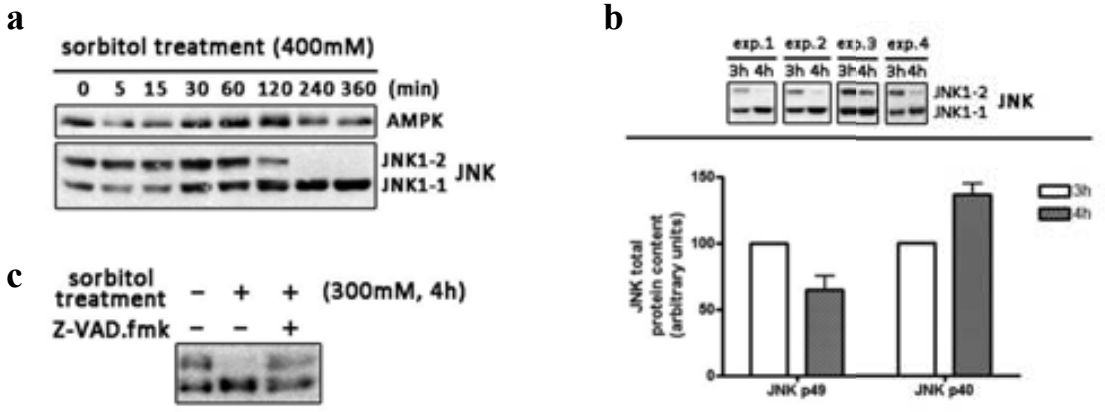

Figure 33 . **JNK1-2 was proteolyzed in osmotic shock induced apoptosis.** *Xenopus* oocytes were treated in sorbitol (300 mM/400 mM) and samples were collected at indicated times and analyzed by western blot. (a) Proteolysis of JNK1-2 induced by osmotic shock. Western blots at 3 h and 4 h were quantified by densitometry. Comparing the protein amount at 4 h to 3 h, the amount of JNK1-2 (p49) decreased about 40% while the amount of JNK1-1 (p40) increased 40% correspondingly. (b) Quantification of JNK1-2 proteolysis. When oocytes were treated by 300 mM sorbitol with the presence of pan caspase inhibitor Z-VAD.fmk, the proteolysis of JNK1-2 was inhibited. (c) JNK1-2 proteolysis is protected by Z-VAD.fmk.

Hyperosmotic shock induces a rapid activation of two JNK isoforms (JNK1-1 p40, and JNK1-2 p49) in *Xenopus* oocytes (Messaoud NB, Thesis D issertation, 2014). I ncubation of the oocy tes w ith 300mM sorbitol during several hours induced the disappearance of JNK1-2 (p49), and an apparent increase i n the b and co rresponding to JNK1-1 (p40) (Fig. 3 3a). Sev eral W estern b lots were quantified by densitometry showing that decreases in JNK1-2 were well correlated with increases in the band corresponding to JNK1-1 (Fig. 33b). The proteolysis of JNK1-2 was inhibited by the broad caspase i nhibitor Z -VAD.fmk (Fig. 3 3c), i ndicating t hat caspase-dependent c leavage of JNK1-2 resulted into a JNK1-1 like fragment.

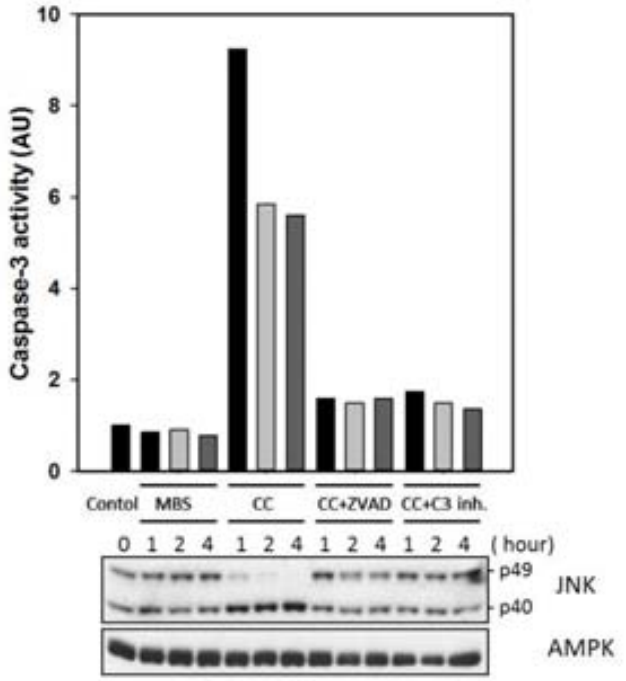

Figure 34. ***Xenopus* JNK1-2 is p roteolyzed into a J NK1-1 li ke p rotein b y caspase-3.** *Xenopus* oocytes were in jected w ith M BS o r cytochrome c (0.5µM, f inal c oncentration i n the o ocyte) then th ese o ocytes w ere trea ted with o smotic sh ock (3 00 m M so rbitol). Samples at 1 h, 2 h , 4 h were collected and analyzed b y western b lot. F or c ytochrome c injection, so me o ocytes were p reincubated with p an cas pase inhibitor Z -VAD.fmk o r caspase-3 sp ecific inhibitor Z -DEVD.fmk f or 1 h , a nd m aintained d uring osmotic sh ock treatment.

Although there are no previous reports about the proteolysis of *Xenopus* JNKs by caspases, it has been reported that human JNK1 and JNK2 are proteolyzed by caspase-3 (Enomoto et al. 2003). To address the role of caspase-3 in the proteolysis of *Xenopus* JNK1-2 we microinjected oocytes with cytochrome c, w hich has been reported t o ac tivate caspase-3 qui ckly (Bhuyan et al . 200 1). As depicted in f ig. 34, cytochrome c m icroinjection initiated r apid caspase-3 activation and disappearance of JNK1-2 (p49) with a corresponding increase of the JNK1-1 (p40) band. In contrast, when the broad caspase i nhibitor Z -VAD.fmk or t he spe cific caspase-3 i nhibitor (Z-DEVD.fmk) was present in the medium, cytochrome c microinjection did not induce JNK1-2 pr oteolysis (Fig. 34). These data clearly indicate that JNK1-2 is a substrate of caspase-3 *in vivo*.

Caspase substrate cleavage sites scanning via an online software “Cascleave” (Song et a l. 2010) indicated t hat t here a re two po tential caspase-3 cl eavage sites a t A sp385 and Asp412 at t he C-terminal of J NK1-2 (Fig. 3 5a). Therefore, w e generated t he mutants JNK1-2D385A and J NK1-

2D412A by site-directed mutagenesis, expressed them in *Xenopus* oocytes, and treated these oocytes with 300 mM sorbitol. Both mutants and the wild type JNK1-2 contained a Myc tag at the N-terminal which allowed detection with Myc antibodies by Western blot. As shown in Fig. 33b, JNK1-2D385A was not proteolyzed 3h after hyperosmotic shock, whereas JNK1-2D412A and wild type JNK1-2 were cleaved. Furthermore, truncated JNK1-2Δ385 had a similar molecular weight as cleaved wild type JNK1-2 (Fig. 35b). In contrast, truncated JNK1-2Δ412 showed a higher molecular weight than cleaved JNK1-2 and was proteolyzed after hyperosmotic shock (Fig. 35b). An additional experiment showed that cleaved JNK1-2, JNK1-2Δ385, and JNK1-1 have the same molecular weight (Fig. 35c).

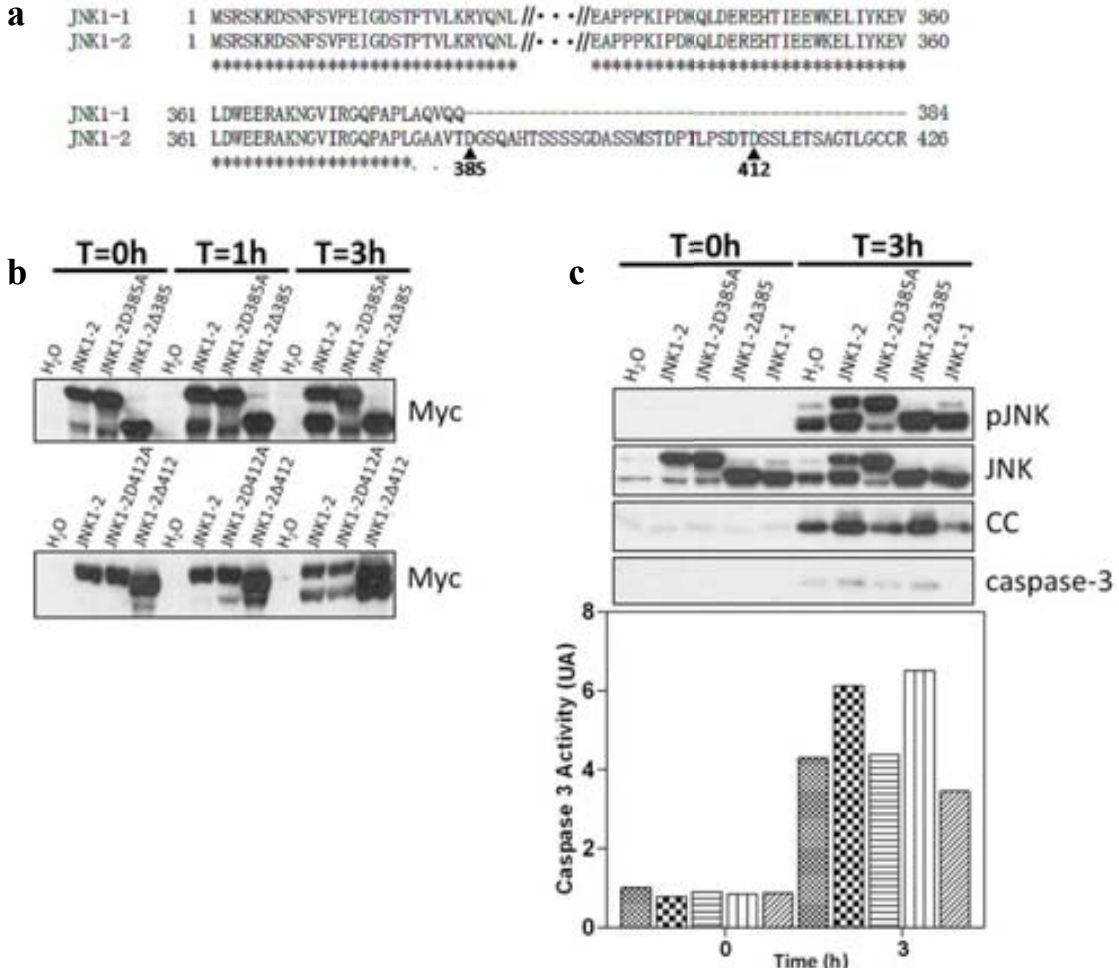

Figure 35. **JNK1-2 cleavage at Asp385 by caspase-3 positively regulates caspase-3 activation.** Wild type JNK1-1, JNK1-2 or JNK1-2 mutants JNK1-2D385A, JNK1-2Δ385, JNK1-2D412A, or JNK1-2Δ412 were overexpressed in *Xenopus* oocytes, the oocytes were then exposed to osmotic shock, samples were collected every hour and analyzed by western blot and caspase-3 assay. (a) N-terminal sequences of *Xenopus* JNK1-2, JNK1-1 and JNK1-2 proteolyzed by caspase-3. (b) Hyperosmotic shock induces cleavage of JNK1-2 at Asp385 but not at Asp412. (c) JNK1-2 cleaved at Asp385 positively regulates cytochrome c release and caspase-3 activation.

Next, we addressed the role of JNK1-2 proteolysis in the regulation of osmostress-induced apoptosis. We expressed JNK1-1, JNK1-2, JNK1-2D385A, or JNK1-2Δ385 in *Xenopus* oocytes, treated them with sorbitol 300 mM for 3 h, and measured cytochrome c release and caspase-3 activation compared with water-injected oocytes as a control. Expression of JNK1-2 increased the release of cytochrome c and caspase-3 activity induced by osmostress compared with JNK1-2D385A, JNK1-1 or water-injected oocytes (Fig. 35c). This result clearly indicates that cleavage of JNK1-2 by caspase-3 accelerates the apoptotic program via increasing the release of cytochrome c and caspase-3 activation, and therefore creates a positive feedback loop. Accordingly, expression of JNK1-2Δ385, the cleaved product of JNK1-2 by caspase-3, also enhaced the release of cytochrome c and caspase-3 activity compared with water-injected oocytes (Fig. 35c). Since expression of JNK1-2Δ385 has a clear apoptotic effect compared with JNK1-1 (Fig. 35c), this imply that the last amino acids of JNK1-2Δ385 might be important for regulating cytochrome c release and caspase-3 activation in the positive feedback loop engaged after JNK1-2 cleavage (Fig. 35a).

6.13 Cloning and expression of Bcl-2 family members in *Xenopus* oocytes

Bcl-2 family members are key proteins in regulating mitochondrial membrane permeability during apoptosis. One anti-apoptotic protein, Bcl-x_L, and three pro-apoptotic proteins (Bak, Bax, and Bid) were cloned by RT-PCR from *Xenopus* oocytes (stage VI). Bcl-x_L, Bak, and Bid were cloned into Ftx5 plasmid that contains a Myc tag at the N-terminal, whereas Bax was cloned into Ftx4 plasmid, without a Myc tag.

As shown in figure 36a, microinjection of Bak, Bax or Bid cRNAs induced rapid caspase-3 activity, without osmotic shock treatment, and the membrane of the oocytes was broken 16 h later (data not shown). However, microinjection of Bcl-x_L cRNA did not alter oocyte morphology and did not induce caspase-3 activity, even 18 h after microinjection. Importantly, overexpression of Bcl-x_L blocked caspase-3 activation induced by osmostress (Fig. 36a). Expression of Bcl-2 family members was monitored by Western blot using Myc antibodies. As shown in Fig. 36a, Bcl-x_L was located in the mitochondria before and 4 h after hyperosmotic shock. When we analyzed expression of Bak and Bid 3 h after microinjection of the corresponding cRNAs, most of Bak protein was located in the mitochondria while almost equal amounts of Bid were located both in the mitochondria and the cytosol (Fig. 36a). However, the amounts of Bak and Bid decreased markedly at 18 h after microinjection of the corresponding cRNAs (Fig. 36a). The localization of Bax was not

monitored in the present experiment because it was not Myc tagged. An unspecific band was detected with the Myc antibodies in all the lanes and is marked with an asterisk (*) in the Western blot.

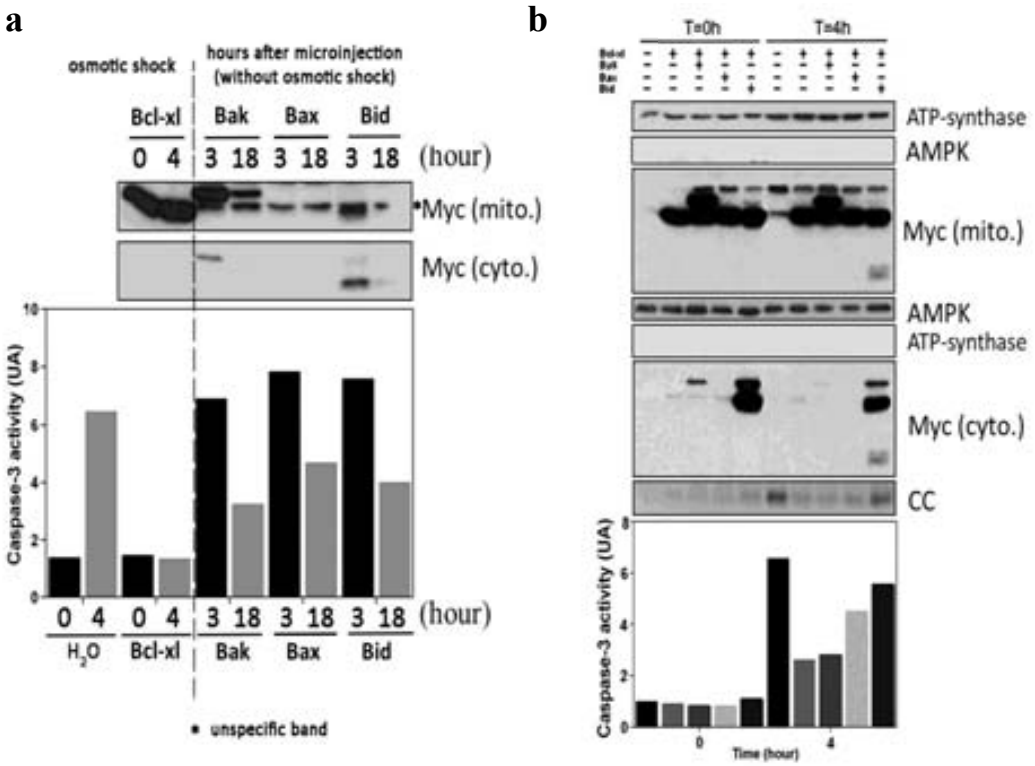

Figure 36. **Bcl-2 family proteins in *Xenopus* oocytes.** (a) Bak, Bax or Bid induce caspase-3 activation while Bcl-x_L blocks osmotic shock-induced caspase-3 activation. cRNAs of Bcl-2 family members were injected into *Xenopus* oocytes, for pro-apoptotic members samples were collected 3 h and 18 h after microinjection. For Bcl-x_L, the oocytes were exposed to osmotic shock 18 h after microinjection, and samples were collected at 0 h and 4 h after treatment. Samples were analyzed by western blot and caspase-3 activity assay. (b) Co-expression of Bcl-x_L with Bak, Bax or Bid and subcellular localization in response to osmotic shock. Pro-apoptotic proteins were coexpressed with Bcl-x_L, then oocytes were exposed to osmotic shock and samples were collected at 0 h and 4 h and analyzed by western blot and caspase-3 activity assay.

When Bcl-x_L was expressed in combination with any of these pro-apoptotic proteins, it saved the oocytes from apoptosis, since there was not caspase-3 activation even 18 h after microinjection (Fig. 36b, lower graphic, time 0 h). In these conditions, Bcl-x_L and most Bak protein were located in the mitochondria; however, unlike described above, a higher amount of Bid protein seems to be present in the cytosolic fraction (Fig. 36b, upper panel), although this Western-blot does not allow to differentiate Bcl-x_L and Bid mitochondrial proteins, cause they have similar molecular weight (see next section to clarify this point). After osmotic shock treatment, the amounts of cytosolic Bak and Bid decreased. Intriguingly, a short fragment with Myc tag was detected 4 h after osmostress in the

oocytes microinjected with Bcl-x_L and Bid (Fig. 36b). In this experiment we cannot conclude whether this fragment came up as a consequence of Bcl-x_L or Bid proteolysis, since both proteins are Myc tagged. This issue will be addressed in the next section. When we analyzed cytochrome c release and caspase-3 activation induced by osmostress in all sets of combinations, we observed that Bcl-x_L expression preserved from osmostress-induced apoptosis the oocytes expressing Bak, but not the oocytes expressing Bid, and with partial protection the oocytes expressing Bak (Fig. 36a, lower graph, time 4 h). Note that in this experiment, Bcl-x_L did not block as described in Fig. 36a, but markedly reduced osmostress-induced apoptosis (Fig. 36b).

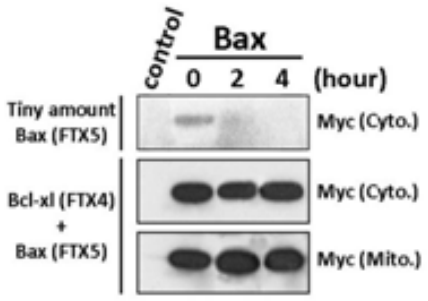

Figure 37. **Bax expression and localization in *Xenopus* oocytes.** Tiny amount of cRNA of FTX5-Bax (upper blot) or combination of FTX4-Bcl-x_L and FTX5-Bax (middle and bottom blots) were injected into *Xenopus* oocytes. Oocytes were exposed to osmotic shock 18 h after microinjection, and samples were collected at 0 h, 2 h, 4 h and analyzed by western blot.

To address properly the distribution of Bax in *Xenopus* oocytes, we cloned the complete sequence into Ftx5 plasmid to add a Myc tag at the N-terminal, and the Bax cRNA was microinjected and expressed in the oocytes. Interestingly, when tiny amount of Bax cRNA were injected to obtain low levels of protein (Fig. 37), oocytes survived and caspase-3 was not activated (data not shown). However, in this condition osmotic shock treatment induced the disappearance of Bax protein in the cytosol, suggesting that a protease activated by osmotic shock might cleave its N-terminal (Fig. 37). When Bax was expressed in higher amounts in combination with Bcl-x_L (not Myc tagged), about half of the Bax protein was located in the mitochondrial fraction and osmotic shock did not induce a significant proteolysis of Bax located in the cytoplasm or in the mitochondria (Fig. 37). However, the western blot suggests that maybe small amounts of cytosolic Bax are translocated to the mitochondria at 2 h after hyperosmotic shock (Fig. 37).

6.14 Bid and mono-ubiquitinated Bid are proteolyzed during osmostress-induced apoptosis in *Xenopus* oocytes

In order to confirm which protein, Bcl-x_L or Bid, is proteolyzed during osmostress-induced apoptosis (Fig. 36d), two different combinations of Bcl-x_L and Bid cRNAs were injected in

Xenopus oocytes: FTX5-Bcl-x_L/FTX4-Bid or FTX4-Bcl-x_L/FTX5-Bid. This allowed us to express high levels of both proteins without any apoptotic effect on untreated oocytes and to detect by Western blot Bcl-x_L or Bid, when the Myc tag is attached at the N-terminal (FTX5 constructs).

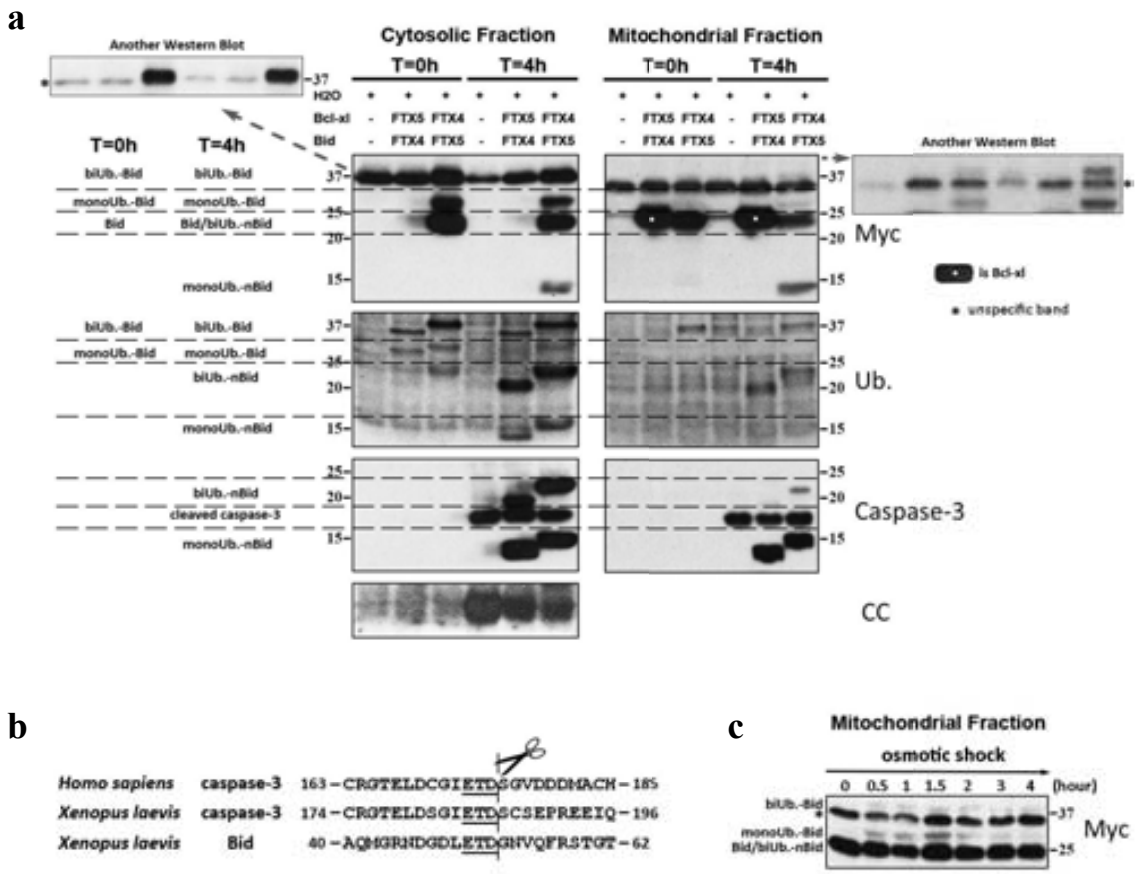

Figure 38. **Bid is ubiquitinated and cleaved during osmotic shock-induced apoptosis.** Two protein combinations (FTX5-Bcl-xL/FTX4-Bid or FTX4-Bcl-xL/FTX5-Bid) were overexpressed in *Xenopus* oocytes. These oocytes were then exposed to osmotic shock. Samples were collected at different times and analyzed by western blot. (a) Bid is mono-and bi-ubiquitinated in *Xenopus* oocytes and osmotic shock induces proteolysis of Bid and monoUb.-Bid, generating N-terminal fragments of Bid that can be recognized by ubiquitin antibodies and by cleaved caspase-3 antibodies. (b) Sequence alignment of *Xenopus* Bid with caspase-3 proteins indicates that the potential cleavage site in Bid is similar to caspase-3 activation cleavage site. c) Osmotic shock induces a slight and rapid increase of monoUb.-Bid and biUb.-Bid in the mitochondrial fraction.

As shown in figure 38 non-treated oocytes (T= 0h) expressed Bcl-x_L (23 kDa, but 24.5 kDa with myc tag) in the mitochondria (second lane of the blots), whereas approximately 50% of Bid (21 kDa, but 22.5 kDa with myc tag) was located in the mitochondria and 50% in the cytosol (third lane of the blots, only Myc tagged proteins were observed in each combination). Besides the 22.5 kDa Bid band, another two extra bands (31 kDa and 39 kDa) were clearly detected in the cytosolic fraction, with little amounts also present in the mitochondria (see additional Western blots on the sides of

Figure 38a). An unspecific protein (*) detected with Myc antibodies overlapped with the 39 kDa Bid protein, but in some Westerns, as shown in the side blots of figure 38a, the background was lower and the proteins separated better. It has been reported that Bid expressed in *Xenopus* egg extracts can be detected as mono and biubiquitinated forms (Saitoh et al. 2009), and since ubiquitin has an expected molecular weight of 8.5 kDa, this could explain the two extra bands obtained in our blots. Western blot analysis with ubiquitin antibodies confirmed that these two bands corresponded to mono- and bi-ubiquitinated Bid (monoUb.-Bid and biUb.-Bid) (Fig. 38a, middle panel). The bands detected with ubiquitin antibodies corresponded to Bid protein confirmed by the shift in molecular weight of Bid caused by the Myc tag attached at the N-terminal (compare lanes 2 and 3, middle panel in Fig. 38a). In the mitochondrial fraction it was detected the bi-Ub.-Bid (39 kDa), but not the mono-Ub.-Bid (31 kDa) by using the ubiquitin antibodies, although in the Western blot using Myc antibodies the amounts of mono-Ub.-Bid and biUb.-Bid looked quite similar (Fig. 38a top and side blots). We speculate that this might be due to some posttranslational modification in the mitochondrial mono-Ub.-Bid pool which could interfere with its ubiquitin detection by Western blot. Alternatively, low amounts of mono-ub.-Bid in the mitochondria are not well detected with the ubiquitin antibody.

We can conclude that in untreated oocytes Bid exists in three different forms: Bid, monoUb.-Bid and biUb.-Bid. Bid is located in the cytosol and the mitochondria (probably interacting with Bcl-x_L), whereas monoUb.-Bid and biUb.-Bid are mainly located in the cytosol, although some little amounts of biUb.-Bid and modified Ub.-Bid might be located in the mitochondria (see Fig. 47, Bid ubiquitination model). After osmotic shock, a 15 kDa band was detected both in the cytosolic and mitochondrial fractions in the combination FTX4-Bcl-x_L/FTX5-Bid but not in the combination FTX5-Bcl-x_L/FTX4-Bid (Fig. 38a, compare lanes 5 and 6 in the upper panels), which means that this fragment resulted from cleavage of Bid instead of Bcl-x_L. Western Blot shown that this 15 kDa band was ubiquitinated, and the shift in molecular weight induced by Myc tag at the N-terminal indicated that this was the N-terminal of Bid (Fig. 38a, lanes 5 and 6 middle panel). In consideration of the molecular weight of ubiquitin (8.5 kDa) and the molecular weight expected for nBid after caspase cleavage of Bid (6 kDa) (Kominami et al. 2006, Saitoh et al. 2009), this 15 kDa band might be mono-ubiquitinated N-terminal of Bid (monoUb.-nBid) (expected molecular weight 14.5 kDa, but 16 kDa with myc tag). Another pair of ubiquitinated bands (22 and 23 kDa) with a molecular weight shift caused by Myc was detected too, and must correspond to biubiquitinated N-terminal of Bid (biUb.-nBid). biUb.-nBid was detected by Western blot with ubiquitin antibodies in both the cytosolic and the mitochondrial fractions, whereas monoUb.-nBid was mainly detected in the cytosol, with very small amounts in the mitochondria (Fig. 38b, lanes 5 and 6 middel panel). The

above results clearly indicate that hyperosmotic shock induces Bid cleavage at a specific site in the N-terminal. Osmostress induced the proteolysis of Bid and monoUb.-Bid since the amount of both proteins were reduced in the cytosol (Fig. 38a). Note that the reduction Bid induced by osmostress was difficult to appreciate with Myc antibodies due to the generation of biUb.-nBid, which has a similar molecular weight to Bid (22,5 kDa for Bid and 24 kDa for biUb.-nBid), but careful inspection of the blot at higher resolution clearly indicated the presence of the two bands. Although Bid and monoUb.-Bid decreased in the cytosol after osmotic shock treatment, the amount of cytosolic biUb.-Bid was maintained quite constant (Fig. 38a). In addition, monoUb.-nBid and biUb.-nBid accumulated in the cytosol, whereas only significant amounts of biUb.-nBid accumulated in the mitochondria. Therefore, it seems that biUb.-nBid came from the ubiquitination of monoUb.-Bid instead of direct cleavage of biUb.-Bid. In addition, osmotic shock quickly induced a slightly increase of monoUb.-Bid and biUb.-Bid in the mictochondrial fraction (Fig. 38c. lane 2 at 30 min after treatment; and Fig. 38a, side blot at 4 h after treatment). All this information is depicted as a working Bid ubiquitination model (Fig. 47).

In traditional signaling pathways, Bid is cleaved by caspase-8 generating the so called tBid fragment to regulate the mitochondrial outer membrane permeability. For *Xenopus* Bid, this cleavage site has been reported at Asp52 (Kominami et al. 2006). As shown in Figure 38b, Bid proteolysis at Asp52 exposes three amino acids (-ETD-), similar to activated caspase-3. It has been reported that cleaved-Caspase-3 antibody from Cell Signaling Technology (Ref. #9661) recognizes the epitope –ETD, and therefore it can be used for detection of other caspase-9 substrates (Fan Yun and Bergmann 2009). Since the epitope –ETD at N-terminal fragment of Bid (nBid) is identical to cleaved caspase-3, it should be detected by the Cell Signaling antibody. As shown in Fig. 38a, lower panel, besides of the activated caspase-3 (18kDa) extra bands corresponding to monoUb.-nBid and biUb.-nBid were recognized by caspase-3 antibody, thus confirming the identity of the Bid fragments. Interestingly, the mitochondrial fraction showed high levels of monoUb.-nBid detected with the cleaved-caspase 3 antibodies from Cell Signaling, whereas the Western blot with ubiquitin antibodies only detected small amount of monoUb.-nBid. We speculate, as described above for the mitochondrial monoUb-Bid, that some modification in the mitochondrial pool of monoUb.-nBid might exist. Actually, a tiny shift of mitochondrial monoUb.-nBid respect to cytosolic monoUb.-nBid was observed (data not shown).

6.15 Hypeosmotic shock induces Bid proteolysis by initiator caspases and by caspase-3

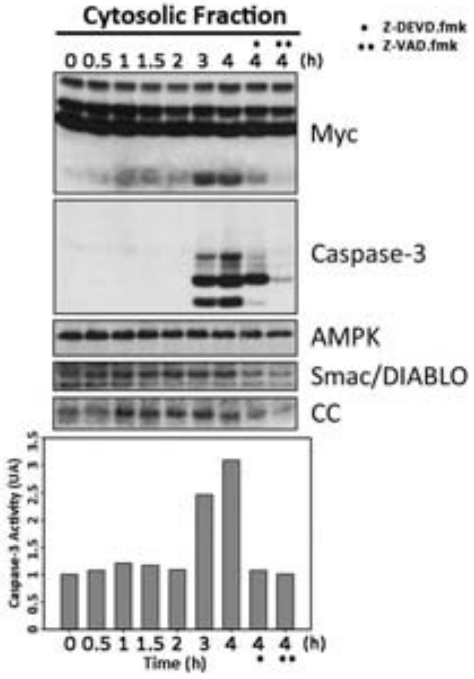

Figure 39. **Hyperomotic shock induces early and late proteolysis of Bid Bid by caspases.** cRNA combination of FTX4-Bcl-xL and FTX5-Bid was injected into *Xenopus* oocytes and 18 h later the oocytes were exposed to osmotic shock in the presence or absence of caspase inhibitor, samples were collected at different times and analyzed by western blot and caspase-3 activity.

Next, we analyzed the proteolysis of Bid induced by osmostress in a time-course experiment. Hyperosmotic shock induced weak proteolysis of Bid at 1 h, detected by the appearance of a 15 kDa band corresponding to monoUb.-Bid as determined in the previous section, which was synchronized with Smac/DIABLO and cytochrome c release (Fig. 39, compare Myc with Smac/DIABLO and cytochrome c blots). At 1 h a significant amount of cytochrome c was realeased into the cytosol, but no caspase-3 activity was detected by Western blot or by enzymatic assay (Fig. 39, lower blot and graph). At 3 and 4 h after osmostress caspase-3 activity was detected by Western blot and by enzymatic assay, which was well correlated with a marked proteolysis of Bid (Fig. 39, upper panel and lower graph). Incubation with the specific caspase-3 inhibitor Z-DEVD.fmk clearly reduced Bid proteolysis at 4 h, measured by quantification of cytosolic monoUb.-nBid with the Myc antibody or by quantification of monoUb.-nBid and biUb.-nBid cytosolic fragments with the Cell Signaling cleaved-caspase-3 antibody (Fig. 39, middle panel, compare samples at 4 h in the presence or absence of inhibitor). Note that caspase-3 inhibitor markedly reduced, but did not block completely the generation of monoUb.-nBid and biUb.-nBid. The cleavage of caspase-3, supposedly induced by caspase-9, was unchanged in the presence of caspase-3 inhibitor as expected, but it was near completely blocked with the broad caspase inhibitor Z-VAD.fmk. Bid proteolysis,

measured as monoUb.-nBid fragment detected with Myc antibodies or as monoUb.-nBid and biUb.-nBid detected with cleaved-Caspase 3 antibody, was completely blocked by Z-VAD.fmk (Fig. 39). Of note, Smac/DIABLO and cytochrome c release induced by osmostress at 4 h were slightly reduced in the presence of caspase-3 inhibitor, and more clearly decreased in the presence of Z-VAD.fmk (Fig. 39 lower blots). We have previously reported that Smac/DIABLO release is a very early event in osmostress-induced apoptosis and both Smac/DIABLO and cytochrome c release decrease in the presence of Z-VAD.fmk due to inhibition of several positive feedback loops (Messaoud NB, Thesis Dissertation, 2014). In addition, previous results suggest that Z-VAD.fmk delays osmostress induced apoptosis by inhibition of a caspase distinct to caspase-3 (Messaoud NB, Thesis Dissertation, 2014). Altogether, the above results suggest that Bid seems to be proteolyzed in low amounts by an initiator caspase that might be activated by early Smac/DIABLO release and low amounts of cytochrome c in the cytosol, and when caspase-3 is fully active, a massive proteolyisis of Bid occurs, which can be clearly detected by Western blot. The proteolysis of Bid induced by osmostress was accelerated by co-expression of Bax in oocytes expressing Bid and Bcl-x_L (Fig. 40), confirming that changes in the equilibrium between pro- and anti-apoptotic members of the Bcl-2 family can modify the kinetics of omostress-induced apoptosis via regulating mitochondrial protein release.

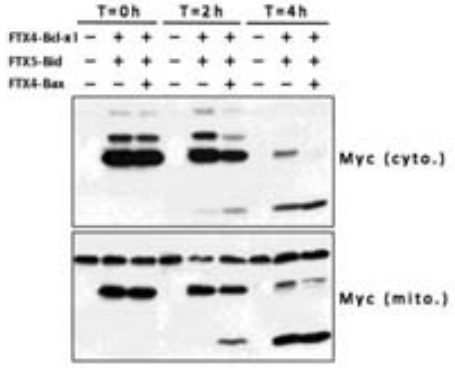

Figure 40. **Bax overexpression accelerates the Bid proteolysis induced by osmotic shock.** Two cRNA combinations, FTX4-Bcl-x_L + FTX5-Bid or FTX4-Bcl-xL + FTX5-Bid + FTX4-Bax, were injected into *Xenopus* oocytes and 18 h later oocytes were exposed to osmotic shock. Samples were collected at different times and analyzed by western blot.

We have previously reported that hyperosmotic shock induces early calpain activation, which contributes to regulate osmostress-induced apoptosis (Messaoud NB, Thesis Dissertation, 2014). Calpains have been reported to proteolyze Bid and Bax at the N-terminal (Gao and Dou 2001, Mandic et al. 2002). In addition, it has been reported that in Fas-induced apoptosis JNK activation can mediate Bid proteolysis generating a specific jBid fragment by a yet unknown protease (Deng Yibin et al. 2003). Therefore, we treated oocytes with a specific calpain inhibitor or expressed a constitutive active MKK7 mutant (MKK7DED) kinase to activate endogenous JNK1-1 and JNK1-2 to address the roles of these signaling pathways in Bid proteolysis induced by osmostress. As shown in Fig. 41 the calpain inhibitor MDL28170 did not have any significant effect on Bid proteolysis at

4 h after osmostress, measured as the amount of monoUb.-Bid fragment detected with Myc antibodies, even though the inhibitor decreased the activation of caspase-3 induced by osmostress (Fig. 41, compare in caspase-3 graph Bcl-x_L + Bid with or without MDL28170). Indeed, expression of MKK7DED induced the phosphorylation of JNK1-1 and JNK1-2 (Fig. 41, time 0 h of Bcl-x_L + Bid + MKK7-DED) but did not change Bid proteolysis and caspase-3 activity induced by osmostress. As a control, Z-VAD.fmk efficiently blocked Bid proteolysis and caspase-3 activation.

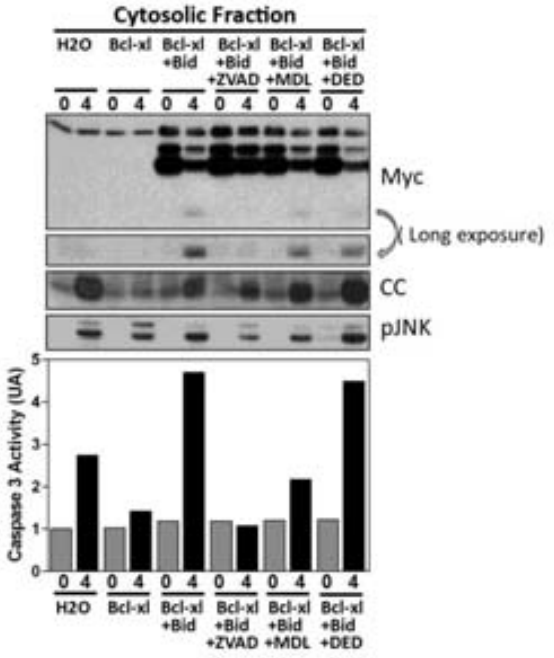

Figure 41. **Calpain inhibitor sustained JNK activation does not alter Bid proteolysis induced by osmostress.** cRNA combination of FTX4-Bcl-xL and FTX5-Bid was injected into *Xenopus* oocytes and 18 h later the oocytes were exposed to osmotic shock in the presence or absence of pan caspase inhibitor Z-VAD.fmk or calpain inhibitor MDL28170 and samples were collected at 4 h and analyzed by western blot and caspase-3 activity. Some oocytes were injected with H_2O or Bcl-x_L cRNA and 18 h later exposed to osmotic shock for 4 h and samples analyzed as described above.

The previous results clearly show that Bid is mainly proteolyzed by caspase-3 at later times of osmostress and that it might be proteolyzed early at low levels by an initiator caspase. To address whether the role of cytochrome c release in the proteolysis of Bid is independent of other signaling patways activated by osmostress, we microinjected cytochrome c (0.5µM, final concentration) in *Xenopus* oocytes expressing Bcl-x_L and Bid, and the cleaved products of Bid by Western blot in the presence or absence of caspase inhibitors. As expected, cytochrome c induced a high caspase-3 activity 1 h after microinjection without any osmotic shock stimulation, and both, the specific caspase-3 inhibitor or the pan-caspase inhibitor Z-VAD-fmk, completely inhibited caspase-3 activity, measured by the enzymatic assay (Fig. 42). Western blot analysis with the cleaved-caspase-3 Cell Signaling antibody showed a marked proteolysis of caspase-3 and Bid in the presence or absence of inhibitors, suggesting that the apoptosome formation and activation was not impaired by the inhibitor Z-VAD.fmk when an excess of cytochrome c existed in the cytosol (Fig. 42). Considering the similar aminoacids residues around the cleavage site of both caspase-3 and Bid

(Fig. 38b), it seems probable that caspase-9 mediates Bid cleavage at Asp52 when high levels of cytochrome c are present in the cytosol.

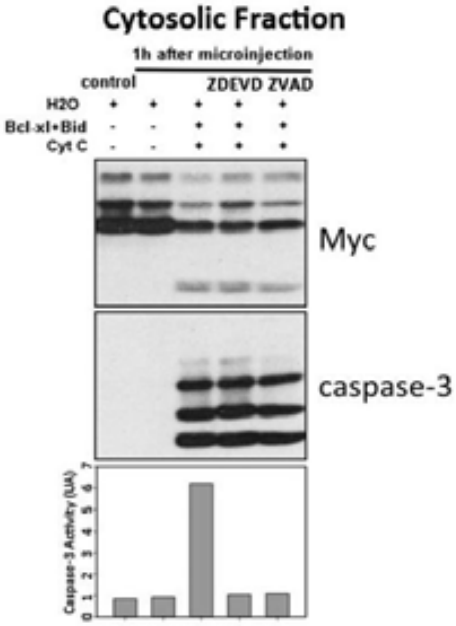

Figure 42. **High amount of cytochrome c induces Bid cleavage even when caspase-3 activity is inhibited.** cRNA combination of FTX4-Bcl-x_L and FTX5-Bid was injected into *Xenopus* oocytes and 18 h later a second microinjection of cytochrome c was performed. Samples were collected 1 h later and analyzed by western blot and caspase-3 activity assay.

Potential initiator caspases activated during osmostress that might induce Bid cleavage include caspase-8, caspase-9 and caspase-10. We could not clone caspase-8 in stage VI oocytes, but it has been reported very low levels, if any, of caspase-8 in *Xenopus* oocytes at stage VI, and high levels at stages 15/16 in early embryogenesis. However, caspase-10 is reported to be highly expressed in stage VI oocytes (Kominami et al. 2006). We cloned caspase-10 from stage VI oocytes and expressed with a Myc tag at the N-terminal in the presence or absence of the usual combination Bcl-x_L and Bid. Low amounts of caspase-10 were expressed in the oocytes 4 h after cRNA injection, and high levels of cytochrome c were detected in the cytosol (Fig. 43), indicating that a small increase of caspase-10 in the oocyte induces apoptosis. The combined expression of caspase-10 with Bcl-x_L and Bid induced the release of cytochrome c and the proteolysis of Bid (Fig. 43), as expected. Although we do not know whether Bid proteolyisis is mediated directly by caspase-10 or indirectly by activation of caspase-9 or caspase-3, there are reports describing in vitro direct proteolyisis of Bid by *Xenopus* caspase-10β (Kominami et al. 2006) or by human caspase-10 (Milhas et al. 2005). Future experiments will address whether caspase-10 is activated early by osmostress and their role in primary Bid cleavage.

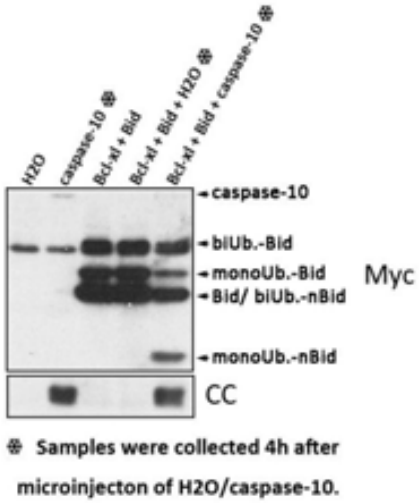

Figure 43. **Expression of caspase-10 induces Bid proteolysis and cytochrome c release.** cRNA combination of FTX4-Bcl-xL and FTX5-Bid was injected into Xenopus oocytes and 18 h later a second microinjection of caspase-10 was performed and samples were collected 4 h later and analyzed by western blot. Some oocytes were injected only with H_2O or caspase-10 cRNA and samples were collected 4 h later.

6.16 Osmostress-induced proteolysis of Bid at Asp52 engages a positive feedback loop increasing cytochrome c release and caspase-3 activation

As we described above, osmostress induces two important modifications in Bid: ubiquitination and cleavage. It has been reported that *Xenopus* Bid is mono-ubiquitinated and di-ubiquitinated in egg extracts, and three sites (K18/21/37) at the N-terminal of *Xenopus* Bid (not conserved in human Bid) were found to be important for ubiquitination. In addition, *Xenopus* Bid has been reported to be cleaved by caspases at Asp52 (Kominami et al. 2006, Saitoh et al. 2009). Therefore, to investigate the function of Bid ubiquitination and cleavage in osmotic shock-induced apoptosis, wild type Bid, triple mutant Bid-K18/21/37R (Bid-nonUb) or mutant Bid-D52N were expressed in *Xenopus* oocytes in combination with Bcl-x_L, and then the oocytes were submitted to hyperosmotic shock. Western Blot shown that mutant Bid-D52N cannot be proteolyzed by osmostress in contrast to wild type Bid or Bid-nonUb (Fig. 44a, see the disappearance of cytosolic Bid in the middle panel). Proteolysis of wild type Bid generated the 15 kDa fragment corresponding to monoUb.-nBid, which was not observed after proteolysis of Bid-nonUb, as expected. Note that proteolysis of wild type Bid also generates biUb.-nBid, as reported previously, which overlaps with Bid in Western blot detection. This explains why Bid-nonUb proteolysis looked apparently faster than wild type Bid (Fig. 44a, see levels of cytosolic Bid at 4 h after treatment). However, this is probably due to the absence of biUb.-nBid after proteolyisis of Bid-nonUb (Fig. 44b).

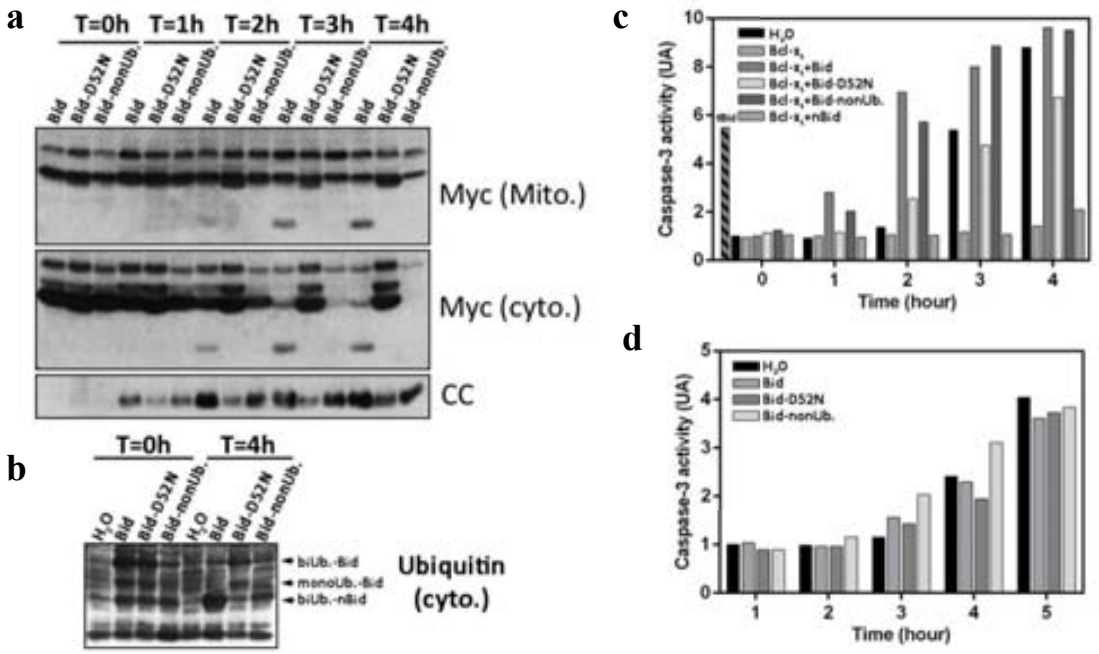

Figure 44. **Functional effects of Bid modification on osmostress-induced apoptosis.** Wild type Bid or mutants combined with FTX4-Bcl-x_L or tiny amount of these proteins were expressed in *Xenopus* oocytes. Then oocytes were exposed to osmotic shock and samples were collected at different times and analyzed by western blot or caspase-3 activity assay. (a) Site-directed mutation of Bid at Asp52 (Bid-D52N) blocks its proteolysis in osmotic shock-induced apoptosis and reduces cytochrome c release. (b) The triple mutant Bid-K18/21/37R (Bid-nonUb) presents marked reduction of ubiquitination before and after hyperosmotic shock treatment. (c) Caspase-3 activity in response to osmostress in oocytes expressing wild type Bid or mutants combined with Bcl-x_L. (d) Caspase-3 activity in response to osmostress in oocytes expressing tiny amount of wild type Bid or mutants.

In an additional experiment, where osmostress-induced apoptosis was accelerated by the expression of Bax in combination with wild type Bid or mutant Bid-nonUb, we detected increased levels of nBid in the oocytes expressing Bid-nonUb. suggesting that Bid-nonUb. might be proteolyzed faster than wild type Bid (Fig. 45).

Ubiquitination analysis by Western blot indicated that Bid-nonUb presented a clear reduction of the mono- and bi- ubiquitinated bands before treatment and also of the bi-ubiquitinated-N-terminal fragment (biUb.-nBid) after osmotic shock, compared with the wild type Bid (Fig. 44b). Despite this marked reduction, low levels of ubiquitination were still detected in the Bid-nonUb mutant (Fig. 44b), as previously reported by other authors (Saitoh et al. 2009). Importantly, expression of mutant Bid-nonUb did not modify cytochrome c release and caspase-3 activation induced by osmostress, compared with wild type Bid, whereas mutant BidD52N clearly reduced cytochrome c release and caspase-3 activation induced by osmostress (Fig. 44a and 44c). This result clearly indicates that Bid

cleavage by caspases, but not Bid ubiquitination, regulates osmostress-induced apoptosis through activation of caspase-3 and therefore creating a positive feedback loop.

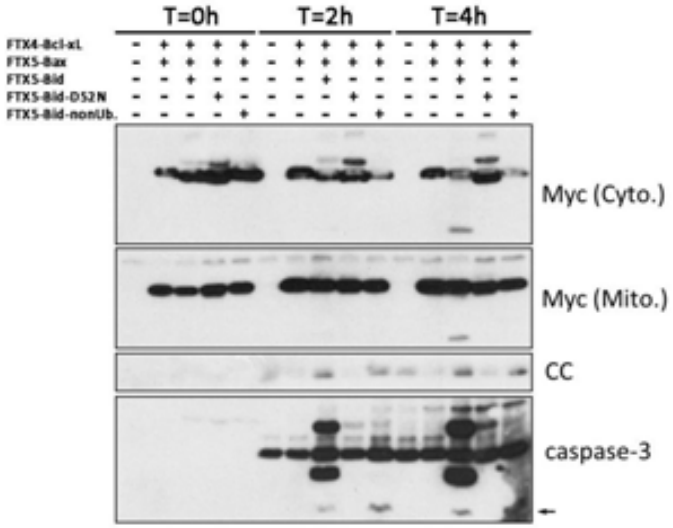

Figure 45. **Mutant Bid-nonUb. is proteolyzed faster than wild type Bid.** Wild type Bid or mutants combined with both FTX4-Bcl-x_L and FTX5-Bax were expressed in *Xenopus* oocytes. Then oocytes were exposed to osmotic shock and samples were collected at different times and analyzed by western. Water injected oocytes were treated and analyzed as control.

Expression of truncated C-terminal Bid (53-184 aa), also known as tBid, induced high caspase-3 activity in oocytes co-expressing Bcl-xL even without hyperosmotic shock treatment (Fig. 44c, time 0 h). On the contrary, expression of nBid (1-52 aa) did not have any effect on osmostress-induced apoptosis compared with water-injected oocytes (Fig. 44c). A small functional effect in osmostress-induced apoptosis by the lack of Bid ubiquitination was observed when tiny amounts of wild type Bid or mutants were expressed in the oocytes. As shown in figure 44d, expression of the mutant Bid-nonUb increased caspase-3 activity induced by osmostress compared with wild type Bid, whereas BidD52N slightly decreased caspase-3 activity at 3 or 4 h after osmostress (Fig. 44d). However, the levels of Bid expression were so low that we could no detect the proteins by Western blot to prove equal levels of expression for wild type Bid and their mutants.

7. DISCUSSION

7.1 JNK proteins and activities in *Xenopus laevis* oocytes

Six JNK transcripts (JNK1-1 and -2, JNK3-1, -2, -3 and -4) were cloned by RT-PCR using total RNA extracted from *Xenopus laevis* oocytes (stage VI). Sequence alignment shows that the JNK sequences are quite conserved. However, *Xenopus* oocytes express only JNK1-1 (40kDa) and JNK1-2 (49kDa) proteins detected by Western blot with total JNK antibodies. In mammalian, there are three JNK genes, the *jnk1* and *jnk2* are ubiquitously expressed, whereas *jnk3* expression is brain-, heart-, and testis-restricted (Gupta et al. 1996). *Xenopus* oocytes do not express enough amounts of JNK3 proteins to be detected by Western blot, and probably the *jnk3* transcripts are maternal stockpiles like many other mRNAs in the oocyte. It was reported that JNKs are necessary to promote embryonic survival and regulate eye development in vertebrates. During goldfish development, JNK1 and JNK2 are expressed at every stage from cleavage to hatching larvae, whereas JNK3 is turned on at the gastrulation stage and expressed at similar levels to that of JNK2 (Huang et al. 2013). Similarly, *Xenopus* JNK3 isoforms might be expressed after fertilization to regulate early embryogenesis and differentiation.

In *Xenopus laevis*, when oocytes are treated with osmotic shock, both JNK1-1 and JNK1-2 are phosphorylated (Messaoud NB, Thesis Dissertation, 2014). It is also reported that in oocytes treated with progesterone JNK activity increases rapidly when oocytes mature (Bagowski et al. 2001a). We addressed the role of JNK activation in meiotic progression by expressing upstream kinases of JNK, as well as different JNK isoforms.

MKK4 and MKK7 are the only upstream kinases known to directly activate JNK proteins (Asaoka and Nishina 2010, Moriguchi et al. 1997). Overexpression of a constitutively active mutant MKK7-DED in *Xenopus* oocytes can activate JNK1-1 and JNK1-2 isoforms without affecting the phosphorylation of ERK2 and p38 family members. Here we show that JNK activation induced by MKK7-DED does not affect the oocyte maturation induced by progesterone, but previous results in our laboratory demonstrated that MKK7-DED overexpression in combination with JNK1-1 or JNK1-2 accelerates apoptosis induced by hyperosmotic shock (Messaoud NB, Thesis Dissertation, 2014). In other cellular systems it has also been reported that sustained activation of JNK induces apoptosis (Ventura et al. 2006).

In *Xenopus* there are no JNK2 isoforms reported. We ectopically expressed human JNK2-1 or the four JNK3 isoforms cloned in our laboratory in *Xenopus* oocytes. Similar to JNK1, all these proteins are phosphorylated by osmotic shock and are recognized with total JNK antibodies while none of them can increase the amount of XpJNK-p42 in mature oocytes.

We confirmed that the protein XpJNK-p42 recognized by pJNK antibody but not total JNK antibody in GVBD oocyte extracts is phosphorylated ERK2 (pERK2). ERK2 can be phosphorylated by both osmostress treatment and progesterone incubation, however, phosphorylated ERK2 induced by osmotic shock can only be recognized by pERK antibodies while activated ERK2 in mature oocytes is detected by both pJNK and pERK antibodies, which indicates that a posttranslational modification is induced in ERK2 by progesterone treatment. Given the close relative of JNK to ERK in the MAPK family and since it was reported that ERK activation may induce c-jun phosphorylation (Pulverer et al. 1991), we considered the possibility that the JNK activity in mature oocytes may come from the activated ERK2. However, here we show that overexpression of ERK2 does not affect JNK activity in mature oocytes (Fig. 29). Similar to our result, it has been reported that MEK1/2 inhibitor U1026 effectively blocked progesterone induced ERK2 activation but had no apparent effect on JNK activity (Bagowski et al. 2001a). Surprisingly, we also show that the JNK inhibitor SP600125 does not inhibit c-Jun phosphorylation in mature oocytes extracts (Fig. 29). All these information imply that the JNK activity (c-Jun phosphorylation) detected in mature oocytes (GVBD) results from activation of another protein kinase, instead of JNK or ERK2, induced by progesterone. It has been reported that cdc2 (Cdk1) can phosphorylate c-Jun (Baker et al. 1992) and, more recently, that Cdk3 can mediate c-Jun phosphorylation at Ser63 and Ser73 in mouse skin epidermal cells (Cho et al. 2009). More experiments are necessary to identify the protein responsible for JNK activity in mature oocytes. The inhibitor SP600125 reduces progesterone-induced maturation of *Xenopus* oocytes (Fig. 19). Since JNKs are not activated during meiotic progression, this implies that SP600125 may targets another protein regulating meiosis. It has been reported that SP600125 inhibits Cdc2 (Cdk1) (Kim JA et al. 2010).

7.2 The role of ERK2 and p38 in *Xenopus laevis* oocyte maturation

Besides the Mos/MEK/ERK signal pathway described in oocyte maturation, another extensively researched cascade that involves ERK activation is Ras/Raf/MEK/ERK signaling pathway. This signaling pathway plays a crucial role in almost all cell functions. Upon receptor activation, GTP-

loaded Ras recruits Raf kinases forming a complex where Raf becomes activated. Then, Raf phosphorylates MEK1⁄2 on same residues to that phosphorylated by Mos, which leads to ERK1⁄2 activation by dual phosphorylation of threonine and tyrosine residues on the dual-specificity motif (T-E-Y) (Cagnol and Chambard 2010). In *Xenopus* oocytes activation of the ERK2 cascade by either Mos, Raf or MEK leads to oocyte GVBD (Bagowski et al. 2001a). It was also reported that MEKK1 phosphorylates MEK1 and thus activates ERK2 (Karandikar et al. 2000). MEKK1 is also implicated in the activation of MKK4 that leads to phosphorylation of JNK and p38 kinases (Xu et al. 1995). Here we show that constitutively active MEKK1Δ activates all p38, JNK, and ERK signaling pathways and accelerates progesterone induced oocyte maturation significantly. We also show that activation p38γ and the ERK signaling pathway are important for MEKK1Δ-induced acceleration.

Induction of G2/M phase transition in mitotic and meiotic cell cycles requires activation by phosphorylation of the protein phosphatase Cdc25. In *Xenopus*, ERK2 is a major Cdc25 kinase. During meiotic induction, ERK2 phosphorylates Cdc25 at T48, T138, and S205, increasing Cdc25 phosphatase activity (Wang Ruoning et al. 2007a). Cdc25 is a specific tyrosine phosphatase that directly activates Cdc2, which in turn activates cdc25 in a positive feedback loop (Gautier et al. 1991, Haccard and Jessus 2006, Wang Ruoning et al. 2007a). Ectopic expression of MKK6 accelerates *Xenopus* oocyte maturation, through p38γ which can also activate the phosphatase Cdc25C, and it seems that endogenous p38γ activation is important for the progesterone induced meiotic G2/M progression (Perdiguero et al. 2003). Ectopic expression of MEKK1Δ accelerates *Xenopus* oocyte maturation, and co-expression of p38γ-DA combined with MEKK1Δ decreases the maturation process, implying that MEKK1Δ may activate p38γ. In oocytes expressing MEKK1Δ, when ERK2 activity is inhibited by U0126 or FR180204 activated p38γ may compensate the ERK cascade to some extent, because oocytes can still mature, although the acceleration of oocyte maturation induced by MEKK1Δ is attenuated.

In MEKK1Δ overexpression experiments, U0126 blocks MEKK1Δ induced ERK activation absolutely by inhibiting the MEK1/2 activity before progesterone stimulation. Intriguingly, this blocking effect disappears after progesterone treatment and ERK2 is phosphorylated. However, when control oocytes, not expressing MEKK1Δ, are treated with progesterone in the presence of U0126, ERK2 phosphorylation is markedly reduced (Fig. 30d). We speculate that there may be another kinase that can phosphorylate ERK2 besides MEK1/2 in mature *Xenopus* oocytes and this kinase may depend on progesterone-induced protein translation and may be under control of p38 cascade associated proteins, and its activation is involved in ERK associated positive regulation. This speculation is supported by antibody reactions. Phosphorylated ERK2 induced by MEKK1Δ

ectopic expression or osmotic shock cannot be recognized by pJNK antibody but, as we proved above, phosphorylated ERK2 in mature oocyte can be detected by both pERK and pJNK antibodies. In consideration of MEK1 kinase activity described above, and the effective inhibition MEK1 by U0126, there should be a MEK1 independent pathway for ERK2 phosphorylation. In *Xenopus* oocytes protein synthesis is absolutely required for ERK activation, and suppression of Mos translation inhibits MAP kinase activation in both mouse and *Xenopus* oocytes (Abrieu et al. 2001). In MEKK1Δ overexpression experiments, the inhibitor U0126 does not inhibit oocyte maturation when ERK2 is already phosphorylated (18 h after MEKK1Δ cRNA injection); however, the inhibitor SP 600125 still works, indicating that SP 600125 inhibits an unknown ERK2 upstream kinase instead of MEK1. A plausible candidate for ERK2 modification beyond the phosphorylation executed by MEK1 is Cdk1/Cdc2. It was reported that active cyclin-B/Cdc2 kinase can activate ERK2 with the absence of detectable Mos (Guadagno and Ferrell 1998, Minshull et al. 1994) and we observed that SP600125 attenuated the phosphorylation of ERK2 in mature oocytes thereby decreasing the percent of mature oocytes (GVBD). Importantly, it has been reported that SP600125 can suppress Cdk1activity thus blocking the progression of human G2 cells into mitosis, independent of JNK inhibition (Kim JA et al. 2010).

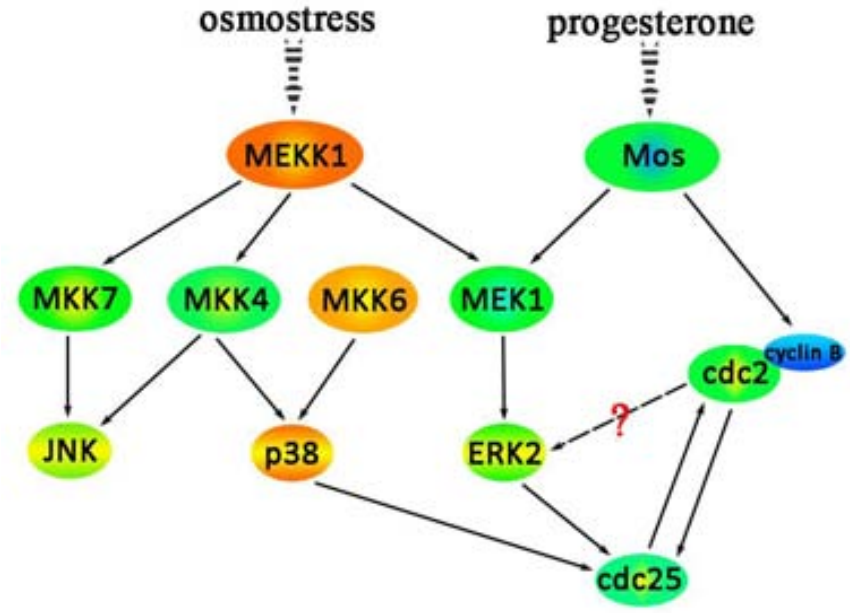

Figure 46. **Schematic diagram of MAP Kinase interaction in *Xenopus* oocytes.** JNK and p38 signaling pathways are mainly involved in cellular stress response, while ERK signaling pathway is crucial for cellular cycle regulation. However, it is also reported that p38 isoforms are implicated in mitotic and meiotic cell cycle regulation by activating CDC proteins. Additionally, a cdc2 dependent posttranslational modification of ERK2 may exist.

Interestingly, in oocytes expressing MEKK1Δ and treated with FR180204, an ERK inhibitor, some phosphorylated ERK2 can be recognized by pJNK antibody. X-ray crystal structure analysis of the human ERK2/FR180204 complex revealed that the ATP-binding pocket on ERK formed by residues Q105, D106, L156, and C166 plays important roles in the ERK2-FR180204 interaction (Ohori et al. 2005). We speculate that FR180204 binding to phosphorylated ERK2 may induce a conformational change that allows detection with pJNK antibodies. It has been reported that the glycine-rich loop of the FR180204-ERK2 complex had a different conformation from those of the other complexes previously reported (Ohori et al. 2005).

It has been reported that ERK activity is very low in cells transfected with constitutively active MEKK1-C or in MEKK1-C and MEK1/2 co-transfection experiments (Xu et al. 1995). Similarly, we found very low level of ERK activity in apoptotic oocytes induced by osmotic shock although ERK2 phosphorylation signal was quite strong; however, ERK activity was high in mature oocytes. Our results suggest that an ERK2 posttranslational modification, independent of MEK1/2 activity, exists in *Xenopus* oocyte maturation, and this modification is critical for ERK2 activity (using MBP as a substrate). Alternatively, ERK phosphorylation induced by MEK1/2 would be sufficient to engage ERK activity, but in apoptotic oocytes (induced by osmotic shock) some modification would induce ERK inactivation. So more experiments are needed to solve these questions.

Osmostress-induced cleavage of JNK1-2 by caspase-3 promotes cytochrome c release and caspase-3 activation in a positive feedback loop

Previous work in our laboratory has shown that sustained activation of JNK1-1 and JNK1-2 contributes to hyperosmotic shock-induced apoptosis of *Xenopus* oocytes, with a higher pro-apoptotic function for JNK1-2 (Messaoud NB, Thesis Dissertation, 2014). It has been shown that JNK may have a pro- or anti-apoptotic role in a stimulus and tissue dependent mechanism (Davis Roger J 2000b, Weston and Davis 2007). It seems that a transient activation of JNK is a struggle for survival, while sustained activation of JNK induces apoptosis (Ventura et al. 2006). Incubation of *Xenopus* oocytes with the JNK inhibitor SP600125 slightly increases caspase-3 activity 1 h after osmostress, suggesting that early activation of JNK might be anti-apoptotic (Messaoud NB, Thesis Dissertation, 2014). JNK has been reported to prevent cell death by up-regulating transcription of survival genes (Lamb et al. 2003). However, in *Xenopus* oocytes there is no transcriptional control, which might also explain why JNK activation is sustained, since phosphatases transcriptionally induced by JNK activation down-regulate JNK phosphorylation in mammalian cells (Owens and Keyse 2007, Ventura et al. 2006). It has also been reported that transient activation of human JNK p46 splice variant (similar to *Xenopus* JNK1-1) delays activation of caspase-9 by direct interaction with Apaf-1 and cytochrome c in the apoptosome complex (Tran et al. 2007). Sustained activation

of JNK could induce apoptosis through phosphorylation of Bax sequestration proteins 14-3-3, which promotes Bax translocation to mitochondria (Tsuruta et al. 2004), phosphorylation of Bad at Ser128 (Donovan et al. 2002), or modulating the activities of other pro-apoptotic BH3-only proteins such as Bim and Bmf (Lei and Davis 2003) (see Introduction for a review). In this work, we have not addressed the posttranslational modifications of the Bcl-2 family members induced by JNK1-1 or JNK1-2 activation after hyperosmotic shock treatment. We do not observe any significant change in Bax distribution during osmostress-induced apoptosis (Fig. 35). However, these measurements were performed in oocytes overexpressing Bax combined with Bcl-x_L, and small changes in the distribution of Bax could be difficult to detect in these conditions. It would be interesting to check how the endogenous levels of Bax respond to hyperosmotic shock. It has also been reported that JNK activation can induce apoptosis through Bid proteolysis and generation of truncated jBid (Deng et al. 2003). However, our results show that expression of a constitutively active MKK7 mutant (MKK7-DED) in *Xenopus* oocytes activates endogenous JNK1-1 and JNK1-2, but neither increases the proteolysis of Bid induced by osmostress (which generates tBid and nBid mono- or bi-ubiquitinated) nor produces a different N-terminal fragment as would be expected after generation of truncated jBid (Fig. 37b). In fact, the protolytic site reported in human Bid that is responsible for the generation of jBid (Deng et al. 2003) is not conserved in *Xenopus*. In the present work we also demonstrate that in osmotic stress-induced apoptosis *Xenopus* JNK1-2 is cleaved into a JNK1-1 like protein after caspase-3 activation. There are two potential caspase-3 recognition sites at D385 and D412. In humans, JNK1 and JNK2 are proteolyzed by caspase-3 at D413 and D410, respectively (Enomoto et al. 2003), in a sequence identical to *Xenopus* recognition site D412 (SDTD). In humans, JNKs do not have an optimal sequence for caspase-3 cleavage (DXXD), but the atypical cleavage site SDTD is recognized and cleaved by caspase-3 (Enomoto et al. 2003). However, our data clearly demonstrates that cleavage of *Xenopus* JNK1-2 occurs only at the consensus recognition site D385 but not at the atypical cleavage site D412. It might be possible that the atypical sequence at D412 in *Xenopus* serves as a binding site for recruitment of caspase-3 but not for cleavage. Alternatively, the atypical sequence might be masked by some kind of protein interaction distinct to caspase-3. We have not determined the JNK activity of the phosphorylated *Xenopus* JNK1-1 like fragment generated by osmostress. However, in humans, the proteolyzed fragments of pJNK1 and pJNK2 generated by caspase-3 have similar activities that full length pJNKs (Enomoto et al. 2003). Importantly, here we show, for the first time, that proteolysis of JNK has a functional role in apoptosis. Cleavage of JNK1-2 by caspase-3 positively regulates cytochrome c release and caspase-3 activity induced by osmostress, thus creating a positive feedback loop.

It seems that the positive feedback comes from the JNK1-1 like fragment (aminoacids 1-385) generated by proteolysis of JNK1-2, since overexpression of the JNK1-1 like fragment mimics the effect of JNK1-2 overexpression accelerating osmostress-induced apoptosis (Fig. 35b). JNK1-2 is more pro-apoptotic that JNK1-1 (Fig. 35b), the only distinction of these two proteins are the aminoacids located at the C-terminal (Fig. 35a), which are generated by alternative splicing. We propose that these different residues could determine different protein interactions. JNK1-1 like fragment may interact preferentially with Bcl-2 family members, thus inhibiting anti-apoptotic or activating pro-apoptotic proteins, and therefore increasing the release of cytochrome c from the mitochondria. Alternatively, the JNK1-1 like fragment increases the activity of the apoptosome complex, competing with JNK1-1, which has been reported previously to interact with Apaf1 and cytochrome c to inhibit the apoptosome complex (Tran et al. 2007).

7.3 Bcl-2 family members in osmostress induced apoptosis

Bcl-2 family members are central proteins in regulating mitochondrial permeability in apoptosis. Anti-apoptotic proteins, such as Bcl-x_L, bind and sequester pro-apoptotic proteins, including activator BH3-only proteins and executor Bax and Bak, to prevent apoptosis. Here we show that *Xenopus* oocytes overexpressing the anti-apoptotic protein Bcl-x_L present a marked reduction of cytochrome c release and caspase-3 activation induced by hyperosmotic shock. In some experiments the inhibition of caspase-3 activity was complete (Fig. 36a). This result indicates that osmostress-induced apoptosis is mainly regulated by activation of the mitochondrial pathway, and that the extrinsic pathway is not activated or has a minor role in caspase-3 activation. On the contrary, ectopic expression of pro-apoptotic Bcl-2 member Bid, that was initially identified as a protein binding to both pro-apoptotic Bax and anti-apoptotic Bcl-2 (Wang Kun et al. 1996), induces oocyte apoptosis without any stress stimulation (Fig. 34a). Although it is reported that Bid locates in the cytosol, and the full activity of Bid is not exerted until proteolytic cleavage by caspase-8 (Li Honglin et al. 1998), full length Bid can still translocates to mitochondria, and it is sufficient to induce apoptosis of cultured cells (König et al. 2007, Valentijn and Gilmore 2004). Overexpression of Bax and Bak also induces apoptosis in *Xenopus* oocytes, as expected, but co-expression of Bcl-x_L with Bax, Bak or Bid blocks the apoptosis induced by the pro-apoptotic family members. Bcl-x_L expression also reduces cytochrome c release and caspase-3 activitation induced by osmostress in oocytes co-expressing Bak, but not in the oocytes expressing Bax or Bid. Although this might seems an artificial system it allowed us to express high levels of both pro- and anti-apoptotic proteins to study some modifications induced by osmostress that would be difficult to detect

analyzing the small amounts of endogenous proteins present in the oocytes. In addition, there are not good commercial antibodies to detect *Xenopus* Bcl-2 family members, but ectopic expression of the proteins with a Myc tag at the N-terminal can be easily detected. In *Xenopus* oocytes, overexpressed full-length Bid is located in the cytosol and the mitochondria and hyperosmotic shock induces *Xenopus* Bid proteolysis in both pools. We also demonstrate that cleavage of Bid induced by osmostress occurs after residue Asp52, in the conserved caspase-8/9/10 site ETD, and is markedly reduced in oocytes incubated with the specific caspase-3 inhibitor, and completely blocked in the presence of Z-VAD.fmk. Therefore, it seems that most of Bid proteolysis is due to caspase-3 activity, but an additional caspase also participates to a minor extent in the proteolyisis of Bid. It has been reported that caspase-3 can cleaves human Bid at residue Asp60, and cell extracts depleted of caspase-3 or extracts of MCF-7 cells that are devoid of caspase-3, due to a deletion in exon3 of the *caspase-3* gene, fails to induce Bid cleavage (Slee et al. 2000). Interestingly, we show here that in *Xenopus* oocytes, cytochrome c microinjection in the presence or absence of Z-VAD.fmk induces the proteolysis of Bid at Asp52, probably through activation of caspase-9. It has been reported that Z-VAD.fmk does not inhibit caspase-9, moreover, in front of some apoptotic stimuli it could activate it (Rodríguez-Enfedaque et al. 2012). The cleavage site in *Xenopus* Bid is similar to the cleavage activation site in *Xenopus* caspase-3 (Fig. 38b), and therefore caspase-9 could cleave both proteins. It has also been reported that *Xenopus* Bid can be proteolyzed by *Xenopus* caspase-8 and caspase-10β (Kominami et al. 2006). We have confirmed that caspase-10 expression in *Xenopus* oocytes induces Bid proteolysis and cytochrome c release. Altogether the above data indicates that the ETD site present in *Xenopus* Bid can be recognized by caspase-3, caspase-8, caspase-9 and caspase-10. *Xenopus* caspase-8, however, is mainly expressed at stages 15/16 in early embryogenesis with very low levels, if any, in stage VI oocytes (Kominami et al. 2006). During apoptosis, Bid can be cleaved not only by caspases, but also by granzyme B, calpains and cathepsins (Billen et al. 2008). We have reported previously that calpain inhibitors, but not cathepsin inhibitors, delay osmostress induced apoptosis in *Xenopus* oocytes (Messaoud NB, Thesis Dissertation, 2004). However, we show here that calpain inhibitor MDL28170 does not decrease Bid proteolysis induced by osmostress, although decreases caspase-3 activation (Fig. 41). The time-course analysis of Bid-cleaved induced by osmostress combined with the data obtained in the presence of inhibitors indicate that low amounts of Bid are proteolyzed very early after hyperosmotic shock by an initiator caspase, whereas most of Bid is cleaved by caspase-3 at later times. Candidates for early proteolysis of Bid are caspase-10, which is highly expressed in stage VI oocytes (Kominami et al. 2006), and caspase-9. Future experiments wil address the role of these caspases in early cleavage of Bid induced by osmostress. The C-terminal product of Bid-cleaved at

residue Asp52, tBid, is more active than full-length Bid inducing cytochrome c release and caspase-3 activation. Whereas overexpression of Bcl-x_L can block the apoptotic function of wild type Bid in the oocytes, tiny amount of tBid (1/100 of wild type Bid) is enough to induce apoptosis without any stress stimulation (Fig. 44c). Therefore, osmostress-induced Bid cleavage mediated by initiator caspases generates tBid that could migrate to the mitochondria and induce cytochrome c release and caspase-3 activation, which in turn generates more tBid, thus creating a positive feedback loop. Indeed, we demonstrate that expression of Bid mutated at the cleavage caspase site ETD (BidD52N) reduces the release of cytochrome c and caspase-3 activity induced by osmostress compared with the wild type Bid (Fig. 44c).

7.4 Bid is mono- and bi-ubiquitinated in *Xenopus* oocytes, but the function of ubiquitinated Bid is not clear

It has been reported that three Lys residues in the N-terminal region of *Xenopus* Bid (not conserved in human) are important for mono- and biubiquitination of Bid, and both mono and biubiquitinated Bid are not degraded by the proteasome in oocyte extracts (Saitoh et al. 2009). In human Bid the C-terminal fragment (tBid) is polyubiquitinated and degraded by the proteasome (Breitschopf et al. 2000), and it has been reported that the N-terminal fragment (nBid) is also polyubiquitinated in Ser/Thr/Cys residues in an unconventional manner and degraded by the proteasome (Tait et al. 2007). Here we show that when *Xenopus* Bid and Bcl-x_L are overexpressed in the oocyte, a significant portion of Bid is mono- and biubiquitinated in the cytosol. Some small amounts of mono- and biubiquitinated Bid are present in the mitochondria, which are slighly increased after osmotic shock treatment. We do not know if this increase is due to migration of cytosolic Bid to the mitochondria or to ubiquitination of the mitochondrial Bid pool. To address this issue we should analyze oocytes treated with hyperosmotic shock in the presence or absence of specific ubiquitination inhibitors. Not only ubiquitinated full-length Bid but also ubiquitinated N-terminal Bid fragments obtained by proteolyisis of Bid are quite stable. The quantification of these fragments by Western blot indicates that proteolysis of Bid and monoUb-Bid in the cytosol generate N-terminal fragments that are ubiquitinated and accumulated in the cytosol and the mitochondria as monoUb-nBid and biUb-nBid. Non ubiquitinated N-terminal Bid is difficult to be detected after hyperosmotic shock, even after microinjection of a cRNA coding for N-terminal Bid. It looks like the non-ubiquitinated N-terminal Bid is not a stable peptide in the oocyte. As described above, hyperosmotic stress produces a marked increase of monoUb-nBid and biUb-nBid in the cytosolic

and mitochondrial fractions, detected with the cleaved caspase-3 Cell Signaling antibodies, although monoUb-nBid (and also monoUb-Bid) was difficult to detect in the mitochondria with anti-Ub antibodies. We speculate, as described in the Results, that some posttranslational modification in the mitochondrial pool of monoUb-nBid and monoUb-Bid may mask their detection with anti-Ub antibodies. It is difficult to know the role of mono- and biubiquitination in Bid, but in other proteins it has been reported that these modifications can alter the localization in the cell, the interaction with other proteins, and their function (Kerscher et al. 2006). Human Bid is subject to autoinhibition in the absence of stimuli, since the N- and C- terminal fragments bind each other through interactions of the BH3-like region at the N-terminal and the BH3 region at the C-terminal (Tan et al. 1999). As described above, unconventional ubiquitination and degradation of its N-terminal fragment is required to unleash the proapoptotic ability of human tBid (Tait et al. 2007). Removal of the N-terminal of Bid has been suggested to increase the number of exposed hydrophobic residues in tBid thereby facilitating binding of the protein to membranes (McDonnell et al. 1999). However, in *Xenopus* Bid the BH3-like region at the N-terminal fragment is not conserved. Therefore, mono and bi-ubiquitination of the N-terminal fragment could be a protective mechanism in *Xenopus* Bid to avoid its interaction with the mitochondrial membrane to induce cytochrome c release in the absence of a stressfull stimulus. Alternatively, Bid ubiquitination may inhibits Bid cleavage mediated by caspases, like phosphorylation of human Bid inhibits Bid cleavage by caspase-8 or caspase-3 (Degli Esposti et al. 2003, Desagher et al. 2001). However, when we expresse a triple mutant Bid (K18/21/37R) (Bid-nonUb.) with a marked reduction in ubiquitination in *Xenopus* oocytes, and compare its effect with wild type Bid, we do not find a clear effect on osmostress-induced apoptosis (Fig. 44c and 44d). It is possible that Bid-nonUb. mutant does not affect the small pool of endogenous Bid ubiquitinated present in the mitochondria. Therefore, an excess of the Bid-nonUb. mutant expressed in the oocytes does not necessarily have to affect the function of this mitochondrial pool. To address this issue properly, we should deplete the endogenous ubiquitinated Bid, which could be achieved by microinjection of specific antibodies for *Xenopus* ubiquitinated Bid (not available yet). We only find a functional effect of the mutant Bid-nonUb. when tiny amounts of wild type or mutant Bid are expressed in the oocytes in the absence of Bcl-x_L (Fig 44d), or when Bax is co-expressed with Bcl-x_L and Bid to accelerate osmostress-induced apoptosis (Fig 40). In the first experiment Bid-nonUb. mutant is slightly more pro-apoptotic that wild type Bid, and in the second experiment Bid-nonUb. seems to be proteolyzed faster that wild type Bid. Because these effects are small, and only found under certain conditions, we conclude that the function of mono- and bi- ubiquitinated Bid on osmostress-induced apoptosis is not yet clear.

7.5 A model for osmostress-induced apoptosis in *Xenopus* oocytes

Hyperosmotic shock induces rapid calpain activation, Smac/DIABLO release and JNK/p38 activation in *Xenopus* oocytes (Messaoud NB, Thesis Dissertation, 2014). The stress protein kinases JNK and p38 are efficient sensors, with high ultrasensitivity, that evaluate stressful situations in the cells. When oocytes are exposed for several hours to hyperosmotic shock sustained activation of p38 and JNK in combination with calpain activation and Smac/DIABLO release induce cytochrome c release and caspase-3 activation (Messaoud NB, Thesis Dissertation, 2014). Here we show that hyperosmotic shock induces early Bid cleavage at very low levels, probably by activation of an initiator caspase, generating tBid that would induce cytochrome c release (Fig. 47, top). Hyperosmotic shock also induces a slight and rapid increase of mono- and bi-ubiquitinated Bid in the mitochondria (Fig. 47, bottom), although their role in osmostress-induced apoptosis in not clear. We cannot discard that rapid Bid ubiquitination might delay Bid proteolysis and therefore be a protective response to hyperosmotic shock. In an early stress situation it is expected that anti-apoptotic and pro-apoptotic responses occurs synchronically. Oocytes exposed to hyperosmotic shock must evaluate carefully all the information to assess the strength and duration of the stress, as well as the damage suffered in the cell machinery, before engaging an irreversible program. Bcl-x_L overexpression protects oocytes from hyperosmotic shock-induced apoptosis, indicating that cytochrome c release from the mitochondria is crucial for caspase-3 activation. However, when cytochrome c is released and reaches a threshold level, caspase-3 is activated and engages several positive feedback loops (Fig. 47, top). For instance, caspase-3 increases calpain activation (Pörn-Ares et al. 1998, Wang Kevin KW et al. 1998), Smac/DIABLO release and p38 phosphorylation (Messaoud NB, Thesis Dissertation, 2014), which in turn increase cytochrome c release and caspase-3 activity. Here we show that caspase-3 also induces JNK1-2 proteolysis, which in turn positively regulates cytochrome c release and caspase-3 activation. In addition, we demonstrate that a massive proteolysis of Bid at Asp52, generating t-Bid, is mediated by caspase-3, thus creating another positive feedback loop. In conclusion, hyperosmotic shock induces the activation of different pathways that converge on the activation of caspase-3, which engages an irreversible apoptotic program through activation of multiple positive feedback loops.

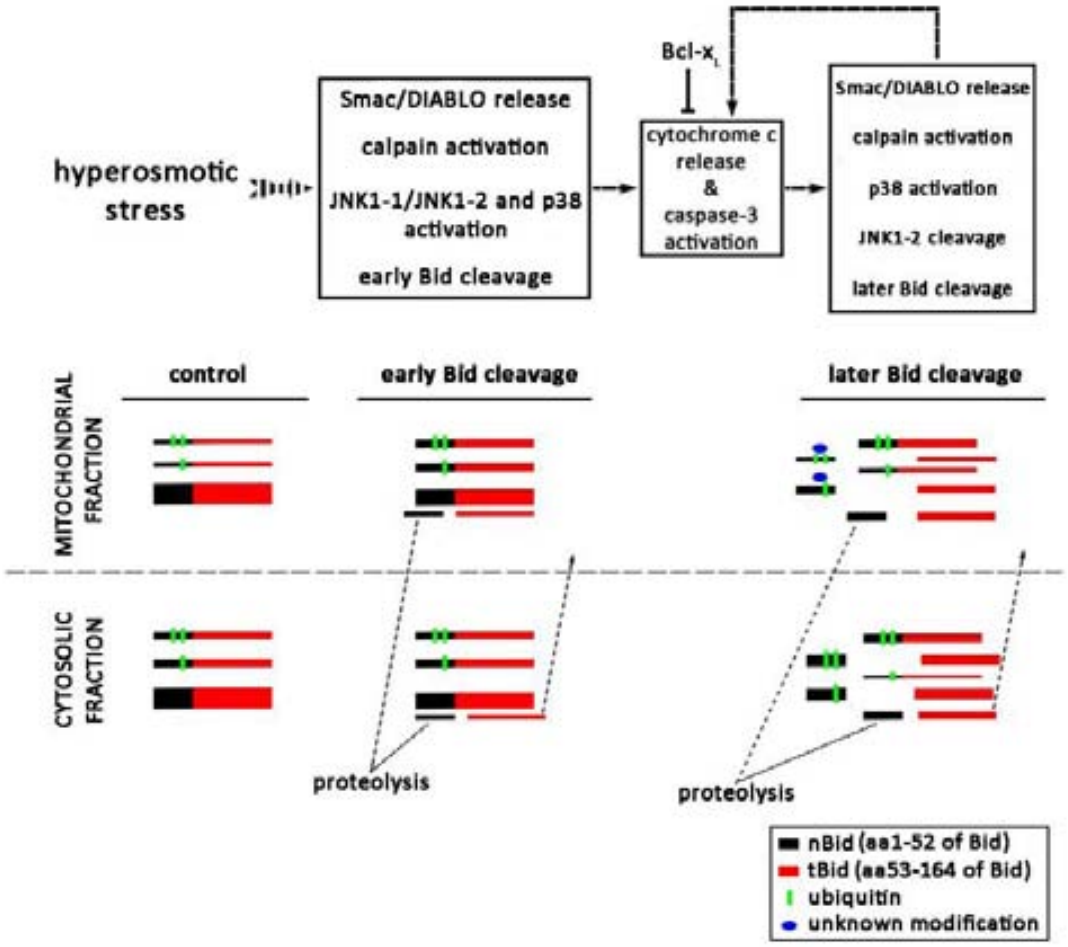

Figure 47. **Model for for osmostress-induced apoptosis in *Xenopus* oocytes.** *Top*: Hyperosmotic stress induces early Smac/DIABLO release, calpain activation, JNK1-1/JNK1-2/p38 activation, and Bid cleavage independently of caspase-3. Activation of these pathways regulate cytochrome c release and caspase-3 activation, which in turn induces more Smac/DIABLO release, calpain activation, p38 activation, and cleavage of JNK1-2 and Bid, that positively feedbacks on cytochrome c release and caspase-3 activation. In contrast, over-expression of Bcl-x_L protects from osmostress-induced apoptosis. *Bottom*: In control oocytes Bid is present in the cytosolic and mitochondrial fractions as non-, mono- or bi-ubiquitinated forms (horizontal black and red bars for Bid and green bars for ubiquitin). Hyperosmotic shock quickly induces a slight increase in the mitochondrial pool of mono- and bi-ubiquitinated Bid. Hyperosmotic shock also induces early cleavage of small amounts of non-ubiquitinated Bid and late cleavage of massive amounts of non- and mono-ubiquitinated Bid in the cytosol and mitochondria. The N-terminal Bid fragment generated (black) is subsequently mono- and bi-ubiquitinated and accumulates in both cytosol and mitochondria, whereas n-Bid non-ubiquitinated is degraded by proteolysis. As depicted in the figure, some unknown modification might be present in n-Bid mono- and bi-ubiquitinated in the mitochondrial fraction. The thickness of the bars representing Bid and its fragments (with or without ubiquitination) is proportional to the amounts detected by Western blot.

8. CONCLUSIONS

1. There are at least six different *jnk* transcripts in *Xenopus laevis* oocytes (stage VI), two for *jnk1* and four for *jnk3*; however the oocytes only express significant levels of JNK1-1 and JNK1-2 proteins.
2. Ectopic expression of a constitutively active MEKK1 accelerates progesterone-induced oocyte maturation through activation of the ERK and p38 signaling pathways.
3. Progesterone treatment does not activate any JNK isoform in mature oocytes.
4. Phosphorylation of c-jun (JNK activity) detected in mature oocytes extracts is independent of ERK2 and JNK.
5. A protein of 42 kDa detected with pJNK antibodies (XpJNKp42) is a posttranslational modification of pERK2 induced during meiotic progression.
6. Hyperosmotic shock induces the activation of JNK1-1 and JNK1-2, but JNK1-2 is cleaved at Asp385 by caspase-3 to generate a JNK1-1 like fragment, which positively regulates cytochrome c release and caspase-3 activation, creating a positive feedback loop.
7. A pool of Bid mono- and bi-ubiquitinated is located in the cytosol and mitochondria of *Xenopus* oocytes. Hyperosmotic shock induces a rapid increase of mono- and bi-ubiquitinated Bid in the mitochondria. However, the effect of Bid ubiquitination in the regulation of osmostress-induced apoptosis is not clear.
8. Osmostress induces an early cleavage of small amounts of Bid at Asp52 by an initiator caspase, and a massive cleavage of Bid at later times in the same residue by caspase-3. The cleavage of Bid positively regulates cytochrome c release and caspase-3 activation, creating a positive feedback loop.

In conclusion, JNK proteins are not involved in *Xenopus* oocyte maturation, and the phosphorylation of c-Jun detected in mature oocytes is independent of JNK and ERK2. Caspase-3 activation induced by hyperosmotic shock engages two positive feedback loops through the cleavage of JNK1-2 and Bid, thus promoting an irreversible death of the oocytes.

9. REFERENCES

Abrieu A, Dorée M, Fisher D. 2001. The interplay between cyclin-B-Cdc2 kinase (MPF) and MAP kinase during maturation of oocytes. Journal of Cell Science 114: 257-267.

Adler V, Qu Y, Smith SJ, Izotova L, Pestka S, Kung H-F, Lin M, Friedman FK, Chie L, Chung D. 2005. Functional interactions of Raf and MEK with Jun-N-terminal kinase (JNK) result in a positive feedback loop on the oncogenic Ras signaling pathway. Biochemistry 44: 10784-10795.

Ambrosino C, Nebreda AR. 2001. Cell cycle regulation by p38 MAP kinases. Biology of the Cell 93: 47-51.

Asaoka Y, Nishina H. 2010. Diverse physiological functions of MKK4 and MKK7 during early embryogenesis. Journal of biochemistry 148: 393-401.

Bagowski CP, Ferrell Jr JE. 2001. Bistability in the JNK cascade. Current Biology 11: 1176-1182.

Bagowski CP, Xiong W, Ferrell JE. 2001a. c-Jun N-terminal kinase activation in Xenopus laevis eggs and embryos a possible non-genomic role for the JNK signaling pathway. Journal of Biological Chemistry 276: 1459-1465.

Bagowski CP, Myers JW, Ferrell JE. 2001b. The Classical Progesterone Receptor Associates with p42 MAPK and Is Involved in Phosphatidylinositol 3-Kinase Signaling inXenopus Oocytes. Journal of Biological Chemistry 276: 37708-37714.

Baker SJ, Kerppola T, Luk D, Vandenberg MT, Marshak D, Curran T, Abate C. 1992. Jun is phosphorylated by several protein kinases at the same sites that are modified in serum-stimulated fibroblasts. Molecular and cellular biology 12: 4694-4705.

Bao Q, Riedl SJ, Shi Y. 2005. Structure of Apaf-1 in the auto-inhibited form: a critical role for ADP. Cell Cycle 4: 1001-1003.

Barr FA, Silljé HH, Nigg EA. 2004. Polo-like kinases and the orchestration of cell division. Nature reviews Molecular cell biology 5: 429-441.

Bayaa M, Booth RA, Sheng Y, Liu XJ. 2000. The classical progesterone receptor mediates Xenopus oocyte maturation through a nongenomic mechanism. Proceedings of the National Academy of Sciences 97: 12607-12612.

Berger L, Wilde A. 2013. Glycolytic Metabolites Are Critical Modulators of Oocyte Maturation and Viability. PloS one 8: e77612.

Bhuyan A, Varshney A, Mathew M. 2001. Resting membrane potential as a marker of apoptosis: studies on Xenopus oocytes microinjected with cytochrome c. Cell death and differentiation 8: 63-69.

Billen L, Shamas-Din A, Andrews D. 2008. Bid: a Bax-like BH3 protein. Oncogene 27: S93-S104.

Boonyaratanakornkit V, Scott MP, Ribon V, Sherman L, Anderson SM, Maller JL, Miller WT, Edwards DP. 2001. Progesterone receptor contains a proline-rich motif that directly interacts with SH3 domains and activates c-Src family tyrosine kinases. Molecular cell 8: 269-280.

Boulton TG, Yancopoulos GD, Gregory JS, Slaughter C, Moomaw C, Hsu J, Cobb MH. 1990. An insulin-stimulated protein kinase similar to yeast kinases involved in cell cycle control. Science 249: 64-67.

Boulton TG, Nye SH, Robbins DJ, Ip NY, Radzlejewska E, Morgenbesser SD, DePinho RA, Panayotatos N, Cobb MH, Yancopoulos GD. 1991. ERKs: a family of protein-serine/threonine kinases that are activated and tyrosine phosphorylated in response to insulin and NGF. Cell 65: 663-675.

Breitschopf K, Zeiher AM, Dimmeler S. 2000. Ubiquitin-mediated Degradation of the Proapoptotic Active Form of Bid A FUNCTIONAL CONSEQUENCE ON APOPTOSIS INDUCTION. Journal of Biological Chemistry 275: 21648-21652.

Brenner B, Koppenhoefer U, Weinstock C, Linderkamp O, Lang F, Gulbins E. 1997. Fas-or ceramide-induced apoptosis is mediated by a Rac1-regulated activation of Jun N-terminal kinase/p38 kinases and GADD153. Journal of Biological Chemistry 272: 22173-22181.

Cagnol S, Chambard JC. 2010. ERK and cell death: Mechanisms of ERK-induced cell death–apoptosis, autophagy and senescence. FEBS journal 277: 2-21.

Campbell L, Hardwick KG. 2003. Analysis of Bub3 spindle checkpoint function in Xenopus egg extracts. Journal of cell science 116: 617-628.

Cargnello M, Roux PP. 2011. Activation and function of the MAPKs and their substrates, the MAPK-activated protein kinases. Microbiology and Molecular Biology Reviews 75: 50-83.

Chen C-L, Lin C-F, Chang W-T, Huang W-C, Teng C-F, Lin Y-S. 2008. Ceramide induces p38 MAPK and JNK activation through a mechanism involving a thioredoxin-interacting protein-mediated pathway. Blood 111: 4365-4374.

Chen J, Downs SM. 2008. AMP-activated protein kinase is involved in hormone-induced mouse oocyte meiotic maturation in vitro. Developmental biology 313: 47-57.

Chen J, Hudson E, Chi MM, Chang AS, Moley KH, Hardie DG, Downs SM. 2006. AMPK regulation of mouse oocyte meiotic resumption in vitro. Developmental biology 291: 227-238.

Chen Y-R, Wang X, Templeton D, Davis RJ, Tan T-H. 1996. The role of c-Jun N-terminal kinase (JNK) in apoptosis induced by ultraviolet C and γ radiation duration of JNK activation may determine cell death and proliferation. Journal of Biological Chemistry 271: 31929-31936.

Chipuk JE, Green DR. 2008. How do BCL-2 proteins induce mitochondrial outer membrane permeabilization? Trends in cell biology 18: 157-164.

Chipuk JE, Moldoveanu T, Llambi F, Parsons MJ, Green DR. 2010. The BCL-2 family reunion. Molecular cell 37: 299-310.

Cho Y-Y, Tang F, Yao K, Lu C, Zhu F, Zheng D, Pugliese A, Bode AM, Dong Z. 2009. Cyclin-dependent kinase-3–mediated c-jun phosphorylation at Ser63 and Ser73 enhances cell transformation. Cancer research 69: 272-281.

Cirman T, Orešić K, Mazovec GD, Turk V, Reed JC, Myers RM, Salvesen GS, Turk B. 2004. Selective disruption of lysosomes in HeLa cells triggers apoptosis mediated by cleavage of Bid by multiple papain-like lysosomal cathepsins. Journal of Biological Chemistry 279: 3578-3587.

Coll O, Morales A, Fernández-Checa JC, Garcia-Ruiz C. 2007. Neutral sphingomyelinase-induced ceramide triggers germinal vesicle breakdown and oxidant-dependent apoptosis in Xenopus laevis oocytes. Journal of lipid research 48: 1924-1935.

Cooper JA, Bowen-Pope DF, Raines E, Ross R, Hunter T. 1982. Similar effects of platelet-derived growth factor and epidermal growth factor on the phosphorylation of tyrosine in cellular proteins. Cell 31: 263-273.

Cortese JD, Voglino AL, Hackenbrock CR. 1998. Multiple conformations of physiological membrane-bound cytochrome c. Biochemistry 37: 6402-6409.

Cuadrado A, Nebreda A. 2010. Mechanisms and functions of p38 MAPK signalling. Biochem. J 429: 403-417.

Davis RJ. 1995. Transcriptional regulation by MAP kinases. Molecular reproduction and development 42: 459-467.

Davis RJ. 2000a. Signal transduction by the JNK group of MAP kinases. Cell 103: 239-252.

Davis RJ. 2000b. Signal transduction by the JNK group of MAP kinases. Pages 13-21. Inflammatory Processes:, Springer.

Degli Esposti M, Ferry G, Masdehors P, Boutin JA, Hickman JA, Dive C. 2003. Post-translational modification of Bid has differential effects on its susceptibility to cleavage by caspase 8 or caspase 3. Journal of Biological Chemistry 278: 15749-15757.

Deng H, Yu F, Chen J, Zhao Y, Xiang J, Lin A. 2008. Phosphorylation of Bad at Thr-201 by JNK1 promotes glycolysis through activation of phosphofructokinase-1. Journal of biological chemistry 283: 20754-20760.

Deng Y, Ren X, Yang L, Lin Y, Wu X. 2003. A JNK-dependent pathway is required for TNFα-induced apoptosis. Cell 115: 61-70.

Derijard B, Raingeaud J, Barrett T, Wu I-H, Han J, Ulevitch RJ, Davis RJ. 1995. Independent human MAP-kinase signal transduction pathways defined by MEK and MKK isoforms. Science 267: 682-685.

Desagher S, Osen-Sand A, Montessuit S, Magnenat E, Vilbois F, Hochmann A, Journot L, Antonsson B, Martinou J-C. 2001. Phosphorylation of bid by casein kinases I and II regulates its cleavage by caspase 8. Molecular cell 8: 601-611.

Dhanasekaran DN, Reddy EP. 2008. JNK signaling in apoptosis. Oncogene 27: 6245-6251.

Dhanasekaran N, Reddy EP. 1998. Signaling by dual specificity kinases. Oncogene 17.

Dirsch VM, Müller IM, Eichhorst ST, Pettit GR, Kamano Y, Inoue M, Xu J-P, Ichihara Y, Wanner G, Vollmar AM. 2003. Cephalostatin 1 selectively triggers the release of Smac/DIABLO and subsequent apoptosis that is characterized by an increased density of the mitochondrial matrix. Cancer research 63: 8869-8876.

Donovan N, Becker EB, Konishi Y, Bonni A. 2002. JNK phosphorylation and activation of BAD couples the stress-activated signaling pathway to the cell death machinery. Journal of Biological Chemistry 277: 40944-40949.

Dougherty MK, Müller J, Ritt DA, Zhou M, Zhou XZ, Copeland TD, Conrads TP, Veenstra TD, Lu KP, Morrison DK. 2005. Regulation of Raf-1 by direct feedback phosphorylation. Molecular cell 17: 215-224.

Downs SM, Hudson ER, Hardie DG. 2002. A potential role for AMP-activated protein kinase in meiotic induction in mouse oocytes. Developmental biology 245: 200-212.

Du C, Fang M, Li Y, Li L, Wang X. 2000. Smac, a mitochondrial protein that promotes cytochrome c–dependent caspase activation by eliminating IAP inhibition. cell 102: 33-42.

Du Pasquier D, Dupré A, Jessus C. 2011. Unfertilized Xenopus eggs die by Bad-dependent apoptosis under the control of Cdk1 and JNK. PloS one 6: e23672.

Dupré A, Haccard O, Jessus C. 2010. Mos in the oocyte: how to use MAPK independently of growth factors and transcription to control meiotic divisions. Journal of signal transduction 2011.

Dupré A, Buffin E, Roustan C, Nairn AC, Jessus C, Haccard O. 2013. The phosphorylation of ARPP19 by Greatwall renders the auto-amplification of MPF independently of PKA in Xenopus oocytes. Journal of cell science 126: 3916-3926.

Edlich F, Banerjee S, Suzuki M, Cleland MM, Arnoult D, Wang C, Neutzner A, Tjandra N, Youle RJ. 2011. Bcl-xL Retrotranslocates Bax from the Mitochondria into the Cytosol. Cell 145: 104-116.

Elmore S. 2007. Apoptosis: a review of programmed cell death. Toxicologic pathology 35: 495-516.

Enomoto A, Suzuki N, Morita A, Ito M, Liu CQ, Matsumoto Y, Yoshioka K, Shiba T, Hosoi Y. 2003. Caspase-mediated cleavage of JNK during stress-induced apoptosis. Biochemical and biophysical research communications 306: 837-842.

Eskes R, Desagher S, Antonsson B, Martinou J-C. 2000. Bid induces the oligomerization and insertion of Bax into the outer mitochondrial membrane. Molecular and cellular biology 20: 929-935.

Falkenstein E, Meyer C, Eisen C, Scriba PC, Wehling M. 1996. Full-length cDNA sequence of a progesterone membrane-binding protein from porcine vascular smooth muscle cells. Biochemical and biophysical research communications 229: 86-89.

Fan H-Y, Sun Q-Y. 2004. Involvement of mitogen-activated protein kinase cascade during oocyte maturation and fertilization in mammals. Biology of reproduction 70: 535-547.

Fan Y, Bergmann A. 2009. The cleaved-Caspase-3 antibody is a marker of Caspase-9-like DRONC activity in Drosophila. Cell Death & Differentiation 17: 534-539.

Favata MF, Horiuchi KY, Manos EJ, Daulerio AJ, Stradley DA, Feeser WS, Van Dyk DE, Pitts WJ, Earl RA, Hobbs F. 1998. Identification of a novel inhibitor of mitogen-activated protein kinase kinase. Journal of Biological Chemistry 273: 18623-18632.

Ferrell JE. 1999. Xenopus oocyte maturation: new lessons from a good egg. Bioessays 21: 833-842.

Frank-Vaillant M, Jessus C, Ozon R, Maller JL, Haccard O. 1999. Two distinct mechanisms control the accumulation of cyclin B1 and Mos in Xenopus oocytes in response to progesterone. Molecular biology of the cell 10: 3279-3288.

Freeman RS, Meyer AN, Li J, Donoghue DJ. 1992. Phosphorylation of conserved serine residues does not regulate the ability of mosxe protein kinase to induce oocyte maturation or function as cytostatic factor. The Journal of cell biology 116: 725-735.

Gallo KA, Johnson GL. 2002. Mixed-lineage kinase control of JNK and p38 MAPK pathways. Nature reviews Molecular cell biology 3: 663-672.

Gao G, Dou QP. 2001. N-terminal cleavage of Bax by calpain generates a potent proapoptotic 18-kDa fragment that promotes Bcl-2-independent cytochrome C release and apoptotic cell death. Journal of cellular biochemistry 80: 53-72.

Gautier J, Solomon MJ, Booher RN, Bazan JF, Kirschner MW. 1991. cdc25 is a specific tyrosine phosphatase that directly activates p34 cdc2. Cell 67: 197-211.

Giam M, Huang D, Bouillet P. 2008. BH3-only proteins and their roles in programmed cell death. Oncogene 27: S128-S136.

Godeau JF, Schorderet-Slatkine S, Hubert P, Baulieu E-E. 1978. Induction of maturation in Xenopus laevis oocytes by a steroid linked to a polymer. Proceedings of the National Academy of Sciences 75: 2353-2357.

Gonzalez FA, Raden DL, Rigby MR, Davis RJ. 1992. Heterogeneous expression of four MAP kinase isoforms in human tissues. FEBS letters 304: 170-178.

Gotoh Y, Masuyama N, Dell K, Shirakabe K, Nishida E. 1995. Initiation of Xenopus oocyte maturation by activation of the mitogen-activated protein kinase cascade. Journal of Biological Chemistry 270: 25898-25904.

Gross A, McDonnell JM, Korsmeyer SJ. 1999. BCL-2 family members and the mitochondria in apoptosis. Genes & development 13: 1899-1911.

Guadagno TM, Ferrell JE. 1998. Requirement for MAPK activation for normal mitotic progression in Xenopus egg extracts. Science 282: 1312-1315.

Gubern A, Barceló-Torns M, Barneda D, López JM, Masgrau R, Picatoste F, Chalfant CE, Balsinde J, Balboa MA, Claro E. 2009. JNK and ceramide kinase govern the biogenesis of lipid droplets through activation of group IVA phospholipase A2. Journal of Biological Chemistry 284: 32359-32369.

Gupta S, Barrett T, Whitmarsh AJ, Cavanagh J, Sluss HK, Derijard B, Davis RJ. 1996. Selective interaction of JNK protein kinase isoforms with transcription factors. The EMBO Journal 15: 2760.

Gurdon J, Woodland H, Lingrel J. 1974. The Translation of mammalian globin mRNA injected into fertilized eggs of Xenopus laevis: I. Message stability in development. Developmental biology 39: 125-133.

Haccard O, Jessus C. 2006. Extra View Oocyte Maturation, Mos and Cyclins. Cell Cycle 5: 1152-1159.

Han J, Lee J, Bibbs L, Ulevitch R. 1994. A MAP kinase targeted by endotoxin and hyperosmolarity in mammalian cells. Science 265: 808-811.

Han J, Lee J-D, Jiang Y, Li Z, Feng L, Ulevitch RJ. 1996. Characterization of the structure and function of a novel MAP kinase kinase (MKK6). Journal of Biological Chemistry 271: 2886-2891.

Hibi M, Lin A, Smeal T, Minden A, Karin M. 1993. Identification of an oncoprotein-and UV-responsive protein kinase that binds and potentiates the c-Jun activation domain. Genes & development 7: 2135-2148.

Howard EL, Charlesworth A, Welk J, MacNicol AM. 1999. The Mitogen-Activated Protein Kinase Signaling Pathway Stimulates Mos mRNA Cytoplasmic Polyadenylation duringXenopus Oocyte Maturation. Molecular and cellular biology 19: 1990-1999.

Hu Y, Ding L, Spencer DM, Núñez G. 1998. WD-40 repeat region regulates Apaf-1 self-association and procaspase-9 activation. Journal of Biological Chemistry 273: 33489-33494.

Huang X-Q, Huang Z-X, Li Z-L, Chen X-W, Li X, Tang X-C, Liu F-Y, Liu Y, Chen L, Han W-J. 2013. C-Jun Terminal Kinases Play an Important Role in Regulating Embryonic Survival and Eye Development in Vertebrates. Current molecular medicine 13: 228-237.

Hurley RL, Anderson KA, Franzone JM, Kemp BE, Means AR, Witters LA. 2005. The Ca2+/calmodulin-dependent protein kinase kinases are AMP-activated protein kinase kinases. Journal of Biological Chemistry 280: 29060-29066.

Igea A, Méndez R. 2010. Meiosis requires a translational positive loop where CPEB1 ensues its replacement by CPEB4. The EMBO journal 29: 2182-2193.

Inoue H, Nojima H, Okayama H. 1990. High efficiency transformation of Escherichia coli with plasmids. Gene 96: 23-28.

Ishikawa K, Hanaoka Y, Kondo Y, Imai K. 1977. Primary action of steroid hormone at the surface of amphibian oocyte in the induction of germinal vesicle breakdown. Molecular and cellular endocrinology 9: 91-100.

Izumi T, Maller JL. 1993. Elimination of cdc2 phosphorylation sites in the cdc25 phosphatase blocks initiation of M-phase. Molecular biology of the cell 4: 1337-1350.

—. 1995. Phosphorylation and activation of the Xenopus Cdc25 phosphatase in the absence of Cdc2 and Cdk2 kinase activity. Molecular biology of the cell 6: 215-226.

Jeong DG, Yoon T-S, Kim JH, Shim MY, Jung S-K, Son JH, Ryu SE, Kim SJ. 2006. Crystal structure of the catalytic domain of human MAP kinase phosphatase 5: structural insight into constitutively active phosphatase. Journal of molecular biology 360: 946-955.

Jiang X, Wang X. 2000. Cytochrome c promotes caspase-9 activation by inducing nucleotide binding to Apaf-1. Journal of Biological Chemistry 275: 31199-31203.

Jiang Y, Chen C, Li Z, Guo W, Gegner JA, Lin S, Han J. 1996. Characterization of the structure and function of a new mitogen-activated protein kinase (p38β). Journal of Biological Chemistry 271: 17920-17926.

Jiang Y, Gram H, Zhao M, New L, Gu J, Feng L, Di Padova F, Ulevitch RJ, Han J. 1997. Characterization of the structure and function of the fourth member of p38 group mitogen-activated protein kinases, p38δ. Journal of Biological Chemistry 272: 30122-30128.

Jones SW, Erikson E, Blenis J, Maller JL, Erikson R. 1988. A Xenopus ribosomal protein S6 kinase has two apparent kinase domains that are each similar to distinct protein kinases. Proceedings of the National Academy of Sciences 85: 3377-3381.

Josefsberg Ben-Yehoshua L, Lewellyn AL, Thomas P, Maller JL. 2007. The role of Xenopus membrane progesterone receptor β in mediating the effect of progesterone on oocyte maturation. Molecular Endocrinology 21: 664-673.

König H-G, Rehm M, Gudorf D, Krajewski S, Gross A, Ward MW, Prehn JH. 2007. Full length Bid is sufficient to induce apoptosis of cultured rat hippocampal neurons. BMC cell biology 8: 7.

Kallunki T, Su B, Tsigelny I, Sluss HK, Dérijard B, Moore G, Davis R, Karin M. 1994. JNK2 contains a specificity-determining region responsible for efficient c-Jun binding and phosphorylation. Genes & Development 8: 2996-3007.

Karandikar M, Xu S, Cobb MH. 2000. MEKK1 binds raf-1 and the ERK2 cascade components. Journal of Biological Chemistry 275: 40120-40127.

Keady BT, Kuo P, Martínez SE, Yuan L, Hake LE. 2007. MAPK interacts with XGef and is required for CPEB activation during meiosis in Xenopus oocytes. Journal of cell science 120: 1093-1103.

Kerr JF, Wyllie AH, Currie AR. 1972. Apoptosis: a basic biological phenomenon with wide-ranging implications in tissue kinetics. British journal of cancer 26: 239.

Kerscher O, Felberbaum R, Hochstrasser M. 2006. Modification of proteins by ubiquitin and ubiquitin-like proteins. Annu. Rev. Cell Dev. Biol. 22: 159-180.

Kholodenko BN, Birtwistle MR. 2009. Four-dimensional dynamics of MAPK information processing systems. Wiley Interdiscip Rev Syst Biol Med 1: 28-44.

Kim B-J, Ryu S-W, Song B-J. 2006. JNK-and p38 kinase-mediated phosphorylation of Bax leads to its activation and mitochondrial translocation and to apoptosis of human hepatoma HepG2 cells. Journal of Biological Chemistry 281: 21256-21265.

Kim H-E, Du F, Fang M, Wang X. 2005. Formation of apoptosome is initiated by cytochrome c-induced dATP hydrolysis and subsequent nucleotide exchange on Apaf-1. Proceedings of the National Academy of Sciences of the United States of America 102: 17545-17550.

Kim J, Lee J, Margolis R, Fotedar R. 2010. SP600125 suppresses Cdk1 and induces endoreplication directly from G2 phase, independent of JNK inhibition. Oncogene 29: 1702-1716.

Kluck RM, Martin SJ, Hoffman BM, Zhou JS, Green DR, Newmeyer DD. 1997. Cytochrome c activation of CPP32-like proteolysis plays a critical role in a Xenopus cell-free apoptosis system. The EMBO journal 16: 4639-4649.

Kominami K, Takagi C, Kurata T, Kitayama A, Nozaki M, Sawasaki T, Kuida K, Endo Y, Manabe N, Ueno N. 2006. The initiator caspase, caspase-10β, and the BH-3-only molecule, Bid, demonstrate evolutionary conservation in Xenopus of their pro-apoptotic activities in the extrinsic and intrinsic pathways. Genes to Cells 11: 701-717.

Kroemer G, Galluzzi L, Brenner C. 2007. Mitochondrial membrane permeabilization in cell death. Physiological reviews 87: 99-163.

Kuwana T, Smith JJ, Muzio M, Dixit V, Newmeyer DD, Kornbluth S. 1998. Apoptosis induction by caspase-8 is amplified through the mitochondrial release of cytochrome c. Journal of Biological Chemistry 273: 16589-16594.

Kuwana T, Bouchier-Hayes L, Chipuk JE, Bonzon C, Sullivan BA, Green DR, Newmeyer DD. 2005. BH3 domains of BH3-only proteins differentially regulate Bax-mediated mitochondrial membrane permeabilization both directly and indirectly. Molecular cell 17: 525-535.

Kvansakul M, Yang H, Fairlie W, Czabotar P, Fischer S, Perugini M, Huang D, Colman P. 2008. Vaccinia virus anti-apoptotic F1L is a novel Bcl-2-like domain-swapped dimer that binds a highly selective subset of BH3-containing death ligands. Cell Death & Differentiation 15: 1564-1571.

Kyriakis JM, Avruch J. 1990. pp54 microtubule-associated protein 2 kinase. A novel serine/threonine protein kinase regulated by phosphorylation and stimulated by poly-L-lysine. Journal of Biological Chemistry 265: 17355-17363.

Lösel R, Dorn-Beineke A, Falkenstein E, Wehling M, Feuring M. 2004. Porcine spermatozoa contain more than one membrane progesterone receptor. The international journal of biochemistry & cell biology 36: 1532-1541.

Lösel RM, Besong D, Peluso JJ, Wehling M. 2008. Progesterone receptor membrane component 1—many tasks for a versatile protein. Steroids 73: 929-934.

Lamb JA, Ventura J-J, Hess P, Flavell RA, Davis RJ. 2003. JunD mediates survival signaling by the JNK signal transduction pathway. Molecular cell 11: 1479-1489.

Lawler S, Fleming Y, Goedert M, Cohen P. 1998. Synergistic activation of SAPK1/JNK1 by two MAP kinase kinases in vitro. Current Biology 8: 1387-1391.

Lee JC, Kumar S, Griswold DE, Underwood DC, Votta BJ, Adams JL. 2000. Inhibition of p38 MAP kinase as a therapeutic strategy. Immunopharmacology 47: 185-201.

Lei K, Davis RJ. 2003. JNK phosphorylation of Bim-related members of the Bcl2 family induces Bax-dependent apoptosis. Proceedings of the National Academy of Sciences 100: 2432-2437.

Lei K, Nimnual A, Zong W-X, Kennedy NJ, Flavell RA, Thompson CB, Bar-Sagi D, Davis RJ. 2002. The Bax subfamily of Bcl2-related proteins is essential for apoptotic signal transduction by c-Jun NH2-terminal kinase. Molecular and cellular biology 22: 4929-4942.

Letai A, Bassik MC, Walensky LD, Sorcinelli MD, Weiler S, Korsmeyer SJ. 2002. Distinct BH3 domains either sensitize or activate mitochondrial apoptosis, serving as prototype cancer therapeutics. Cancer cell 2: 183-192.

Li H, Zhu H, Xu C-j, Yuan J. 1998. Cleavage of BID by caspase 8 mediates the mitochondrial damage in the Fas pathway of apoptosis. Cell 94: 491-501.

Li P, Nijhawan D, Budihardjo I, Srinivasula SM, Ahmad M, Alnemri ES, Wang X. 1997. Cytochrome c and dATP-dependent formation of Apaf-1/caspase-9 complex initiates an apoptotic protease cascade. Cell 91: 479-489.

Liu X, Kim CN, Yang J, Jemmerson R, Wang X. 1996. Induction of apoptotic program in cell-free extracts: requirement for dATP and cytochrome c. Cell 86: 147-157.

Lorenz K, Schmitt JP, Schmitteckert EM, Lohse MJ. 2008. A new type of ERK1/2 autophosphorylation causes cardiac hypertrophy. Nature medicine 15: 75-83.

Lovell JF, Billen LP, Bindner S, Shamas-Din A, Fradin C, Leber B, Andrews DW. 2008. Membrane binding by tBid initiates an ordered series of events culminating in membrane permeabilization by Bax. Cell 135: 1074-1084.

Luo X, Budihardjo I, Zou H, Slaughter C, Wang X. 1998. Bid, a Bcl2 interacting protein, mediates cytochrome c release from mitochondria in response to activation of cell surface death receptors. Cell 94: 481-490.

Lutter M, Fang M, Luo X, Nishijima M, Xie X-s, Wang X. 2000. Cardiolipin provides specificity for targeting of tBid to mitochondria. Nature cell biology 2: 754-761.

Lutz L, Cole L, Gupta M, Kwist K, Auchus R, Hammes S. 2001. Evidence that androgens are the primary steroids produced by Xenopus laevis ovaries and may signal through the classical androgen receptor to promote oocyte maturation. Proceedings of the National Academy of Sciences 98: 13728-13733.

Madesh M, Antonsson B, Srinivasula SM, Alnemri ES, Hajnóczky G. 2002. Rapid kinetics of tBid-induced cytochrome c and Smac/DIABLO release and mitochondrial depolarization. Journal of Biological Chemistry 277: 5651-5659.

Makani S, Gollapudi S, Yel L, Chiplunkar S, Gupta S. 2002. Biochemical and molecular basis of thimerosal-induced apoptosis in T cells: a major role of mitochondrial pathway. Genes and immunity 3: 270-278.

Mandic A, Viktorsson K, Strandberg L, Heiden T, Hansson J, Linder S, Shoshan MC. 2002. Calpain-mediated Bid cleavage and calpain-independent Bak modulation: two separate pathways in cisplatin-induced apoptosis. Molecular and cellular biology 22: 3003-3013.

Manning G, Whyte DB, Martinez R, Hunter T, Sudarsanam S. 2002. The protein kinase complement of the human genome. Science 298: 1912-1934.

Martiáñez T, Francès S, López JM. 2009. Generation of digital responses in stress sensors. Journal of Biological Chemistry 284: 23902-23911.

Martin JH, Mohit AA, Miller CA. 1996. Developmental expression in the mouse nervous system of the p49 3F12 SAP kinase. Molecular brain research 35: 47-57.

Martinez S, Grandy R, Pasten P, Montecinos H, Montecino M, Olate J, Hinrichs MV. 2006. Plasma membrane destination of the classical Xenopus laevis progesterone receptor accelerates progesterone-induced oocyte maturation. Journal of cellular biochemistry 99: 853-859.

Martinou J-C, Youle RJ. 2011. Mitochondria in apoptosis: Bcl-2 family members and mitochondrial dynamics. Developmental cell 21: 92-101.

McCoy F, Darbandi R, Chen S-I, Eckard L, Dodd K, Jones K, Baucum AJ, Gibbons JA, Lin S-H, Colbran RJ. 2013. Metabolic regulation of CaMKII protein and caspases in Xenopus laevis egg extracts. Journal of Biological Chemistry 288: 8838-8848.

McDonnell JM, Fushman D, Milliman CL, Korsmeyer SJ, Cowburn D. 1999. Solution structure of the proapoptotic molecule BID: a structural basis for apoptotic agonists and antagonists. Cell 96: 625-634.

McGrew LL, Dworkin-Rastl E, Dworkin MB, Richter JD. 1989. Poly (A) elongation during Xenopus oocyte maturation is required for translational recruitment and is mediated by a short sequence element. Genes & development 3: 803-815.

Meier R, Rouse J, Cuenda A, Nebreda AR, Cohen P. 1996. Cellular Stresses and Cytokines Activate Multiple Mitogen-Activated-Protein Kinase Kinase Homologues in PC12 and KB Cells. European Journal of Biochemistry 236: 796-805.

Mendez R, Richter JD. 2001. Translational control by CPEB: a means to the end. Nature Reviews Molecular Cell Biology 2: 521-529.

Mendez R, Hake LE, Andresson T, Littlepage LE, Ruderman JV, Richter JD. 2000. Phosphorylation of CPE binding factor by Eg2 regulates translation of c-mos mRNA. Nature 404: 302-307.

Messaoud NB. Mecanismos de regulación de la muerte del oocito por shock hiperosmótico.Thesis Dissertation. Universitat Autònoma de Barcelona, 2014.

Meyer D, Liu A, Margolis B. 1999. Interaction of c-Jun amino-terminal kinase interacting protein-1 with p190 rhoGEF and its localization in differentiated neurons. Journal of Biological Chemistry 274: 35113-35118.

Milhas D, Cuvillier O, Therville N, Clavé P, Thomsen M, Levade T, Benoist H, Ségui B. 2005. Caspase-10 triggers Bid cleavage and caspase cascade activation in FasL-induced apoptosis. Journal of Biological Chemistry 280: 19836-19842.

Minden A, Lin A, McMahon M, Lange-Carter C, Derijard B, Davis RJ, Johnson GL, Karin M. 1994. Differential activation of ERK and JNK mitogen-activated protein kinases by Raf-1 and MEKK. Science 266: 1719-1723.

Minshull J, Sun H, Tonks NK, Murray AW. 1994. A MAP kinase-dependent spindle assembly checkpoint in Xenopus egg extracts. Cell 79: 475-486.

Mood K, Bong Y-S, Lee H-S, Ishimura A, Daar IO. 2004. Contribution of JNK, Mek, Mos and PI-3K signaling to GVBD in Xenopus oocytes. Cellular signalling 16: 631-642.

Moriguchi T, Toyoshima F, Masuyama N, Hanafusa H, Gotoh Y, Nishida E. 1997. A novel SAPK/JNK kinase, MKK7, stimulated by TNFα and cellular stresses. The EMBO Journal 16: 7045-7053.

Morizane Y, Honda R, Fukami K, Yasuda H. 2005. X-linked inhibitor of apoptosis functions as ubiquitin ligase toward mature caspase-9 and cytosolic Smac/DIABLO. Journal of biochemistry 137: 125-132.

Morrill GA, Kostellow AB, Askari A. 2010. Progesterone modulation of transmembrane helix-helix interactions between the α-subunit of Na/K-ATPase and phospholipid N-methyltransferase in the oocyte plasma membrane. BMC structural biology 10: 12.

Morrill GA, Erlichman J, Gutierrez-Juarez R, Kostellow AB. 2005. The steroid-binding subunit of the Na/K-ATPase as a progesterone receptor on the amphibian oocyte plasma membrane. Steroids 70: 933-945.

Morrison DK, Davis RJ. 2003. Regulation of map kinase signaling modules by scaffold proteins in mammals*. Annual review of cell and developmental biology 19: 91-118.

Muzio M, Chinnaiyan AM, Kischkel FC, O'Rourke K, Shevchenko A, Ni J, Scaffidi C, Bretz JD, Zhang M, Gentz R. 1996. FLICE, a novel FADD-homologous ICE/CED-3–like protease, is recruited to the CD95 (Fas/APO-1) death-inducing signaling complex. Cell 85: 817-827.

Nakajima R, Masukata H. 2002. SpSld3 is required for loading and maintenance of SpCdc45 on chromatin in DNA replication in fission yeast. Molecular biology of the cell 13: 1462-1472.

Newmeyer DD, Farschon DM, Reed JC. 1994. Cell-free apoptosis in Xenopus egg extracts: inhibition by Bcl-2 and requirement for an organelle fraction enriched in mitochondria. Cell 79: 353-364.

Nutt LK. 2012. The Xenopus oocyte: A model for studying the metabolic regulation of cancer cell death. Pages 412-418. Seminars in cell & developmental biology: Elsevier.

Nutt LK, Margolis SS, Jensen M, Herman CE, Dunphy WG, Rathmell JC, Kornbluth S. 2005. Metabolic regulation of oocyte cell death through the CaMKII-mediated phosphorylation of caspase-2. Cell 123: 89-103.

Ohori M, Kinoshita T, Okubo M, Sato K, Yamazaki A, Arakawa H, Nishimura S, Inamura N, Nakajima H, Neya M. 2005. Identification of a selective ERK inhibitor and structural determination of the inhibitor–ERK2 complex. Biochemical and biophysical research communications 336: 357-363.

Ott M, Robertson JD, Gogvadze V, Zhivotovsky B, Orrenius S. 2002. Cytochrome c release from mitochondria proceeds by a two-step process. Proceedings of the National Academy of Sciences 99: 1259-1263.

Owens D, Keyse S. 2007. Differential regulation of MAP kinase signalling by dual-specificity protein phosphatases. Oncogene 26: 3203-3213.

Pörn-Ares M, Ares M, Orrenius S. 1998. Calcium signalling and the regulation of apoptosis. Toxicology in vitro 12: 539-543.

Palmer A, Gavin AC, Nebreda AR. 1998. A link between MAP kinase and p34cdc2/cyclin B during oocyte maturation: p90rsk phosphorylates and inactivates the p34cdc2 inhibitory kinase Myt1. The EMBO Journal 17: 5037-5047.

Papkoff J, Verma IM, Hunter T. 1982. Detection of a transforming gene product in cells transformed by Moloney murine sarcoma virus. Cell 29: 417-426.

Pargellis C, Tong L, Churchill L, Cirillo PF, Gilmore T, Graham AG, Grob PM, Hickey ER, Moss N, Pav S. 2002. Inhibition of p38 MAP kinase by utilizing a novel allosteric binding site. Nature Structural & Molecular Biology 9: 268-272.

Parone PA, James DI, Da Cruz S, Mattenberger Y, Donzé O, Barja F, Martinou J-C. 2006. Inhibiting the mitochondrial fission machinery does not prevent Bax/Bak-dependent apoptosis. Molecular and cellular biology 26: 7397-7408.

Peluso JJ, Romak J, Liu X. 2008. Progesterone receptor membrane component-1 (PGRMC1) is the mediator of progesterone's antiapoptotic action in spontaneously immortalized granulosa cells as revealed by PGRMC1 small interfering ribonucleic acid treatment and functional analysis of PGRMC1 mutations. Endocrinology 149: 534-543.

Peluso JJ, Pappalardo A, Losel R, Wehling M. 2006. Progesterone membrane receptor component 1 expression in the immature rat ovary and its role in mediating progesterone's antiapoptotic action. Endocrinology 147: 3133-3140.

Perdiguero E, Pillaire MJ, Bodart JF, Hennersdorf F, Frödin M, Duesbery NS, Alonso G, Nebreda AR. 2003. Xp38γ/SAPK3 promotes meiotic G2/M transition in Xenopus oocytes and activates Cdc25C. The EMBO journal 22: 5746-5756.

Peter ME, Krammer P. 2003. The CD95 (APO-1/Fas) DISC and beyond. Cell Death & Differentiation 10: 26-35.

Petros AM, Olejniczak ET, Fesik SW. 2004. Structural biology of the Bcl-2 family of proteins. Biochimica et Biophysica Acta (BBA)-Molecular Cell Research 1644: 83-94.

Pham CD, Arlinghaus RB, Zheng C-F, Guan K-L, Singh B. 1995. Characterization of MEK1 phosphorylation by the v-Mos protein. Oncogene 10: 1683-1688.

Posada J, Yew N, Ahn N, Woude GV, Cooper J. 1993. Mos stimulates MAP kinase in Xenopus oocytes and activates a MAP kinase kinase in vitro. Molecular and Cellular Biology 13: 2546-2553.

Pulverer BJ, Kyriakis JM, Avruch J, Nikolakaki E, Woodgett JR. 1991. Phosphorylation of c-jun mediated by MAP kinases. Nature 353: 670-674.

Putcha GV, Le S, Frank S, Besirli CG, Clark K, Chu B, Alix S, Youle RJ, LaMarche A, Maroney AC. 2003. JNK-mediated BIM phosphorylation potentiates BAX-dependent apoptosis. Neuron 38: 899-914.

Puthalakath H, Strasser A. 2002. Keeping killers on a tight leash: transcriptional and post-translational control of the pro-apoptotic activity of BH3-only proteins. Cell death and differentiation 9: 505-512.

Qian Y-W, Erikson E, Taieb FE, Maller JL. 2001. The polo-like kinase Plx1 is required for activation of the phosphatase Cdc25C and cyclin B-Cdc2 in Xenopus oocytes. Molecular biology of the cell 12: 1791-1799.

Radford HE, Meijer HA, de Moor CH. 2008. Translational control by cytoplasmic polyadenylation in Xenopus oocytes. Biochimica et Biophysica Acta (BBA)-Gene Regulatory Mechanisms 1779: 217-229.

Raman M, Chen W, Cobb M. 2007. Differential regulation and properties of MAPKs. Oncogene 26: 3100-3112.

Rapp UR, Götz R, Albert S. 2006. BuCy RAFs drive cells into MEK addiction. Cancer Cell 9: 9-12.

Ray LB, Sturgill TW. 1988. Insulin-stimulated microtubule-associated protein kinase is phosphorylated on tyrosine and threonine in vivo. Proceedings of the National Academy of Sciences 85: 3753-3757.

Regan J, Breitfelder S, Cirillo P, Gilmore T, Graham AG, Hickey E, Klaus B, Madwed J, Moriak M, Moss N. 2002. Pyrazole urea-based inhibitors of p38 MAP kinase: from lead compound to clinical candidate. Journal of medicinal chemistry 45: 2994-3008.

Reiners Jr J, Caruso J, Mathieu P, Chelladurai B, Yin X-M, Kessel D. 2002. Release of cytochrome c and activation of pro-caspase-9 following lysosomal photodamage involves Bid cleavage. Cell Death & Differentiation 9.

Richter JD. 2007. CPEB: a life in translation. Trends in biochemical sciences 32: 279-285.

Riedl SJ, Shi Y. 2004. Molecular mechanisms of caspase regulation during apoptosis. Nature Reviews Molecular Cell Biology 5: 897-907.

Riedl SJ, Salvesen GS. 2007. The apoptosome: signalling platform of cell death. Nature Reviews Molecular Cell Biology 8: 405-413.

Rodríguez-Enfedaque A, Delmas E, Guillaume A, Gaumer S, Mignotte B, Vayssière J-L, Renaud F. 2012. zVAD-fmk upregulates caspase-9 cleavage and activity in etoposide-induced cell death of mouse embryonic fibroblasts. Biochimica et Biophysica Acta (BBA)-Molecular Cell Research 1823: 1343-1352.

Rouse J, Cohen P, Trigon S, Morange M, Alonso-Llamazares A, Zamanillo D, Hunt T, Nebreda AR. 1994. A novel kinase cascade triggered by stress and heat shock that stimulates MAPKAP kinase-2 and phosphorylation of the small heat shock proteins. Cell 78: 1027-1037.

Sagata N, Watanabe N, Woude GFV, Ikawa Y. 1989. The c-mos proto-oncogene product is a cytostatic factor responsible for meiotic arrest in vertebrate eggs.

Saitoh T, Tsuchiya Y, Kinoshita T, Itoh M, Yamashita S. 2009. Pro-apoptotic activity and mono-/diubiquitylation of Xenopus Bid in egg extracts. Biochemical and biophysical research communications 384: 491-494.

Salvesen GS, Dixit VM. 1997. Caspases: intracellular signaling by proteolysis. Cell 91: 443-446.

Schaeffer HJ, Weber MJ. 1999. Mitogen-activated protein kinases: specific messages from ubiquitous messengers. Molecular and cellular biology 19: 2435-2444.

Schmitt A, Nebreda AR. 2002. Signalling pathways in oocyte meiotic maturation. Journal of cell science 115: 2457-2459.

Schmitt A, Gutierrez GJ, Lénárt P, Ellenberg J, Nebreda AR. 2002. Histone H3 phosphorylation during Xenopus oocyte maturation: regulation by the MAP kinase/p90Rsk pathway and uncoupling from DNA condensation. FEBS letters 518: 23-28.

Schroeter H, BOYD C, Ahmed R, Spencer J, DUNCAN R, Rice-Evans C, Cadenas E. 2003. c-Jun N-terminal kinase (JNK)-mediated modulation of brain mitochondria function: new target proteins for JNK signalling in mitochondrion-dependent apoptosis. Biochem. J 372: 359-369.

Setoyama D, Yamashita M, Sagata N. 2007. Mechanism of degradation of CPEB during Xenopus oocyte maturation. Proceedings of the National Academy of Sciences 104: 18001-18006.

Shamas-Din A, Brahmbhatt H, Leber B, Andrews DW. 2011. BH3-only proteins: Orchestrators of apoptosis. Biochimica et Biophysica Acta (BBA)-Molecular Cell Research 1813: 508-520.

Sharrocks AD, Yang S-H, Galanis A. 2000. Docking domains and substrate-specificity determination for MAP kinases. Trends in biochemical sciences 25: 448-453.

Shaul YD, Seger R. 2006. ERK1c regulates Golgi fragmentation during mitosis. The Journal of cell biology 172: 885-897.

Shaw AS, Filbert EL. 2009. Scaffold proteins and immune-cell signalling. Nature Reviews Immunology 9: 47-56.

Shi Y. 2002. Mechanisms of caspase activation and inhibition during apoptosis. Molecular cell 9: 459-470.

—. 2008. Chapter Seven Apoptosome Assembly. Methods in enzymology 442: 141-156.

Shieh J-C, Wilkinson MG, Millar JB. 1998. The Win1 mitotic regulator is a component of the fission yeast stress-activated Sty1 MAPK pathway. Molecular biology of the cell 9: 311-322.

Shiozaki K, Russell P. 1995. Cell-cycle control linked to extracellular environment by MAP kinase pathway in fission yeast.

Slee EA, Keogh SA, Martin SJ. 2000. Cleavage of BID during cytotoxic drug and UV radiation-induced apoptosis occurs downstream of the point of Bcl-2 action and is catalysed by caspase-3: a potential feedback loop for amplification of apoptosis-associated mitochondrial cytochrome c release. Cell Death & Differentiation 7.

Sluss HK, Barrett T, Derijard B, Davis RJ. 1994. Signal transduction by tumor necrosis factor mediated by JNK protein kinases. Molecular and Cellular Biology 14: 8376-8384.

Smith LD, Ecker R. 1971. The interaction of steroids with Rana pipiens oocytes in the induction of maturation. Developmental biology 25: 232-247.

Song J, Tan H, Shen H, Mahmood K, Boyd SE, Webb GI, Akutsu T, Whisstock JC. 2010. Cascleave: towards more accurate prediction of caspase substrate cleavage sites. Bioinformatics 26: 752-760.

Srinivasula SM, Datta P, Fan X-J, Fernandes-Alnemri T, Huang Z, Alnemri ES. 2000. Molecular determinants of the caspase-promoting activity of Smac/DIABLO and its role in the death receptor pathway. Journal of Biological Chemistry 275: 36152-36157.

Srinivasula SM, Hegde R, Saleh A, Datta P, Shiozaki E, Chai J, Lee R-A, Robbins PD, Fernandes-Alnemri T, Shi Y. 2001. A conserved XIAP-interaction motif in caspase-9 and Smac/DIABLO regulates caspase activity and apoptosis. Nature 410: 112-116.

Srivastava RK, Mi Q-S, Hardwick JM, Longo DL. 1999. Deletion of the loop region of Bcl-2 completely blocks paclitaxel-induced apoptosis. Proceedings of the National Academy of Sciences 96: 3775-3780.

Strasser A. 2005. The role of BH3-only proteins in the immune system. Nature Reviews Immunology 5: 189-200.

Strum JC, Swenson KI, Turner JE, Bell RM. 1995. Ceramide triggers meiotic cell cycle progression in Xenopus oocytes. A potential mediator of progesterone-induced maturation. Journal of Biological Chemistry 270: 13541-13547.

Sunayama J, Tsuruta F, Masuyama N, Gotoh Y. 2005. JNK antagonizes Akt-mediated survival signals by phosphorylating 14-3-3. The Journal of cell biology 170: 295-304.

Sutton VR, Wowk ME, Cancilla M, Trapani JA. 2003. Caspase activation by granzyme B is indirect, and caspase autoprocessing requires the release of proapoptotic mitochondrial factors. Immunity 18: 319-329.

Sutton VR, Davis JE, Cancilla M, Johnstone RW, Ruefli AA, Sedelies K, Browne KA, Trapani JA. 2000. Initiation of apoptosis by granzyme B requires direct cleavage of bid, but not direct granzyme B–mediated caspase activation. The Journal of experimental medicine 192: 1403-1414.

Tait SW, de Vries E, Maas C, Keller AM, D'Santos CS, Borst J. 2007. Apoptosis induction by Bid requires unconventional ubiquitination and degradation of its N-terminal fragment. The Journal of cell biology 179: 1453-1466.

Takenaka K, Moriguchi T, Nishida E. 1998. Activation of the protein kinase p38 in the spindle assembly checkpoint and mitotic arrest. Science 280: 599-602.

Tan KO, Tan KML, Victor CY. 1999. A novel BH3-like domain in BID is required for intramolecular interaction and autoinhibition of pro-apoptotic activity. Journal of Biological Chemistry 274: 23687-23690.

Tanoue T, Adachi M, Moriguchi T, Nishida E. 2000. A conserved docking motif in MAP kinases common to substrates, activators and regulators. Nature cell biology 2: 110-116.

Tay J, Hodgman R, Sarkissian M, Richter JD. 2003. Regulated CPEB phosphorylation during meiotic progression suggests a mechanism for temporal control of maternal mRNA translation. Genes & development 17: 1457-1462.

Thomas D, Wendt-Nordahl G, Röckl K, Ficker E, Brown AM, Kiehn J. 2001. High-affinity blockade of human ether-a-go-go-related gene human cardiac potassium channels by the novel antiarrhythmic drug BRL-32872. Journal of Pharmacology and Experimental Therapeutics 297: 753-761.

Thomas D, Hammerling BC, Wimmer A-B, Wu K, Ficker E, Kuryshev YA, Scherer D, Kiehn J, Katus HA, Schoels W. 2004. Direct block of hERG potassium channels by the protein kinase C inhibitor bisindolylmaleimide I (GF109203X). Cardiovascular research 64: 467-476.

Tian J, Kim S, Heilig E, Ruderman JV. 2000. Identification of XPR-1, a progesterone receptor required for Xenopus oocyte activation. Proceedings of the National Academy of Sciences 97: 14358-14363.

Tournier C, Whitmarsh AJ, Cavanagh J, Barrett T, Davis RJ. 1999. The MKK7 gene encodes a group of c-Jun NH2-terminal kinase kinases. Molecular and cellular biology 19: 1569-1581.

Tournier C, Hess P, Yang DD, Xu J, Turner TK, Nimnual A, Bar-Sagi D, Jones SN, Flavell RA, Davis RJ. 2000. Requirement of JNK for stress-induced activation of the cytochrome c-mediated death pathway. Science 288: 870-874.

Toyoshima-Morimoto F, Taniguchi E, Nishida E. 2002. Plk1 promotes nuclear translocation of human Cdc25C during prophase. EMBO reports 3: 341-348.

Tran TH, Andreka P, Rodrigues CO, Webster KA, Bishopric NH. 2007. Jun kinase delays caspase-9 activation by interaction with the apoptosome. Journal of Biological Chemistry 282: 20340-20350.

Tsuruta F, Sunayama J, Mori Y, Hattori S, Shimizu S, Tsujimoto Y, Yoshioka K, Masuyama N, Gotoh Y. 2004. JNK promotes Bax translocation to mitochondria through phosphorylation of 14-3-3 proteins. The EMBO journal 23: 1889-1899.

Valentijn AJ, Gilmore AP. 2004. Translocation of full-length Bid to mitochondria during anoikis. Journal of Biological Chemistry 279: 32848-32857.

Vaux DL. 2011. Apoptogenic factors released from mitochondria. Biochimica et Biophysica Acta (BBA)-Molecular Cell Research 1813: 546-550.

Ventura J-J, Hübner A, Zhang C, Flavell RA, Shokat KM, Davis RJ. 2006. Chemical genetic analysis of the time course of signal transduction by JNK. Molecular cell 21: 701-710.

Verhagen AM, Ekert PG, Pakusch M, Silke J, Connolly LM, Reid GE, Moritz RL, Simpson RJ, Vaux DL. 2000. Identification of DIABLO, a mammalian protein that promotes apoptosis by binding to and antagonizing IAP proteins. cell 102: 43-53.

Verheij M, Bose R, Lin XH, Yao B, Jarvis WD, Grant S, Birrer MJ, Szabo E, Zon LI, Kyriakis JM. 1996. Requirement for ceramide-initiated SAPK/JNK signalling in stress-induced apoptosis.

Wagner EF, Nebreda ÁR. 2009. Signal integration by JNK and p38 MAPK pathways in cancer development. Nature Reviews Cancer 9: 537-549.

Wang C, Youle RJ. 2009. The role of mitochondria in apoptosis*. Annual review of genetics 43: 95-118.

Wang K, Yin X-M, Chao DT, Milliman CL, Korsmeyer SJ. 1996. BID: a novel BH3 domain-only death agonist. Genes & development 10: 2859-2869.

Wang KK, Posmantur R, Nadimpalli R, Nath R, Mohan P, Nixon RA, Talanian RV, Keegan M, Herzog L, Allen H. 1998. Caspase-mediated fragmentation of calpain inhibitor protein calpastatin during apoptosis. Archives of biochemistry and biophysics 356: 187-196.

Wang R, He G, Nelman-Gonzalez M, Ashorn CL, Gallick GE, Stukenberg PT, Kirschner MW, Kuang J. 2007a. Regulation of Cdc25C by ERK-MAP Kinases during the G2/M Transition. Cell 128: 1119-1132.

—. 2007b. Regulation of Cdc25C by ERK-MAP Kinases during the G2/M Transition. Cell 128: 1119-1132.

Wang X-T, Pei D-S, Xu J, Guan Q-H, Sun Y-F, Liu X-M, Zhang G-Y. 2007c. Opposing effects of Bad phosphorylation at two distinct sites by Akt1 and JNK1/2 on ischemic brain injury. Cellular signalling 19: 1844-1856.

Wang X. 2001. The expanding role of mitochondria in apoptosis. Genes & development 15: 2922-2933.

Wang X, Destrument A, Tournier C. 2007d. Physiological roles of MKK4 and MKK7: insights from animal models. Biochimica et Biophysica Acta (BBA)-Molecular Cell Research 1773: 1349-1357.

Wang X, McGowan CH, Zhao M, He L, Downey JS, Fearns C, Wang Y, Huang S, Han J. 2000. Involvement of the MKK6-p38γ cascade in γ-radiation-induced cell cycle arrest. Molecular and cellular biology 20: 4543-4552.

Watanabe N, Vande WG, Ikawa Y, Sagata N. 1989. Specific proteolysis of the c-mos proto-oncogene product by calpain on fertilization of Xenopus eggs. Nature 342: 505-511.

Wei MC, Zong W-X, Cheng EH-Y, Lindsten T, Panoutsakopoulou V, Ross AJ, Roth KA, MacGregor GR, Thompson CB, Korsmeyer SJ. 2001. Proapoptotic BAX and BAK: a requisite gateway to mitochondrial dysfunction and death. Science 292: 727-730.

Wessel D, Flügge U-I. 1984. A method for the quantitative recovery of protein in dilute solution in the presence of detergents and lipids. Analytical biochemistry 138: 141-143.

Weston CR, Davis RJ. 2002. The JNK signal transduction pathway. Current opinion in genetics & development 12: 14-21.

—. 2007. The JNK signal transduction pathway. Current opinion in cell biology 19: 142-149.

Whitmarsh AJ, Davis RJ. 1998. Structural organization of MAP-kinase signaling modules by scaffold proteins in yeast and mammals. Trends in biochemical sciences 23: 481-485.

Xu S, Robbins D, Frost J, Dang A, Lange-Carter C, Cobb MH. 1995. MEKK1 phosphorylates MEK1 and MEK2 but does not cause activation of mitogen-activated protein kinase. Proceedings of the National Academy of Sciences 92: 6808-6812.

Yamamoto K, Ichijo H, Korsmeyer SJ. 1999. BCL-2 is phosphorylated and inactivated by an ASK1/Jun N-terminal protein kinase pathway normally activated at G2/M. Molecular and cellular biology 19: 8469-8478.

Yamashita Y, Hishinuma M, Shimada M. 2009. Journal of Ovarian Research. Journal of ovarian research 2: 20.

Yang A, Walker N, Bronson R, Kaghad M, Oosterwegel M, Bonnin J, Vagner C, Bonnet H, Dikkes P, Sharpe A. 2000. p73-deficient mice have neurological, pheromonal and inflammatory defects but lack spontaneous tumours. Nature 404: 99-103.

Yang DD, Kuan C-Y, Whitmarsh AJ, Rinócn M, Zheng TS, Davis RJ, Rakic P, Flavell RA. 1997. Absence of excitotoxicity-induced apoptosis in the hippocampus of mice lacking the Jnk3 gene. Nature 389: 865-870.

Yu L, Xiong B, Gao W, Wang C, Zhong Z, Huo L, Wang Q, Hou Y, Liu K, Liu XJ. 2007. MEK1/2 regulates microtubule organization, spindle pole tethering and asymmetric division during mouse oocyte meiotic maturation. CELL CYCLE-LANDES BIOSCIENCE- 6: 330.

Yujiri T, Ware M, Widmann C, Oyer R, Russell D, Chan E, Zaitsu Y, Clarke P, Tyler K, Oka Y. 2000. MEK kinase 1 gene disruption alters cell migration and c-Jun NH2-terminal kinase regulation but does not cause a measurable defect in NF-κB activation. Proceedings of the National Academy of Sciences 97: 7272-7277.

Yung Y, Yao Z, Hanoch T, Seger R. 2000. ERK1b, a 46-kDa ERK isoform that is differentially regulated by MEK. Journal of Biological Chemistry 275: 15799-15808.

Zaltsman Y, Shachnai L, Yivgi-Ohana N, Schwarz M, Maryanovich M, Houtkooper RH, Vaz FM, De Leonardis F, Fiermonte G, Palmieri F. 2010. MTCH2/MIMP is a major facilitator of tBID recruitment to mitochondria. Nature cell biology 12: 553-562.

Zarubin T, Jiahuai H. 2005. Activation and signaling of the p38 MAP kinase pathway. Cell research 15: 11-18.

Zhu Y, Bond J, Thomas P. 2003. Identification, classification, and partial characterization of genes in humans and other vertebrates homologous to a fish membrane progestin receptor. Proceedings of the National Academy of Sciences 100: 2237-2242.

Zou H, Li Q, Lin S-C, Wu Z, Han J, Ye Z. 2007. Differential requirement of MKK4 and MKK7 in JNK activation by distinct scaffold proteins. FEBS letters 581: 196-202.